Climate Control Using Model Predictive Control to Reduce Energy Consumption in Hjørring Badminton Arena

Master thesis
Michael Harding Givskov
Control & automation
Aalborg University
3rd June 2021

AALBORG UNIVERSITY

Department of Electronic Systems
Control & Automation
Fredrik Bajers Vej 7B
9220 Aalborg
http://www.es.aau.dk/

Titel:

Climate Control Using Model Predictive Control to Reduce Energy Consumption in Hjørring Badminton Arena

Project:

Master thesis

Projectperiod:

01/02-2021 - 03/06-2021

Participants:

Michael Harding Givskov

Supervisors:

Henrik Schiøler
Roozbeh Izadi-Zamanabadi

Page number total: 81 pages
Finished: 03-06-2021

Synopsis:

All over the world a trend of increased energy consumption is seen. This is not only in developing countries but also in developed countries. Naturally increased demand for electricity will increase the use of fossil fuels until green alternatives are in place and the rapid increase in global temperatures will have disastrous consequences. Generally buildings are accountable for 32% of the total energy consumption. That is, energy used for heating, lighting and appliances. Space heating accounts for 33% of the total energy usage in both commercial and residential buildings and is therefore a good candidate for improvements. A badminton arena built in the 1950s is considered. in this work smart planning and usage of the heating system can be used to create large energy savings. This approach is investigated in this work by creating a model of the building and using said model together with a model predictive controller to find the optimal heating strategy. Such a strategy would involve allowing the indoor temperature to drop during the night and unoccupied hours and keep comfortable temperatures when the building is occupied. Simulations have shown that the approach does decrease energy consumption, however further developments on the model are needed for better results.

Preface

This thesis is composed by Michael Harding Givskov, 4th semester of the Control and Automation master education at Aalborg University in the spring of 2021.

The thesis is written with the goal of creating a model predictive controller to decrease energy consumption in large commercial buildings.

Acknowledgement

Special thianks are directed to the supervisors Henrik Schiøler and Roozbeh Izadi-Zamanabadi at Aalborg University for guidance throughout the project period, proof reading and for ideas when i have been stuck on something.

Readers guide

The thesis is intended to be read in chronological order. Figures and equations are assigned numbers which are used in the text to refer to the correct place. Materials such as books, papers or websites that have been used as a source can be found in a compilation at the end of this report. Equations and values in general make use of standard SI-units. The coming section includes a list of variables. If the variable/function is a differential, only the non-differentiated function is included in this list. In this report the time derivative is denoted as a dot above the function. Time dependent variables will generally be noted without the addition of the $x(t)$ notation for convenience (in this case x is any given time dependent variable). However in each of the modelling sections the variables included in the models are noted in a table where time dependent variables will have the $x(t)$ notation.

Summary

This thesis deals with the development of an autonomous control system to be applied to heating ventilation and air conditioning (HVAC) units in outdated commercial buildings. With the current developments in global temperatures and emissions it is important to act fast and in many different areas. In this case it is identified that a third of all energy consumed in both the commercial and residential sector goes to space heating. This makes space heating a good candidate for optimizations. Specifically in the case of commercial buildings there are ample opportunities for improvements as the buildings in most cases will not be occupied at night or even throughout the whole day. This allows for lowering the required temperature when the building is unoccupied. As the required heating is proportional to the difference in indoor and outdoor temperature a lower energy consumption will be the result.

A general investigation into expected outdoor temperature ranges is conducted followed by a definition of occupant comfort levels. The comfort levels are used to ensure the developed controller can maintain an acceptable range of temperatures which together with activity patterns is used to create a basis for the problem formulation.

For this work Hjørring Badminton Arena has been used as a use case. A description of the building and installed HVAC system is given. The system utilizes a cross-flow recuperator to regain some heat that otherwise would be exhausted. The pre-heated air is sent past a water-air heat exchanger that utilizes district heating water. The modelling of this element has been found to be flawed however corrections could not be implemented in time. This unit is the main heating element used to control the inlet temperature to the building. The building is split into three separate parts and only the main zone where the badminton is played is included in this work.

Thermal models have been developed for each of the previously mentioned elements, recuperator, heater and the main room. These have all been combined into a single model containing all the elements. This model has shown to be nonlinear and utilizes the flow rate, heater dissipation, return air temperature and ambient temperatures as inputs, with the room temperature as the output. Furthermore it has been found that the amount of people present in the room can have an impact on the temperature developments in the room and will act as a disturbance.

The control method suggested to solve the problem statement is gain scheduled model predictive control. A general description of model predictive control is given before a design and tuning process is begun. The resulting controller does not utilize the fans in the system other than when cooling is required. This comes as a consequence of the flaw in the heating model. Otherwise the MPC performs as was to be expected and is able to make decisions based on future developments of temperatures and reference values.

The resulting controller has in simulation been able to decrease the energy usage by almost 4% compared to the use case system in the same simulated period. This is less than what was expected however, this is deemed to be the case as the model has a higher heat loss than the real system based on measurements and simulation data.

In the authors opinion the work presented in this thesis does contribute with a proof of concept when it comes to utilizing model predictive control as a way to decrease energy consumption. However further developments are required in order to see a more clear result of how much the energy consumption can be reduced.

Danish Summary

Denne afhandling omhandler udvikling af et automatisk kontrol system som skal anvendes på varme, ventilation og air conditioning systemer i gamle kommercielle bygninger. Med de nuværende udviklinger i forhold til globale temperaturer og emmisioner, er det vigtigt at handle hurtigt og på mange områder. I dette tilfælde er det blevet identificeret at en tredjedel af alt energiforbruget i den kommercielle såvel som bolig sektoren bliver brugt på rumopvarming. Dette gør rumopvarmning til en god kandidat i forhold til optimeringer. Specifikt i det kommercielle tilfælde er der mange muligheder for forbedringer eftersom at bygningerne oftest ikke anvendes om natten eller igennem hele dagen. Det gør det muligt at sænke den krævede indendørs temperatur når bygningen ikke bruges. Eftersom at den påkrævede opvarmning er proportionel med temperatur forskellen indendørs og udendørs vil der blive anvendt mindre energi som resultat deraf.

En generel undersøgelse af forventede udendørs temperaturer udføres og efterfølges af en definition af forbrugernes grader af komfortabilitet. Komfortabilitets graderne anvendes til at sikre at den udviklede kontroller kan opretholde tilfredsstillende temperaturer som sammen med aktivitets mønstre er brugt til at forme en basis for problem formuleringen.

I dette projekt er Hjørring Badminton Arena blevet brugt som en brugssag. En beskrivelse af bygningen samt det installerede ventilations system gives. Systemet anvender en krydsstrøms rekuperator for at genvinde noget af den energi eller varme som ellers ville blive sendt ud af systemet. Den forvarmede luft sendes igennem en vand-luft varme veksler som anvender fjernvarme vand. Modelleringen af dette element har vist sig at være mangelfuld men rettelser kunne imidlertid ikke implementeres i tide. Denne enhed er hoved opvarmnings elementet som anvendes til at styre temperaturen på luften der sendes ind i hallen. Bygningen er delt op i tre zoner hvor kun den vigtigste zone, hvor der spilles badminton er inkluderet i dette projekt.

Termiske modeller er blevet udviklet for hver af de førnævnte elementer, rekuperatoren, varme elementet og hallen. Disse er alle blevet kombineret til en samlet model. Denne model har vist sig at være ikke-lineær og anvender luft strømmen, varme afsættelsen, retur luft temperaturen og udendørs luft temperaturen som inputs og rum temperaturen som output. Endvidere har det vist sig at antallet af personer i hallen kan have en indflydelse på temperatur udviklingen og dette vil virke som en forstyrrelse.

Den metode der er foreslået som kontroller for at løse problemstillingen er Gain Scheduled Model Predictive Control. En generel beskrivelse af model predictive control er givet før design og justerings fasen begynder. Den resulterende kontroller anvender ikke blæserne i systemet undtagen når der er brug for køling i hallen. Dette kommer som en konsekvens af den mangelfulde model af varme elementet. Derudover virker kontrolleren som forventet og er i stand til at tage beslutninger i forhold til kontrol signalerne baseret på fremtidige ændringer i temperaturer og reference værdier. Kontrolleren har i simuleringer været i

stand til at reducere det samlede energiforbrug med 4% sammenlignet med det rigtige system i samme periode. Dette er en mindre reduktion end forventet men det anses for at være tilfældet grundet at den udviklede model har et større varme tab end det virkelige system, hvormed ekstra varme skal tilføjes.

Det er forfatterens holdning at arbejdet der er præsenteret i denne afhandling bidrager med et bevis på konceptet i forhold til energi besparelser ved brug af moderne kontrol metoder såsom model predictive control. Dog er der brug for mere udvikling før det kan ses hvor stor en reduktion der reelt kan findes i energi forbruget.

Nomenclature

Here is a list containing some of the important constant and variables used throughout the report.

Symbols

$T_{cfs}, T_{div}, T_{exh}$	Recuperator temperatures
T_{amb}	Ambient temperatures
T_{sup}	Supply air temperature
T_{room}, T_{wall}	Indoor temperatures
q	Air flow rate
$C_{rec}, C_{div}, C_H, C_r, C_w$	Thermal capacities
$\alpha_{div}, \alpha_{wall}$	Heat transfer coefficient
c_{p_a}	Specific heat capacity of air
c_{p_div}	Specific heat capacity of aluminium
ρ_a	Density of air
ρ_{div}	Density of aluminium
P_{heater}	Power dissipation of heater
V_r	Room volume
V_H	Heater volume
$V_{pHeater}$	Recuperator volume
$T_{r,day}$	Daytime reference temperatures
$T_{r,night}$	Nighttime reference temperatures
$\Phi_t, \Phi_{occupants}, \Phi_{equipment}$	Internal building disturbances
ts	Sample time
H_p	MPC prediction horizon
H_u	MPC control horizon

Contents

1 Introduction

In the recent decades the damaging effects of greenhouse gasses have become more prevalent and the public awareness of this topic has also rapidly increased. Industry contributes heavily to the emission of these gasses, specially in countries with loose regulations for emissions. However, if one considers the general population and the sheer amount of people, carbon footprint produced here is also adding up to quite a significant amount. According to [Berardi 2017], up to 40% of the energy used in developed countries is spent on the heating of homes and buildings.

This report investigates the energy consumption of community / public utility buildings such as sports arenas, sports halls and gymnasiums. Many of these buildings have been build during the 20th century and are becoming outdated in terms of the new policies implemented in developed countries such as Denmark and others. Furthermore, often these buildings are not occupied throughout the whole day and there is therefore room to optimize the amount of energy consumed by for example lowering the heating and general energy usage outside of occupancy hours. Not only will this assist in reducing carbon footprints but also help create savings for the owners as they will have to spend less on the electricity and water bills overall.

This project aims to find a solution that can be retrofitted into buildings such as sports arenas and other similar facilities. Doing so will in the end result in savings for the property/building owners which can trickle down to the end users. Furthermore it will lower the overall carbon emissions produced in the process of heating the building which, if deployed to a great enough extent, will start to have an impact on the overall emissions of the country.

One way to solve this problem is through the use of a control strategy that can utilize future predictions of the system states such that heating can be lowered when the building is unoccupied. One way to implement this is through the use of Model Predictive Controllers (MPC) which is the option that is explored in this work.

Problem analysis 2

2.1 Energy consumption and carbon emissions

Ever since the industrial revolution, humans as a race have steadily been increasing the amount of pollution produced as industries have grown. This trend has now reached a point where some actions have to be taken to reduce the pollution as grave consequences will otherwise have to be faced. Some of these consequences can already be seen today in the form of ice melting on the north and south pole which is leading to a rising sea level and changing ocean currents. In the recent decades the effects of the massive amounts of pollution has reached the awareness of the general population and many new initiatives and regulations have been put in place to reduce general pollution and CO2 emissions.

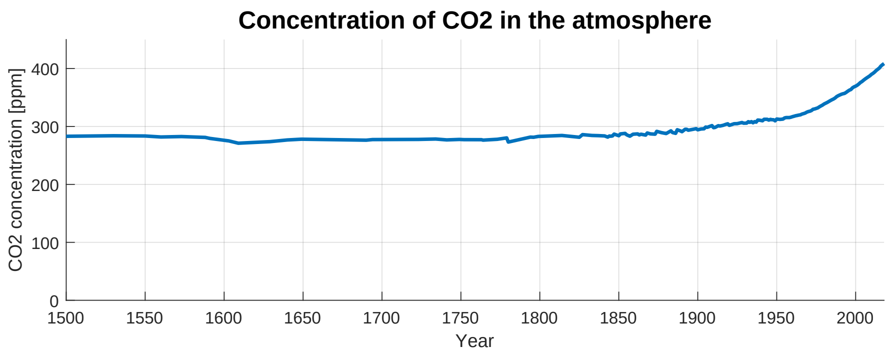

Figure 2.1: Concentration of CO2 in the atmosphere over the last 300 years where the recent increase in CO2 pollution clearly can be seen [Ritchie and Roser 2017]

Predictions of greenhouse gas emissions in the future suggest a worst case scenario where the annual greenhouse gasses roughly will double from the current amount by the year 2050 [Ritchie and Roser 2017] [Berardi 2017], which furthermore is supported by the likes of the U.S. Energy Information Administration [EIA 2020]. British Petrolium suggests that the global demand and consumption of oil will increase from the demand of 2007 by 30% before the year 2035. Furthermore the demand for natural gasses and coal is expected to increase by roughly 50% during the same period [BP 2010].

A paper in the Resources, Conservation and recycling journal by Umberto Berardi has spent some effort on looking at different estimates of energy consumption in different countries and regions. One source suggests that the energy consumption of the building sector can be up to 40% for developed countries which can be related to a similar measure of 40% of the total green house gasses being produced here [Berardi 2017].

A study by the International Panel for Climate Change has shown how the global emissions in the building sector is steadily increasing over time. However, this increase is mainly based on the indirect emissions which means that the buildings are now consuming more electricity. This obviously leads to more electricity production causing these indirect emissions from the building sector [IPCC 2014]. Furthermore this study looked into the global effect of the emissions from the building sector which represents 25% of the total emissions globally. Here 19% represents the greenhouse gas emissions and the last 6% represents other emissions [IPCC 2014]. Considering the indirect emissions it is hard to estimate the actual greenhouse gas emissions as the energy conversion factor from a material into electricity varies a lot based on the material and process. Therefore instead of looking at emissions one could consider the final energy usage which will have some relation to the emissions as those are released when producing the energy in the power plants.

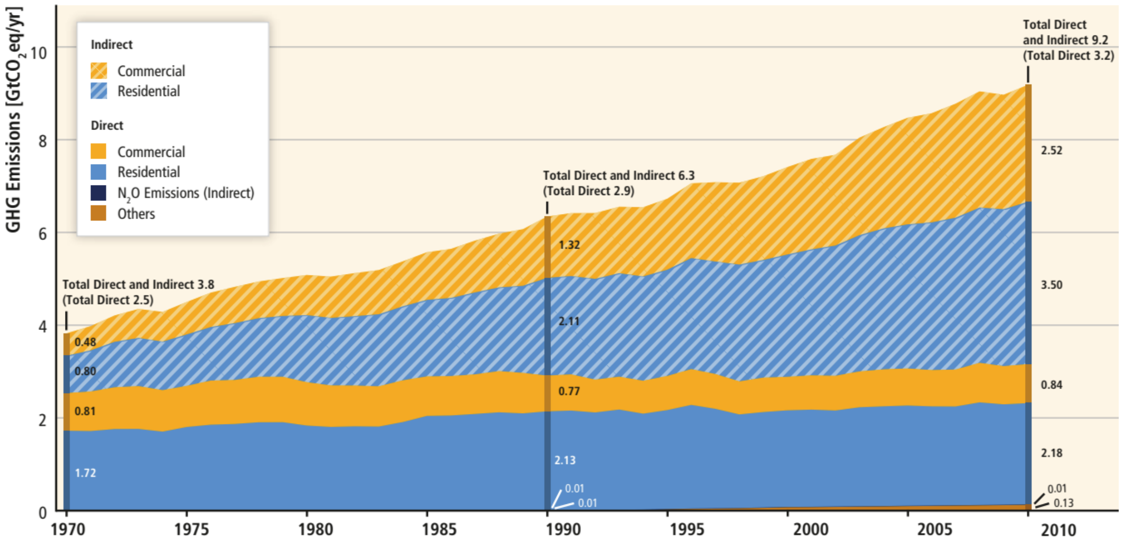

Figure 2.2: Emissions in recent decades shown in terms of direct and indirect emissions and grouped by residential and commercial [IPCC 2014]

When considering the energy usage, buildings were in 2010 responsible for 32% of the total global final energy use, where 24% was for residential and 8% was commercial. Out of this, space heating represented 32-33% in both categories.

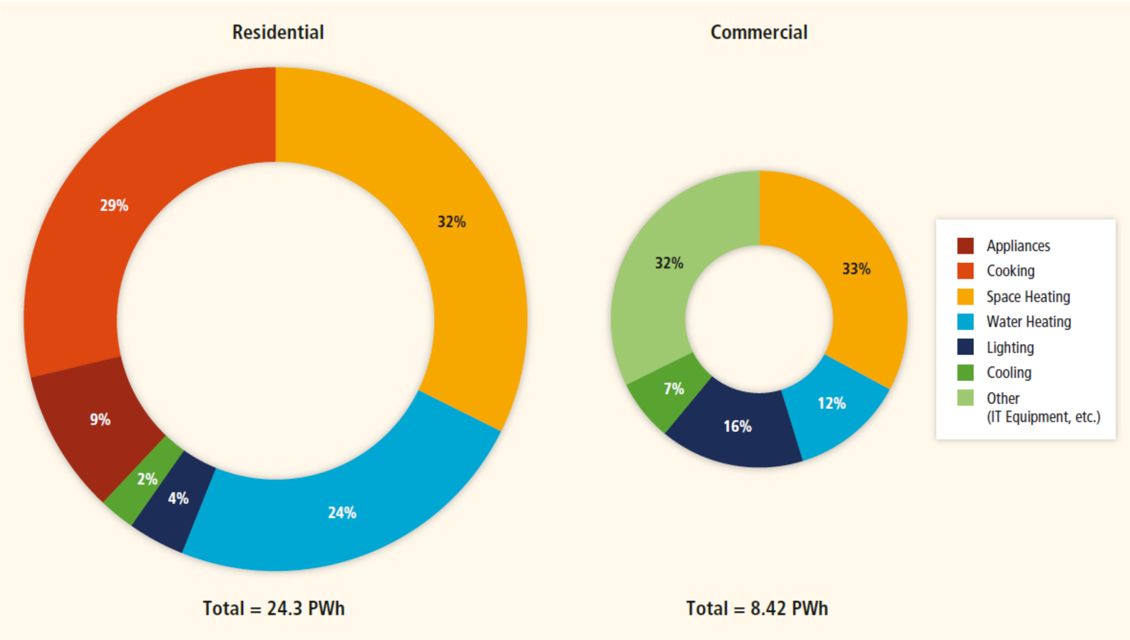

Figure 2.3: Final energy usage in residential and commercial buildings split into categories [IPCC 2014]

As one would expect the consistency of the two categories vary greatly in terms of where most of the energy is used. However, heating being the main contributor of the energy usage is a common factor and therefore a good candidate for an area to attempt to improve the efficiency.

2.2 Retrofitting or building new facilities

As the less developed countries around the world continue to progress they will start to have a greater energy demand. As of 2010, an estimated 0.8 billion people in the world did not have access to adequate housing [UN-Habitat 2008]. Furthermore 1.3 billion people did not have access to electricity and lastly an estimated 3 billion people depend on unhealthy and highly polluting fuels when it comes to cooking meals and heating homes [IPCC 2014]. Clearly as the accessibility of housing and electricity increases this will result in a greater energy consumption. This together with the information presented in the previous section suggests that immediate action should be taken to reduce energy consumption and thereby also limiting the emission of greenhouse gasses if the effects of global warming are to be reduced.

When considering the different approaches to saving energy and limiting CO2 emissions there are two different options when it comes to buildings. Nations could impose new building codes that will ensure some environmental standards and regulations are followed. These could specifically be related to the insulation in the building and the overall energy efficiency. Many nations have already done this. However, it can also be done through entities such as the European Union. As an example take the European union which imposes regulations on all member countries. These European regulations were implemented in the Energy Performance of Buildings Directive, which was implemented in 2002 and updated in 2010 [Berardi 2017]. An example of countries that could show large improvements if new codes and regulations are implemented is Russia. It has been estimated that Russia could potentially reduce final energy usage by 42% due to the many old buildings with poor building codes and the cold climate [Berardi 2017].

In order to limit the climate changes that are happening, rapid changes have to occur if the consequences have to be reduced as much as possible. That means that when the energy saving strategies are to be considered, it has to be with this rapid response in mind. Obviously the building codes only count for new buildings, so therefore they will mainly only affect countries with a high construction rate and or turn-over rate, when considering the rapid response. Turn-over rate here refers to rate at which old buildings are demolished and replaced. For the European union this turn-over rate is in general quite low [Berardi 2017] and therefore a different approach is better in these cases. For countries with low turn-over rates a retrofitting approach should be considered instead. Retrofitting in this case is when the original building is kept and the devices, systems, materials, etc. are replaced with more modern versions that have a better efficiency than the old ones.

For residential buildings the retrofitting could for example consist of new insulation and more efficient appliances. Both of these will affect the main energy consumption areas as seen in **Fig. 2.3**. Furthermore behavioural changes could also assist in reducing the energy consumption, that could be only keeping lights on when necessary and turning off all appliances such as TVs and radios when they are not actively being used.

For commercial buildings the main energy consuming areas (see **Fig. 2.3**) can generally be made more efficient by implementing more modern and smarter systems. Take for example the space heating part of the commercial energy usage. Even though the amount of energy being used here is very similar to the residential buildings there is one key difference between the two. Commercial buildings are usually not occupied 24 hours per day and in some cases also not during weekends. This means that there is an opportunity to implement new systems that lower the indoor temperature when the building is not occupied anyways and then reheats the building before the occupants show up again. Furthermore sections such as the lighting can also be reduced by ensuring that all lights are turned off when the building is unoccupied and only necessary lights are on otherwise. It is harder to argue for good energy saving methods for the IT equipment section as it consists of a diverse array of equipment types. However, one could imagine that ensuring all equipment that does not necessarily have to be on 24 hours per day is turned off when unused.

To reduce the complexity and time requirements it is decided to only focus on the space heating sector in commercial buildings for the rest of this work.

2.3 Seasonal effects on energy consumption

It is well understood that due to the second law of thermodynamics, if there is a temperature difference between two mediums and some possible conduction between the two, then the hottest medium will conduct heat towards the cold medium. In a similar fashion as the ambient temperature decreases, the amount of energy required to heat up an object is increasing as the temperature difference between the two bodies will increase. This effect will impact that amount of heating and time needed to heat up an indoor space as the outdoor ambient temperature will change with the seasons.

Due to the seasonal temperature changes it is beneficial to investigate what the expected temperature ranges are for each season. This will help with estimating the baseline amount of heating required to keep a certain temperature inside when combined with the insulation properties of the building. For simplicity this report will only deal with the danish climate and attempt to expand to other regions of the world in the final discussions. The Danish Meteorological Institute (DMI) records and archives temperature data throughout the country and makes the data available to the public [DMI 2021]. **Fig. 2.4**, **2.5** and **2.6** are produced based on data from 2020 and consists of the averaged temperature measurements from all over the country.

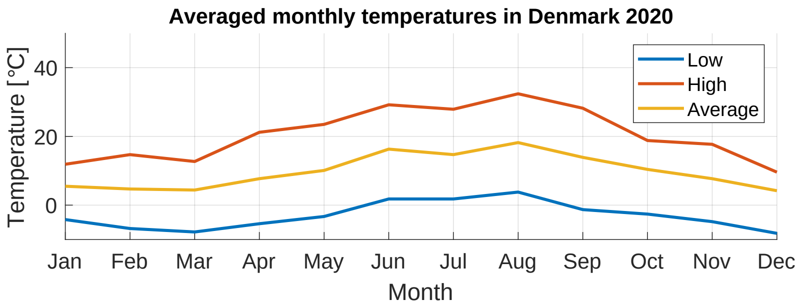

Figure 2.4: Averaged temperatures over each month in Denmark in 2020

By looking at **Fig. 2.4** it is possible to see the maximum and minimum temperatures throughout the whole year. These values will vary from year to year and similarly from region to region. However, It will still give some good indications towards the expected temperature ranges of the outdoor climate. From this it can be determined that the outdoor temperature range (given some extra worst case buffer ranges) will be between -10 °C and 35 °C. These boundaries does not necessarily give any information towards the typical temperature ranges during each season however. Therefore a closer look will also be taken at an arbitrary month in the summer and winter seasons.

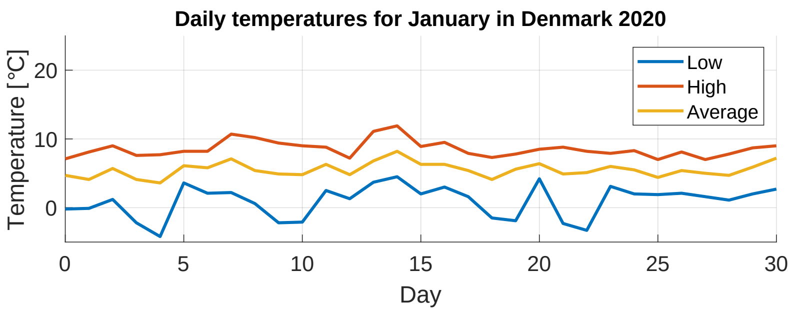

Figure 2.5: Daily temperatures in January of 2020

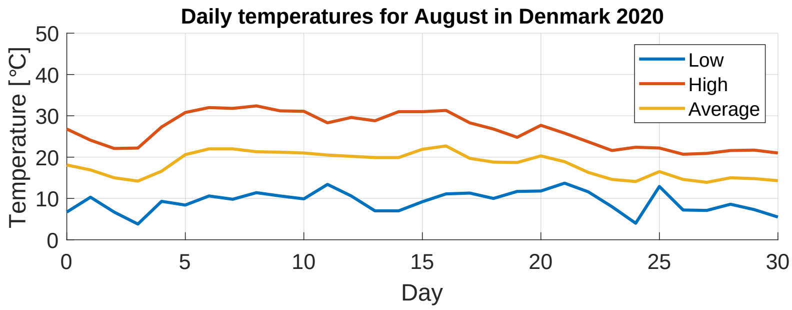

Figure 2.6: Daily temperatures in August of 2020

Fig. 2.5 and **2.6** shows the daily temperature ranges for the months of January and August respectively. By taking the average of the highest and lowest temperatures per day it is possible to estimate the expected temperature at noon/afternoon and during the night. These averages can be seen in **Tab. 2.1** together with the overall highest and lowest temperatures.

	Lowest	Averaged low	Averaged high	Highest
Winter (Jan)	-8.2000	0.9355	8.5452	11.9000
Summer (Aug)	3.8000	9.2419	26.4839	32.4000

Table 2.1: Temperatures (in °C) during the summer and winter seasons

2.4 Vacancy hours and activity patterns

As mentioned in **Sec. 2.1** Many commercial buildings are not occupied throughout the whole day. Examples of these could be shops, office buildings and sports arenas/halls. Which makes it interesting to investigate if some effort has been put into reducing heating when no occupants are present or if the heating system is running continuously throughout the day. Naturally this varies from building to building and therefore this work will be based on a case study which can be seen in **Ch. 4**. Clearly a building is not required to be heated to comfortable levels if no person is indoors, but simply has to be heated to a level where no structural damage occours. The issue with simply turning off the heating when the last person leaves and on again when the first person arrives is that it takes time for the building to heat up again. With the previously mentioned approach it would mean that no comfortable temperatures are achieved inside the building for the first hour or more (depending on the size of the building and capabilities of the heating system).

One way to get around this issue of delayed heating is by having some prediction of when the occupants will show up and expect the indoor climate to be at a comfortable level. In other words, if the activity pattern of the building is known, then the heating can be turned back on at the time that would allow for sufficient heating before the occupants arrive.

Ideally such a system would have the temperature reach the comfortable level exactly as the occupants start to arrive in order to maximize efficiency. However, there are numerous factors that makes the time at which the heating has to start uncertain. First of all the occupants will not necessarily arrive at the same time every day. Furthermore with the case of office buildings some of the workers there might stay late or come in early some days. Then there is also the issue of the outdoor climate as mentioned in the previous section (**Sec. 2.3**). If the building is empty during the night hours and the heating is turned off as the last person leaves, the indoor temperature will start to steadily fall towards the outdoor temperature. Although it likely will not fall too much due to the building insulation it will still require a significant amount of energy to heat the building back up. This will especially be the case during the winter as the temperature difference is greater.

When people are occupying a building they themselves will release some of their body heat into their surroundings. this means that once the building is occupied there might be less heating required than initially estimated. This will however, be dependent on the size of a given room and how many people there are inside. If the size of the room is large enough this effect might be insignificant however it should be investigated further. Specifically for the cases of sports arenas/halls and similar buildings it should be noted that since the activities performed here can be categorized as exercising. This will result in larger amounts of body heat being released into the room and furthermore the moisture content in the room could increase.

A final consideration that also should be made is when to turn off the heating. So far it has been stated that the heating is turned off when the last person leaves the building. However, just like there is a delay before the heating effects start to show when turning on the heating system, the temperature will also stay around the comfortable level initially when the system is turned off. Some considerations should be made in terms of how early the system can be turned off without the occupants noticing a significant difference. Although this will be specific from building to building again and therefore should be considered for the subject of the case study.

2.5 Humidity

When manipulating the heat in an enclosed space the humidity in that space will change. This is an important consideration in buildings since part of the construction can be wood or other materials which can take damage if exposed to high humidity over long periods. On top of the possibility of rot in the wooden structures there is also the risk of mold forming inside the building. It is therefore of great importance to ensure that the humidity stays below a certain level throughout the whole day. Furthermore if a system that lowers the temperature at night or when unoccupied is used, this system will have to also consider the humidity aspect. That is, the temperature will likely not be allowed to go below a certain amount as condensation otherwise then could form inside the building. The recommended indoor humidity level is considered to be between 30% - 60% relative humidity. Where less than 30% and more than 70% is considered to be uncomfortable dry and wet respectively and having the humidity at no higher than 60% reduces the risk of allergenic and pathogenic organisms [ASHRAE 2001].

Due to time limitations it has been determined to not consider indoor humidity levels in this work, however it must be noted that humidity generally is an important factor in comfort levels and due to the possibility of structural damage this effect should be considered in future work.

2.6 Temperature comfort level of occupants

Even though it is possible to save energy when it comes to space heating there is still an aspect that is important to keep at an acceptable level. This aspect is ensuring that the occupants of the building are comfortable at the temperature inside the building. For commercial buildings it can be particularly difficult to find a suitable temperature level that suits most people as a large variety of people will occupy these at any given time.

There are multiple different estimations of best temperatures based on very specific properties from person to person, such as metabolism rate and ratio between clothed and unclothed body area. The most recognized and used thermal comfort model is the Predicted Mean Vote as seen in [Orosa 2010]. However, these models can be overly specific and considering the standards shown in [ASHRAE 2010] the acceptable temperature range to maintain a comfortable level is rather large.

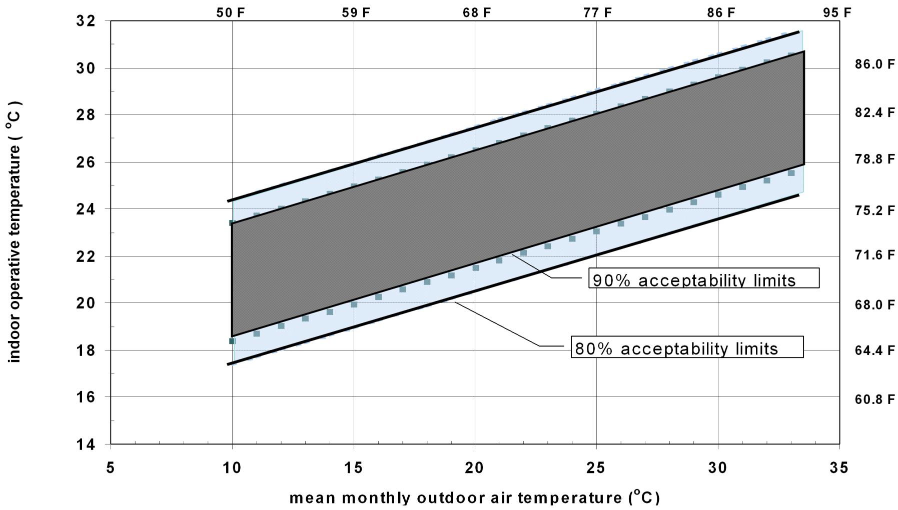

Figure 2.7: Comfortable temperature ranges dependent on the outdoor temperatures [ASHRAE 2010]

As it can be seen in **Fig. 2.7** at any given outdoor temperature, the range at which 90% of people would be comfortable is in a range of 5 °C. if this is to be expanded in such a way that only 80% of people are comfortable the range increases to approximately 7 °C. Noting that the comfortable temperature range changes with the outdoor temperature, this allows for a potential of further energy savings during the winter season which has to be investigated further. Ideally these comfortable temperature ranges are to be tested in the building chosen for the case study, to prove that they are sufficient and gauge the satisfaction of the users of the building. This is however not possible during the period of this work. Since a case study is executed here (further information presented in **Ch. 3**, useful information has been received from the managers of the building with regards to the comfortable indoor temperatures. As the building used in this case study is used for exercising and competitive sports it is noted that the temperatures needed for an acceptable comfort level is reduced compared to the information presented in **Fig. 2.7**. In this case an acceptable indoor temperature is set to be 18 degrees.

2.7 Problem formulation

This chapter has investigated how much energy is being consumed on a global scale and under what categories the energy is used. Furthermore this investigation has looked into the emissions related to the production of this energy. Specially the space heating category uses large amounts of energy both in the commercial and residential sector and could therefore be a good target for improvements. Lastly the things that can affect the amount of heating or that which changes dependent on the heating have also been investigated. This is done in order to get some insight into the effects of changing the heating and when it is beneficial to do so.

This study aims to improve the energy consumption in the space heating category by lowering the required heating on a daily basis in commercial buildings which are not always occupied and therefore have periods where no heating is necessary. For this purpose it is chosen to do a case study on a commercial building where the activity patterns are such that this type of heating is possible. The case study will focus on a badminton arena located in Hjørring, Denmark. The location of this building ties into the new versus retrofitting problem investigated in **Sec. 2.2**. Here it is found that countries such as Denmark should consider retrofitting old buildings with new technologies as the rate at which buildings are replaced is very low.

The energy consumption improvements will in this case not be done through implementation of a brand new heating, ventilation and air-conditioning system (HVAC system) but instead through a smarter use of the already existing system. That is, a new and smarter controller is to be developed. On top of lowering the energy consumption it is important that this new controller does not lower the existing comfort levels of the arena in exchange for the efficiency and therefore effort should also be put into this aspect. Considering this building is being used for sports and physical activity it also has be to robust towards highly fluctuating indoor humidity and temperature levels as well as outdoor seasonal changes.

The aforementioned can be summed up in the following problem formulation:

How can one develop a controller that considers a multitude of factors such as activity patterns, humidity, seasonal changes etc. while keeping the same comfort levels and reducing the energy consumption, be designed and retrofitted into an aging commercial building?

Case study: Hjørring Badminton Arena 3

Looking at the building plans it is possible to estimate the scale of the building. The building can be divided into three distinct zones for convenience. First of all there is the main badminton playing field area referred to as "zone 1" in **Fig. 3.1**. "Zone 2" contains the changing rooms and various utilities such as toilets and a cafeteria. Furthermore in the basement of this area contains the water and heating utility room where the HVAC system is found. Lastly "zone 3" is an external storage unit. This work will mainly focus on zone 1 as it is by far the biggest area that requires heating and will therefore overshadow the requirements of the other zones.

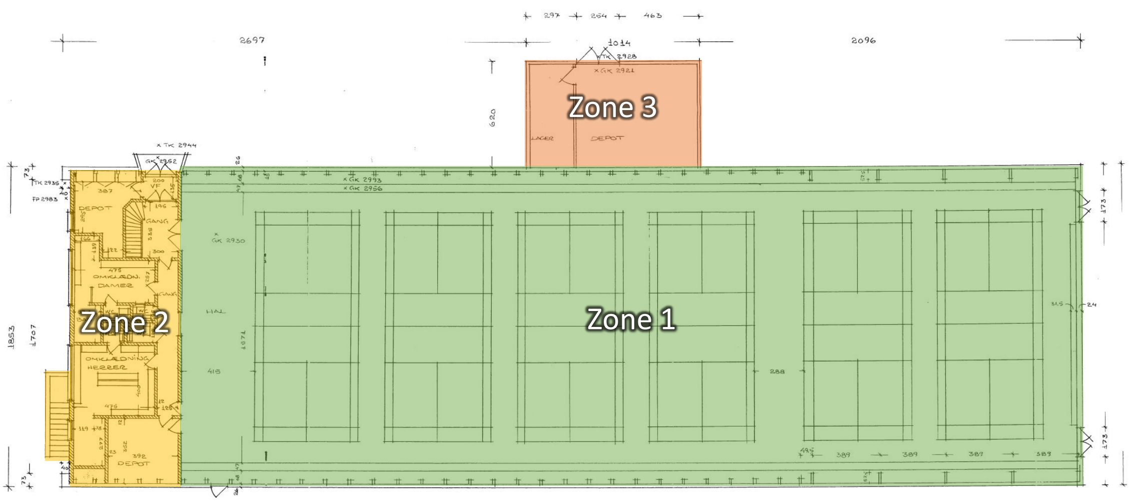

Figure 3.1: Division of the badminton arena into zones

The total area and volume zone 1 is estimated as this is of relevance at a later stage, for example when the heat-loss to the outdoor environment is calculated (see **Sec. 4.4.1**) Firstly, the floor area of zone 1 can easily be estimated by looking at building plans where the width of the building is noted as being $w_{gf} = 18\ m$. The length of the building (disregarding zone 2) before the extension in 1992 was 35.7 m and the extension, which added two extra courts, is noted as having a length of 16 m. This results in a total length of $l_{gf} = 51.7\ m$ and a total ground floor area $A_{gf} \approx 931\ m^2$.

Considering the roof of the building is made up of two arches from the top of the building to the ground, as shown in **Fig. 3.2**, the easiest way of finding the internal volume is through the cross sectional area A_{cr} of the building. The arches are formed as circles with a radius of 10.45 meters and are offset from the center line of the arena floor by 1.45 meters to each side. The angle at points A and C are 82° resulting in a total cross sectional area of $A_{arch} = 78.2\ m^2$ for each of the circular sections. giving a total of 156.3 m^2, however the two will overlap in the middle forming a triangle with an area of $A_{overlap} = 15\ m^2$ which is to be subtracted resulting in a final cross sectional area of $A_{cr} = 2 \cdot A_{arch} - A_{overlap} = 141.3$ m^2.

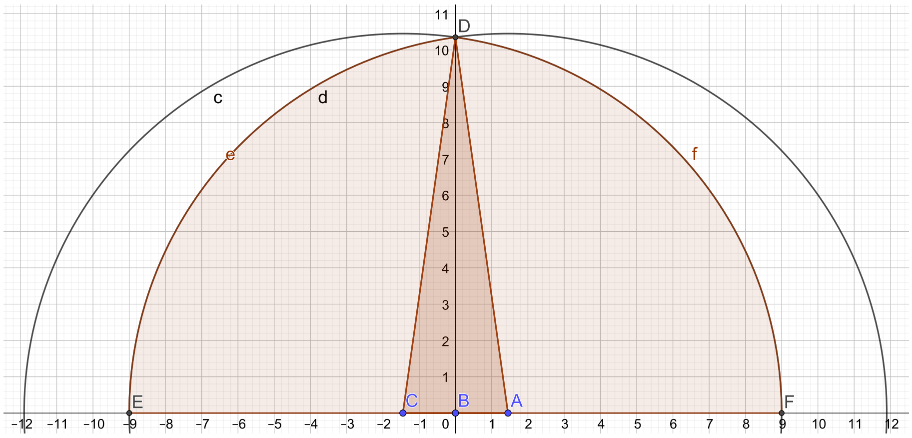

Figure 3.2: Cross sectional area of the arena based on the dimensions of the arches holding up the roof

Combining that with the length of the arena after the extension of zone 1 in 1992 this give a total internal volume of the zone of $V_{Z1} = l_{gf} \cdot A_{cr} \approx 7300\ m^3$.

Lastly the surface area of the roof and the gable (the terminating wall on the right side of zone 1) should be estimated as that also is a boundary through which the heat will dissipate to the outdoor environment. In this particular case the gable will have an area equivalent to the the cross sectional area calculated earlier, $A_{gable} = A_{cr}$. The surface area of the roof can be estimated in a similarly to the way A_{arch} is estimated. Instead of using the area of the circle, this time the circumference of the circle is multiplied with the angle of the circle slice. With a radius of 10.45 m the arc length l_{arc} of one side of the the roof is $l_{arc} = (10.45 \cdot 2 \cdot \pi) \cdot \frac{82}{360} = 14.9557 \approx 15\ m$. The total surface area of the roof is then found by adding up both sides of the roof and multiplying it with the length of the roof, $A_{roof} = 2 \cdot l_{arc} \cdot l_{gf} = 1546.4221 \approx 1546\ m^2$.

3.1 Energy consumption and isolation

As this work is concerning optimizing energy usage, investigating the energy consumption of the case at hand appears as an obvious starting point. A member of the board of the arena has provided a measure of the energy consumption throughout the year 2020 which can be seen in figure **Fig. 3.3**. As it can be seen from this figure the seasons have a large impact on the amount of heating required to keep a comfortable temperature inside the arena. During the summer periods almost no heating is needed whereas almost 10 times that amount is required during the winter. Judging by the expected and actual consumption it appears that 2020 was an unusually warm year overall. From this point on when the energy consumption of the building is referenced, it will be with regards to the expected consumption seen on **Fig. 3.3**.

The energy consumption shown here is only regarding the heating element in the HVAC system and does not include any of the energy used on lighting, water heating and the fan motors.

Regarding the insulation it is known that the roof is made up of 35 mm wood and a 1 mm steel plate on top, possibly with felt roofing between the two. Furthermore the amount of heating required to keep it warm inside can be seen on a monthly basis in **Fig. 3.3**, although it is not known what the indoor temperature reference was during these periods or whether the reference temperature was kept. The insulation and energy usage can be used to make an estimate of the amount of energy being given off to the environment and thereby finding the heat-loss of the building and the required heating at given temperatures. This is investigated further in **Sec. 4.4.1**.

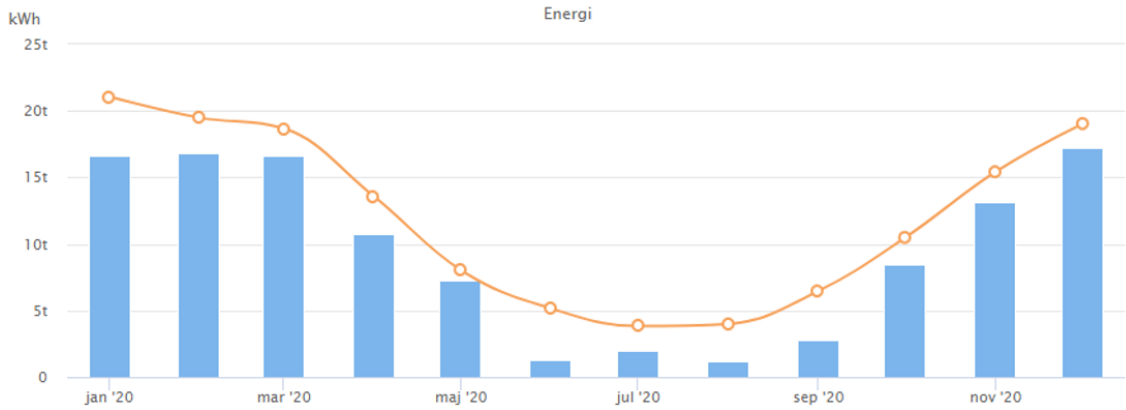

Figure 3.3: Energy consumption in the badminton arena in the year 2020. Blue columns: actual consumption. Orange graph: expected consumption.

3.2 Activity patterns

When it comes to the activity patterns of the arena, the schedule is generally repeated on a weekly basis due to planned activities and is generally known a week in advance. Not all activities will be planned but it is somewhat safe to assume that the activity in the building will generally be throughout the whole day. That is, from 08:00 to 22:00. Throughout the day there can be periods of an hour or more where the building is not occupied. The likelihood of periods like these are increased around the time of opening and closing the building. Furthermore it is assumed that there is a lower amount of activity from morning to the afternoon in the weekdays, as most people are working or at school during this period. Both the case of occupancy through a full day and with no occupants in certain periods can be studied further and used as tests for the controller that is yet to be designed. As of the writing of this work, the website of the badminton arena is being modernized. This includes a new booking and scheduling system which advantageously could be used as a tool for planning the optimal heating strategy. This will be possible if the system is connected to the internet such that it can retrieve the schedule and possibly the expected amount of people. Furthermore this also allows for retrieval of data such as weather forecasts which can assist in decision making if the humidity levels are concerning.

3.3 Heating, ventilation and air conditioning

Now the general layout and properties of the building have been investigated and next the HVAC system is to be explored. Before considering the one installed in this particular building, the general layout of the HVAC systems is investigated to get a better idea of their function.

3.3.1 General HVAC systems

When considering HVAC systems there are two main classes. A central HVAC system and local HVAC systems. Central HVAC systems perform all of the operations on the air in one central unit or location, while the local HVAC systems rely on a distributed network of smaller units in individual rooms or spread out across a large area. Each have their own advantages, for example will the central HVAC system generally not perform well in a situation where multiple rooms with different requirements are present. In such a case the local HVAC systems will have an easier time satisfying the requirements for each zone as the air supplied can be drastically different from zone to zone, which isn't possible in the central HVAC case.

HVAC systems consist of 5 different main elements. All of these except the dampers can be seen in **Fig. 3.4**. Moving from left to right the systems starts off with an inlet where fresh air pulled in and enters a mixing chamber. In the mixing chamber the fresh air is mixed with return air that previously has been heated and now is exiting the zone in which the HVAC system is supplying air. Only part of the exhaust air will enter the mixer and the rest will simply be sent to an exhaust vent where it is released to the outdoor environment.

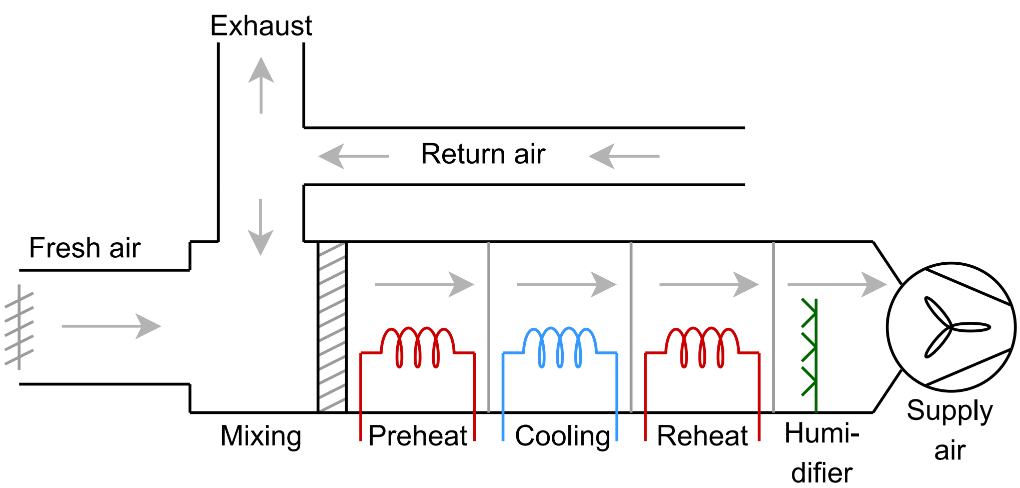

Figure 3.4: A general layout of a central HVAC system

After the mixing box the air will be sent through a filter to remove unwanted elements present in the air stream. This filter can also be placed earlier in the process and in many, if not all, cases there will be more coarse filters placed at the inlet. Furthermore along the duct systems there can be dampers present which is the element not shown on **Fig. 3.4**. These dampers can be used to adjust and control the flow of air in different parts of the system. After the filters the mixed air enters a preheating stage where it is prepared such that a required amount of cooling or heating can be performed in later stages. Next stage is based around a cooler that allows for chilling the air if it is too warm compared to the desired temperature inside the building. Following the cooling stage, a heating stage can be found. This stage is used in the case where the preheated air is too cold and extra heat is added. Last stage of the air conditioning part is a humidifier that allows altering of the moisture content of the air being supplied to the building. Finally the air reaches the fan which is responsible for drawing the air through the previous stages and sending it into the building through the ducting after the fan. Most cases will also contain a fan to draw in the return air and induce the circulation of air inside the building.

Each of the cooling and heating stages can be realised with the use of different types of systems. They are generally split into air-air, water-air and water-water heat exchangers.

3.3.2 HVAC installed in case study

Hjørring badminton arena is outfitted with a HVAC system from Exhausto with the model designation VEX 5.5S, installed in 1998. The system consists of two units, firstly the main unit where some preheating occurs and where the fans are located. Secondly there is an external heat exchanger unit that acts as the heater for the system. The system can be seen in the shape of a diagram in **Fig. 3.5** and an image **Fig. 3.6** of the actual system in the basement of the building.

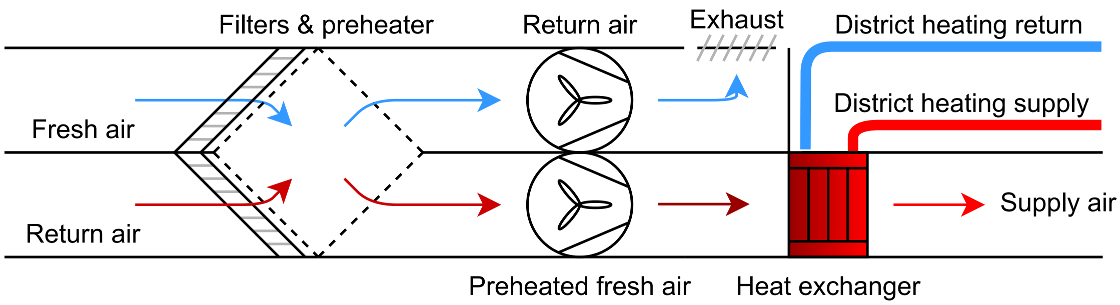

Figure 3.5: Conceptual overview of the HVAC system installed in HBA

Figure 3.6: Main parts of the HVAC system installed at HBA

Taking a closer look at the main unit first. **Fig. 3.7** shows the preheating, or what could be called the waste heat recuperater (referred to as the CFR or recuperator from this point on) in this case. Here some of the energy still present in the return air is used to heat up the incoming fresh air through an air-air heat exchanger (using a cross-flow configuration) before it enters the fans where it is either pushed towards the main heat exchanger or the exhaust outlet.

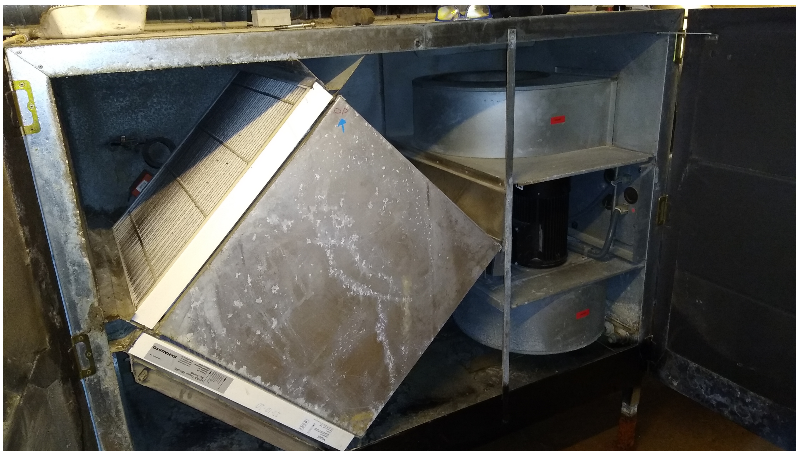

Figure 3.7: Internal view of the main HVAC unit

The preheated fresh air is fed into the main heat exchanger unit which can be seen on **Fig. 3.8**. Here incoming hot district heating water enters the unit in pipes that the air will have to pass by, resulting in a heat exchange between the two bodies and the temperature of the air increasing.

Figure 3.8: Side view of the water-air heat exchanger where the water comes directly from the district heating supply

These elements will be explored more in-depth in **Ch. 4** where the modelling of the building and system can be seen.
Lastly the venting of the arena is investigated. The air vents in the arena are place in the audience stands as small openings at ground level covered by a grate. This can be seen in **Fig. 3.9**. These openings are placed in intervals of a few meters and extend the full length of the room. Even though there are vents in part of the building that was added in 1992, these vents are not connected to the rest of the system and can be deemed inactive.

The vents can be found on both sides of the arena and the system is made such that all the vents on the right side of the room (see **Fig. 3.10**) expel the supply air which rises to towards the ceiling as it is warm air. As the air starts to cool down it will fall towards the ground level and enter the vents on the left side as there will be a smaller pressure there due to the fans in the HVAC. This creates a form of natural convection inside the arena which allows the supply air to spread throughout the whole room.

Figure 3.9: Ventilation in- and outlets, located at bottom of the audience stands in the badminton court area

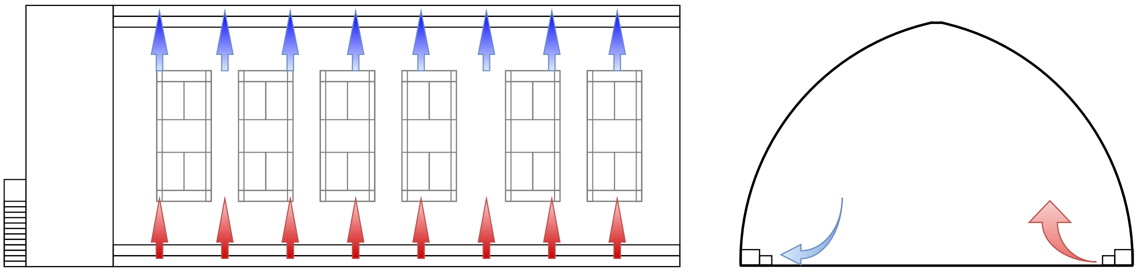

(a) Top view (b) Simplified front view

Figure 3.10: Heating distribution in zone 1

Now all parts of the system have been established and a closer look at the specific parameter values and system dynamics. This is done through modelling of the systems which is done in the following chapter.

Modelling the system 4

In the process of making a controller for a system, one will need to also make a model of said system. The models should be sufficiently accurate for the application. In theory the best option is to make the model as accurate as possible. However, there are limitations such as the capabilities of the system and processors that have to handle the computations required for the controller. Furthermore, some of the lesser dynamics will have small or insignificant impacts on the overall system response and therefore are not necessary for a good controller. Identifying the important dynamics is a big part of the modelling process, specially when limited computing power is present or when dealing with complex systems where the complexity of the control design also can be simplified as a consequence. This chapter seeks to investigate the parts of the system that have been mentioned in previous chapter (**Ch. 3**). Through that investigation mathematical models are created and finally simulated in order to see if the accuracy is sufficient or revisions are needed.

Here an overview of the available sensors on the HVAC is shown. Most of the temperatures in the system is measureable based on the current sensor setup. If a state or parameter is unmeasureable state estimators can be used. However in this case it will be rather easy to add new sensors to the system without a large cost. This leads to the assumption that all required sensor data can be collected.

Identifier	Description
T_1	Temperature sensor on the room inlet
T_2	Temperature sensor on the return air (assumed to be equal to T_{room})
T_3	Temperature sensor on the exhaust outlet
T_4	Temperature sensor on the outlet of the water heat exchanger
$p_1\&p_2$	Combination of pressure sensors to measure pressure drop over filter Δp_{in}
$p_3\&p_4$	Combination of pressure sensors to measure pressure drop over filter Δp_{out}

Table 4.1: Available sensors, see **Fig. 4.1**

The model is split into three different parts as follows: The CFR and fans, the external water-air heater and lastly the room in which the badminton is played (see zone 1 in **Fig. 3.1**). These models can then be combined at a later stage, where the controller can be designed.

4.1 Overall model assumptions

In order to better understand the impacts of actuators on the supply air created by the HVAC system it is beneficial to create a mathematical model.

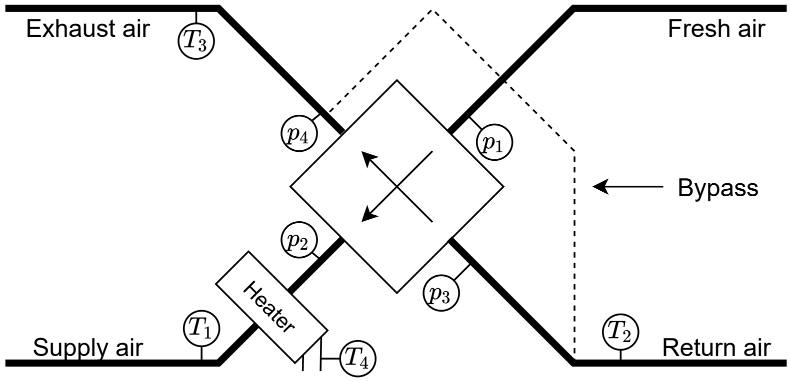

Figure 4.1: Graphical representation of available sensors in the HVAC unit

Before beginning the modelling process a few assumptions will be made. These serve to simplify the system such that the model likewise can be reduced in complexity. Furthermore the assumptions are made for things that will have small impacts on the overall performance of the system. The ones mentioned here will count for all parts of the HVAC system and if there are further assumptions for specific elements in the HVAC, those will be mentioned in the corresponding subsection.

For the overall HVAC system the assumptions are as follows.

- Even though it can be seen on the ventilation ducts in **Fig. 3.6** that there is no external insulation, it is not known whether this is also the case for the ducting outside of the room where the HVAC is placed. For the moment it is assumed that the ducting is insulated to such a degree that heat-loss to the surroundings is eliminated.
- It is assumed that this insulation does not store any significant amount of heat.
- It is assumed that the air is well mixed, both in the ducts and in the champers in the HVAC and heater. If this is not the case it will be necessary to have multiple temperature sensors in every crucial chamber.
- It is assumed that the volume inside the chambers are constant, and that the density and specific heat of the air also remains constant.
- It is assumed that the flow of air in the system remains the same on the output as it is on the input, meaning that there is no leakage in the system.

With these assumptions in place, the modelling process can now commence.

4.2 Cross-flow recuperator and fans

The first part of the system of which a model is created is the recuperator unit and the fans present in the same physical box.

4.2.1 Model

The purpose of the CFR is to regain some of the heat that otherwise will be sent to the exhaust of the system and therefore a model for the CFR outlet temperature T_{cfs}

is required. For the fans the goal is to model the airflow created at different rotational velocities of the blades. **Fig. 4.2** shows some of the different physical parameters used in this part.

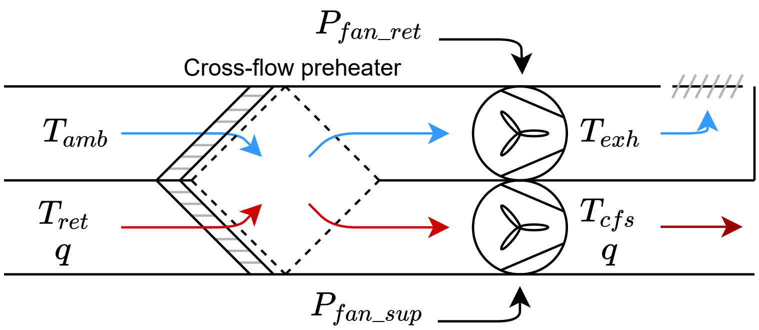

Figure 4.2: Overview of parameters involved in the CFR and fan model

Starting off with the cross-flow pre-heating unit. There are two different options when it comes to modelling this part. Firstly, the datasheet for the HVAC system has been obtained. In this document the manufacturer states that the cross-flow heat exchanger will transfer 60-70% of the available energy between the two air streams. This appears as a quite vague statistic as there is no data in the datasheet to back up the statement. However, in good faith this transfer rate will be tested in simulation along with the model of the unit. The model makes use of the heat transfer between the two air streams which can be estimated through the use of the energy balance equation. This equation can be used to model the exchange of energy between the two flows in the form of a temperature change.

This simple equation comes from the law of conservation of energy: stating that the energy of some mass will stay constant in an isolated system and changes can only happen by giving off or receiving energy from the environment. This allows for the simple formulation that the change in energy will be equivalent to the received energy and loss of energy as seen in **Eq. 4.1**

$$\frac{dE}{dt} = \dot{E}_{in} - \dot{E}_{out} \tag{4.1}$$

The usefulness of the energy balance equation is readily apparent when considering that energy exists in many different forms. In this case the goal is to find the change in temperature of the two air streams when they pass through the unit which can be considered a heat exchanger. The temperature of some fluid or solid can be used as an expression of the internal energy it contains.

In this case the heat exchanger can be seen as three energy balance equations, where each corresponds to one of the following mediums: Fresh inlet air, the aluminium separator and the return air. This can be seen as shown in **Fig. 4.3a** or as a simplified version in **Fig. 4.3b**.

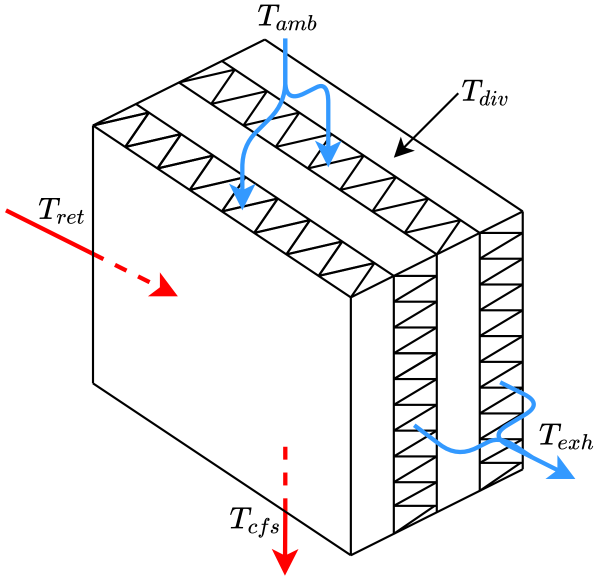

(a) Illustration of flow through the fins of the recuperator

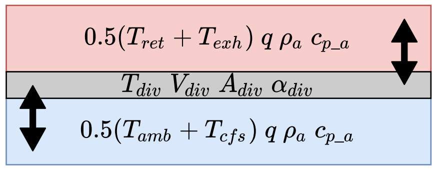

(b) Simplified illustration of heat transfer between the two air streams. The blue zone is the air with T_{amb} as input and T_{cfs} as output. For the red zone it is T_{ret} and T_{exh} respectively. The arrows indicate the heat transfer between the bodies

Figure 4.3: Flows through the water-air heat exchanger

When using this approach and considering the temperatures as the states of this part of the system the energy balance equations will appear as follows.

$$C_{rec}\frac{dT_{exh}}{dt} = (T_{ret} - T_{exh}) \cdot q_{ret} \cdot \rho_a \cdot c_{p\_a} - \left(\frac{T_{ret} + T_{exh}}{2} - T_{div}\right) A_{div} \cdot \alpha_{div} \tag{4.2}$$

$$C_{div}\frac{dT_{div}}{dt} = \left(\frac{T_{ret} + T_{exh}}{2} - T_{div}\right) A_{div} \cdot \alpha_{div} + \left(T_{div} - \frac{T_{amb} + T_{cfs}}{2}\right) A_{div} \cdot \alpha_{div} \tag{4.3}$$

$$C_{rec}\frac{dT_{cfs}}{dt} = (T_{amb} - T_{cfs}) q_{sup} \cdot \rho_a \cdot c_{p\_a} + \left(T_{div} - \frac{T_{amb} + T_{cfs}}{2}\right) A_{div} \cdot \alpha_{div} \tag{4.4}$$

As the air goes through the pre-heater it will gradually decrease or increase in temperature. In this case this effect is taken into account by simply taking the average temperature of the air stream when considering the heat transfer to the dividing wall (example: $\left(\frac{T_{ret}+T_{exh}}{2} - T_{div}\right) A_{div} \cdot \alpha_{div}$). The parameters C_{rec} and C_{div} represents the heat capacity of the air and aluminium and allows for a conversion of temperature to the amount of energy contained in those mediums based on the temperature. C_a is obtained as a combination of the volume, density and specific heat capacity as follows: $C_{rec} = V_{pHeater} \cdot \rho_a \cdot c_{p\_a}$. C_{div} is obtained in the same way, resulting in $C_{div} = V_{div} \cdot \rho_{div} \cdot c_{p\_div}$.

Inserting C_{rec} and C_{div} into **Eq. 4.2**, **4.3** and **4.4** and reducing the equations the following is obtained.

$$\dot{T}_{exh} = (T_{ret} - T_{exh})\frac{q_{ret}}{V_{pHeater}} + \left(\frac{T_{ret} + T_{exh}}{2} - T_{div}\right)\frac{A_{div} \cdot \alpha_{div}}{V_{pHeater} \cdot \rho_a \cdot c_{p\_a}} \tag{4.5}$$

$$\dot{T}_{div} = \left(\frac{T_{ret} + T_{exh}}{2} - T_{div}\right) \frac{A_{div} \cdot \alpha_{div}}{V_{div} \cdot \rho_{div} \cdot c_{p\_div}} + \left(T_{div} - \frac{T_{amb} + T_{cfs}}{2}\right) \frac{A_{div} \cdot \alpha_{div}}{V_{div} \cdot \rho_{div} \cdot c_{p\_div}} \tag{4.6}$$

$$\dot{T}_{cfs} = (T_{amb} - T_{cfs}) \frac{q_{sup}}{V_{pHeater}} + \left(T_{div} - \frac{T_{amb} + T_{cfs}}{2}\right) \frac{A_{div} \cdot \alpha_{div}}{V_{pHeater} \cdot \rho_a \cdot c_{p\_a}} \tag{4.7}$$

Using the temperatures of the different mediums as states and the airflows as control inputs, the system can be set up in the state-space form. Furthermore, assuming that the two airflows are equal this reduces the the controls to a single flowrate q. Firstly there are the states and control input vectors.

$$x = \begin{bmatrix} T_{exh} \\ T_{div} \\ T_{cfs} \end{bmatrix} \tag{4.8}$$

$$u = q \tag{4.9}$$

$$\begin{aligned}\begin{bmatrix} \dot{T}_{exh} \\ \dot{T}_{div} \\ \dot{T}_{cfs} \end{bmatrix} &= \begin{bmatrix} \frac{T_{ret}/T_{exh}+1}{2} \frac{A_{div} \cdot \alpha_{div}}{V_{pHeater}} & -\frac{A_{div} \cdot \alpha_{div}}{V_{pHeater}} & 0 \\ \frac{T_{ret}/T_{exh}+1}{2} \frac{A_{div} \cdot \alpha_{div}}{\rho_a \cdot c_{p\_a}} & 0 & \frac{T_{amb}/T_{cfs}+1}{2} \frac{A_{div} \cdot \alpha_{div}}{\rho_a \cdot c_{p\_a}} \\ 0 & \frac{A_{div} \cdot \alpha_{div}}{V_{pHeater}} & \frac{T_{amb}/T_{cfs}+1}{2} \frac{A_{div} \cdot \alpha_{div}}{V_{pHeater}} \end{bmatrix} \begin{bmatrix} T_{exh} \\ T_{div} \\ T_{cfs} \end{bmatrix} \\ &+ \begin{bmatrix} \frac{T_{ret}}{V_{pHeater}} \\ 0 \\ -\frac{T_{amb}}{V_{pHeater}} \end{bmatrix} \begin{bmatrix} q \end{bmatrix} + \begin{bmatrix} -\frac{q}{V_{pHeater}} & 0 & 0 \\ 0 & 0 & 0 \\ 0 & 0 & -\frac{q}{V_{pHeater}} \end{bmatrix} \begin{bmatrix} t_{exh} \\ t_{div} \\ t_{cfs} \end{bmatrix}\end{aligned} \tag{4.10}$$

By defining the matrices according to the state-space form a greater overview of this system is obtained. Here the C matrix is defined as $C = \begin{bmatrix} 0 & 0 & 1 \end{bmatrix}$

$$\begin{aligned} \dot{x} &= A_0 x + Bu + A_1(u)x \\ y &= Cx \end{aligned} \tag{4.11}$$

Lastly there is the problem of determining the air flow generated by the fans as there is no flow sensor built into the system. Here two different approaches are considered. First approach works by using the pressure difference generated by the pre-heater to estimate the air flow. This can be done in this case as there are pressure sensors on both sides of the recuperator for both air streams. These sensors are normally used to indicate if the filters need to be changed however given sufficient accuracy they could also be used to estimate the flow. The second method that is available is to find the relation between the rotation of the motors and the air flow generated as a consequence. This method is considered to be a better solution in this case as all the required parameters are available and it has proven an efficient method in previous work.

Proceeding by finding the relationship between the rotational velocity of the fan and the flow it generates, a few parameters from the datasheet are useful. Firstly the range of flows that the fan can produce is stated. This range is roughly 750-3800 m^3/h. The lower boundary is due to the fact that the fans only can go down to a certain frequency before they will completely shut off. This lower boundary is set at 30% of the maximum frequency. The motors for the fans are controlled by continuous frequency converters allowing for the frequency range of 15-50 Hz when considering the lower boundary. the rotational velocity of the motor is stated as rotations per minute (RPM) and the maximum speed reachable is 1420 RPM. It is assumed that there is no slip between the motor and the fan. Furthermore, using the so-called "fan laws" which provide a few simple equations and properties that allow for estimation of the flow, pressure and power generated/used by the fan. Using the property that the flow is proportional to the velocity of the fan when the fan diameter is kept constant, the flow rate based on the frequency applied to the motor can then be determined as follows.

$$Q_f = \frac{3800m^3/h}{50Hz} = 76m^3/h/Hz \tag{4.12}$$

Using this relation the flow rate produced by the fans can then be determined. Keeping in mind that only a single flow parameter is used as both air-streams are assumed to have equal flow.

$$q = Q_f \cdot f_r \tag{4.13}$$

4.2.2 Parameter estimation

A few constant parameters for the recuperator can be set with help from the HVAC datasheet (see App. A.1). First of all here it is clearly stated that the surface area of the medium between the two air streams in the recuperator is $A_{div} = 42m^2$. The thickness of the aluminium which divides the two air-streams is not stated in the document. In order to achieve great heat transfer between the two air-streams it is important that the dividing material has a surface area high compared to the volume. Therefore it can be said with high confidence that the dividing plates are very thin. Later measurements during tests resulted in the thickness of the plates being 1 mm which will result in the volume occupied by the divider being $V_{div} = 42m^2 \cdot 0.001m = 0.042m^3$. Using this estimation and the dimensions for the whole unit that is given in the datasheet the volume which the air streams can occupy are $V_{pHeater} = \frac{0.592^3 - V_{div}}{2} = \frac{0.1655m^3}{2} = 0.0827m^3$. Here the value is divided by two as half of the space will be occupied by the return air and the remaining space is dedicated to the fresh air.

4.3 Water-air heater

The main heat exchanger used in this building can be shown illustratively as seen in **Fig. 4.4** and additionally the flow, for both the air and water perspective can be seen in **Fig. 4.5a** and **Fig. 4.5b** respectively. The heater is a water-air heat exchanger which means

Symbol	Value [unit]	Description
$T_{amb}(t)$	[°C]	Ambient outdoor temperature
$T_{cfs}(t)$	[°C]	Temperature of air after the cross-flow pre-heater
$T_{ret}(t)$	[°C]	Temperature of air returning from zone 1
$T_{exh}(t)$	[°C]	Temperature of air leaving the system
$T_{div}(t)$	[°C]	Temperature of the divider material
$q(t)$	$[m^3/h]$	Flow rate of air-streams
ρ_a	1.225 $[kg/m^3]$	Density of air
ρ_{div}	2700 $[kg/m^3]$	Density of divider material (aluminium)
α_{div}	25 $[W/m^2K]$	Heat transfer coefficient
c_{p_a}	1.006 $[J/kgK]$	Specific heat capacity of air
c_{p_div}	910 $[J/kgK]$	Specific heat capacity of divider material (aluminium)
A_{div}	42 $[m^2]$	Surface area where the heat transfer can occur
$V_{pHeater}$	0.0827 $[m^3]$	Internal volume available for the air
V_{div}	0.042 $[m^3]$	Volume of the aluminium

Table 4.2: Parameters used in the recuperator and fan model. Only constants are shown with values

that hot water (or cold if the heat exchanger is used as a chiller) is used to heat up tubes and/or fins which will give off heat to the passing air. In this case the heat transfer happens by letting the tubes containing the hot water run through the path in which the air will flow. This results in the air being forced past the tubes where it will pick up the heat. It is not known if the path of the water is organized in a specific way. However, based on the positions of the inlet and outlet pipes it can be assumed that the heater makes use of the principle of a counter-flow heat exchanger.

Returning to the energy balance equation stated in **Eq. 4.1** which now can be used again to model this unit. Some of the parameters used to describe the model can be seen in **Fig. 4.4**.

Firstly, the air at the inlet has a temperature governed by the previously modelled section, the recuperator which is denoted as T_{cfs}. Furthermore the inlet air has the flowrate generated by the fans q. As stated previously regarding the assumptions, the flowrate is assumed to be constant throughout the elements. The heating supplied by the heater is dependent on the temperature of the incoming district heating water denoted as T_{w_sup} and the outlet will have water returning to the supplier with a temperature of T_{w_ret}. Lastly the energy consumed by the pump is denoted as P_{pump}. This energy will not have a significant effect on the heating of the air but will have an impact on the overall energy consumption of the building. Considering the energy consumption of the rest of the HVAC unit this amount is insignificant and is therefore disregarded.

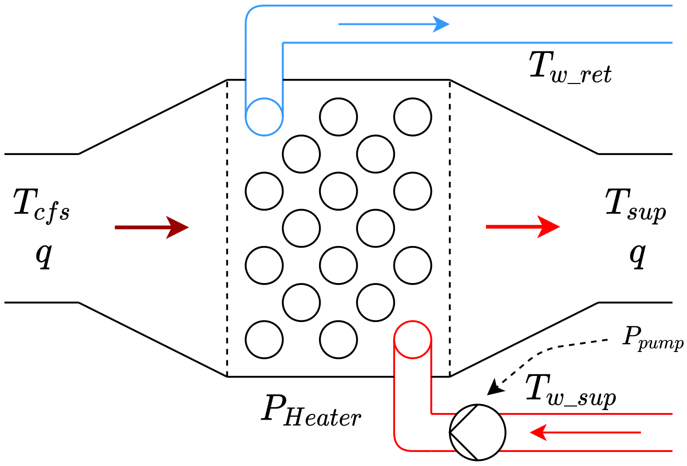

Figure 4.4: overview of parameters involved in the heater model. Each of the tubes in the heater connects to another one, allowing for the water to pass through them all (note that the amount of tubes for the water to pass through is not to scale, see **Fig. 3.8** for full amount)

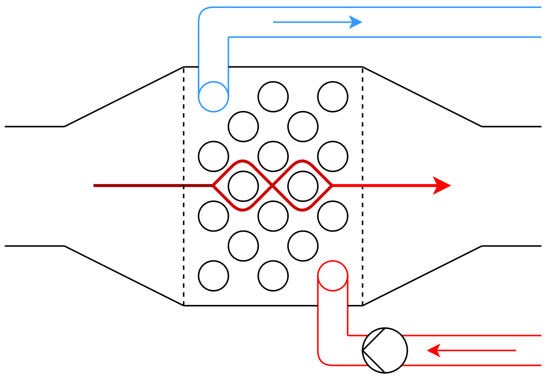

(a) flow of air

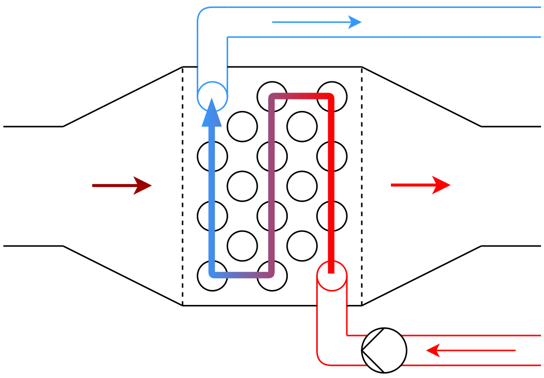

(b) flow of water

Figure 4.5: Flows through the water-air heat exchanger

Using the previously mentioned parameters and **Fig. 4.4** with the energy balance equation **Eq. 4.14** is obtained.

$$C_H \frac{dT_{sup}}{dt} = (T_{cfs} - T_{sup}) \cdot q \cdot \rho_a \cdot c_{p\_a} + P_{heater} \tag{4.14}$$

Where q is the flow-rate generated by the supply fan, ρ_a is the density of the air and c_{p_a} is the specific heat capacity of the air. The parameter C_H represents the heat capacity of the air and allows for a conversion of temperature to the amount of energy contained in the air based on the temperature. C_H is obtained as a combination of the volume, density and specific heat capacity as follows: $C_H = V_{Heater}\rho_a c_{p\_a}$.

In order to estimate the amount of energy that is being added to the air through the water-air heat exchanger (P_{heater}) it is required to know how much energy the water contains and delivers to the system.

The amount of thermal energy in the water can in general be determined with the use of **Eq. 4.15** Where E_t is the thermal energy, m_w is the mass of the water, c_{p_w} is the specific heat capacity of the water and Δt is the temperature change in the water as it passes through the heater. The model developed here does not take the effect of the counter-flow configuration into account, but this could be considered for further development. Lastly the contribution of heat from the pump that pushes the water through the heater is neglected as this will be an insignificant amount compared to the total energy dissipated by the water.

$$E_t = m_w \cdot c_{p\_w} \cdot \Delta T_w \tag{4.15}$$

The capacity of water in the pipes is estimated in **Sec. 4.3.1**. It is worth noting that after passing through the heater, the pipes bend 180 degrees and go back into the heater such that they pass through many times. These bends do not occour inside the air stream but outside of the heater. This will result in some loss of thermal energy from the water. Considering that the air outside the heater is only moved by natural convection, the amount of lost energy will be quite low and is neglected. Seeing the energy from the perspective of the air stream in the heater, the effect provided by the heater can be expressed a **Eq. 4.16**.

$$P_{heater} = (m_w \cdot c_{p\_w} \cdot (T_{w\_ret} - T_{w\_sup})) \tag{4.16}$$

Rearranging the differential equation, inserting C_H and putting it on the state-space form it appears as follows.

$$\dot{T}_{sup} = (T_{cfs} - T_{sup})\frac{q}{V_{Heater}} + \frac{P_{Heater}}{C_H} \tag{4.17}$$

With state and control vectors defined as **Eq. 4.18**.

$$x = T_{sup} \qquad u = \begin{bmatrix} q \\ P_{Heater} \end{bmatrix} \tag{4.18}$$

$$\dot{T}_{sup} = \begin{bmatrix} \frac{q}{V_{Heater}} \end{bmatrix} \begin{bmatrix} T_{sup} \end{bmatrix} + \begin{bmatrix} \frac{T_{cfs}}{V_{Heater}} & \frac{1}{C_H} \end{bmatrix} \begin{bmatrix} q \\ P_{Heater} \end{bmatrix} \tag{4.19}$$

Considering the output as well, a system as seen in **Eq. 4.20** is obtained. with the matrices seen in **Eq. 4.21**.

$$\begin{aligned} \dot{x} &= A(u)x + Bu \\ y &= Cx \end{aligned} \tag{4.20}$$

$$A(u) = \begin{bmatrix} \frac{q}{V_{Heater}} \end{bmatrix}, \quad B = \begin{bmatrix} \frac{T_{cfs}}{V_{Heater}} & \frac{1}{C_H} \end{bmatrix}, \quad C = 1 \tag{4.21}$$

Looking back at the differential equation the transfer function can be determined. First by assuming that the air coming from the cross-flow recuperator has a constant temperature due to the slow changes in the outdoor and return temperature, a new temperature can be defined $\tilde{T} = T_{sup} - T_{cfs} \rightarrow \frac{d\tilde{T}}{dt} = \frac{dT_{sup}}{dt}$. This means that the differential equation can be reduced to the following.

$$C_H \frac{d\tilde{T}}{dt} = -q\rho_a c_{p\_a}\tilde{T} + P_{Heater} \tag{4.22}$$

which then can be transformed into the transfer function through the laplace transform.

$$\rightarrow T(s) = \frac{X(s)}{Y(s)} = \frac{\frac{1}{V_{Heater}\rho_a c_{p\_a}}}{\frac{V_{Heater}}{q}s + 1} \tag{4.23}$$

resulting in a gain K_p and time constant T_p

$$K_p = \frac{1}{V_{Heater}\rho_a c_{p\_a}} \tag{4.24}$$

$$T_p = \frac{V_{Heater}}{q} \tag{4.25}$$

4.3.1 Parameter estimation

The unknown parameters present in this model is m_w and C_H. Firstly in order to find the mass of the water inside the heater some dimensions of the heater are required. As the water is carried through pipes the internal volume of these is needed. Here the outer diameter (OD) of the pipes have been measured to be 15 mm and coincidentally there was an unconnected pipe in one of the openings of the heater. Based on this unconnected pipe the thickness (d_{pipe}) has been measured to 1 mm. Considering the outer diameter and the thickness the inner diameter (ID) is determined, $ID_{pipe} = OD_{pipe} - 2 \cdot d_{pipe} = 13mm$. Using this inner diameter in combination with the length of the pipe which can be calculated based on the amount of times it goes through the heater unit and the width of the unit, the mass of the internal water can be calculated. The width of the heater is measured to be 0.6 m and the amount of times the pipes go through the heater is 42 times. Finally the internal area of the pipe is calculated,

$$V_w = A_{pipe} \cdot l_{pipe} \cdot n_{pipe} = \left(\frac{ID_{pipe}}{2}\right)^2 \cdot \pi \cdot l_{pipe} \cdot n_{pipe} = 42.2mm^2 \cdot \pi \cdot 0.6m \cdot 42 \approx 0.0033m^3 \tag{4.26}$$

Using the calculated volume and applying the density of the water, the mass can be obtained.

$$m_w = V_w \cdot \rho_w = 0.0033 \cdot 997kg/m^3 \approx 3.334kg \tag{4.27}$$

The heat capacity of the air C_H is found using the definition specified earlier where $C_H = V_{Heater}\rho_a c_{p\_a}$. Here the only unknown is the volume of the heater unit V_{Heater} which can be found as a result of the dimensions of the unit and subtracting the space occupied by the pipes containing the water V_{pipe}. The volume of the pipe is simply estimated by using the outer diameter of the pipe and calculating the cross sectional area which then can be multiplied with the length of the pipe inside of the heater as before.

$$V_{pipe} = \left(\frac{OD_{pipe}}{2}\right)^2 \cdot \pi \cdot l_{pipe} \cdot n_{pipe} \approx 0.0044m^3 \tag{4.28}$$

$$V_{Heater} = w_{Heater} \cdot h_{Heater} \cdot d_{Heater} - V_{pipe} = 0.6 \cdot 0.54 \cdot 0.21 - 0.0044 \approx 0.0636 \tag{4.29}$$

The resulting list of parameters and values obtained for constants can be found in the following table 4.3.

Symbol	Value [unit]	Description
$T_{cfs}(t)$	[°C]	Input temperature of air
$T_{sup}(t)$	[°C]	Output temperature of air
$T_{w\_sup}(t)$	[°C]	Input temperature of water
$T_{w\_ret}(t)$	[°C]	Output temperature of water
$q(t)$	$[m^3/s]$	flow rate of the air stream
$P_{heater}(t)$	$[W]$	Effect dissipated from the water to the air
V_{heater}	0.0636 $[m^3]$	Volume of air inside the heater element
m_w	$3.334[kg]$	Mass of the water contained in the pipes
c_{p_a}	1006 $[J/kgK]$	Specific heat capacity of air
c_{p_w}	4180 $[J/kgK]$	Specific heat capacity of water
ρ_a	1.225 $[kg/m^3]$	Density of air

Table 4.3: Parameters used in the heat exchanger model. Only constants shown with values

After the development of this model access had been granted to the arena and measurements and tests could be performed. With this access the operation of the system was further investigated and has been found that the district heating supply water is controlled through an on/off valve, and that the pump can not be controlled through an external signal, resulting in a constant power of $25kW \pm 5\%$ when the heater is on. With this style of operation the system is currently running in a simple on/off configuration. It is assumed that with some form of slow Pulse Width Modulation (PWM) control on the on/off valve, or an exchange of the pump to one that can be controlled, it is possible to get accurate control of the power provided by the heater unit. This is not implemented in this work but rather simply assumed and thereby the variable P_{heater} can obtain a value between 0 and $25 \cdot 10^3$ corresponding to the power dissipation. This will in effect make the model of the heat dissipated by the water obsolete however it can be used in further developments as will be discussed in **Sec. 6.1** and **Sec. 6.2.1**. This approach to controlling P_{heater} has also caused an issue in that it disconnects the relationship between the power dissipation of the heater and the airflow which again will be further discussed in **Sec. 6.1**.

4.4 Arena model

With the HVAC model in place the attention is now shifted towards the area which the air is supplied to. The main goal here is to create a mathematical model that allows for the representation of the temperature of the air inside the room. This can again be done through the use of the energy balance equation shown in **Eq. 4.1**.

There are a few things that have to be considered in this case. Firstly when dealing with a room of this size (see **Sec. 3**) it has to be considered whether the supplied air is spread evenly throughout the room and further if this happens in a time frame that makes it possible to consider that effect negligible. Furthermore, naturally some loss of heat will be encountered and that amount is needed in order to better determine how much heat needs to be supplied to the room.

Firstly according to [Brath 1999] and their sources it is stated that in steady state the temperature difference in different parts of the room can vary between a few degrees. Furthermore it is stated that for fast temperature changes the temperature in different areas of a room will be almost identical in intervals between 1 and 20 minutes. This statement ensures that the air in the room can be considered to be mixed rapidly and also well mixed if it is ventilated. To see how quickly the room will be ventilated in this specific building one can consider standards such as DS 474 [DS n.d.] by Dansk Standard. Here it is stated that the flow of air in ventilated rooms should have a velocity of 0.1 m/s. Using this together with the width of the room w_{gf} it is determined that the air will be fully mixed within 3-10 minutes depending on how the air travels in the room.

The second topic that has to be addressed is the heat transfer between the air and the walls and roof of the building. This is included in the energy balance equation as a loss of energy. Due to this two energy balances are required. One for the transfer between the air and the wall/roof and one for the transfer between the wall/roof and the outside air.

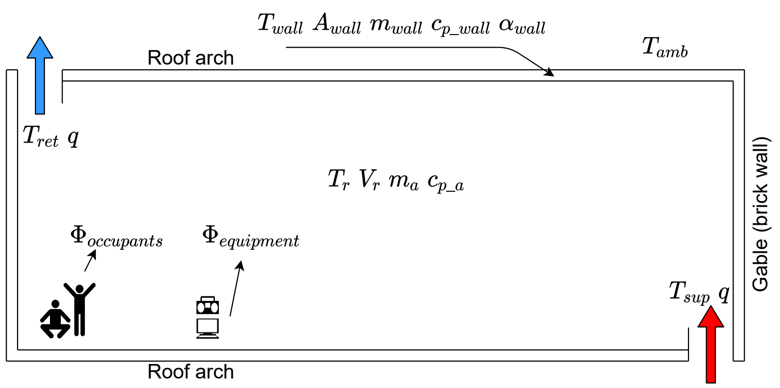

Figure 4.6: Model parameters for the room receiving the controlled air

On **Fig. 4.6** an overview of all parameters used in the model can be seen and the definition of all of these can be found in **Tab. 4.4**.

The energy balance equations are defined as in the previous section. Firstly the balance equation for the room which contains the heat transfer from the indoor air to the walls/roof and from the HVAC outlets to the indoor air. Here $C_r = V_r \cdot \rho_a \cdot c_{p\_a}$ is the heat capacity of the air in the room.

$$C_r \frac{dT_r}{dt} = (T_{sup} - T_r) \cdot q \cdot \rho_a \cdot c_{p\_a} + (T_{wall} - T_r) \cdot A_{wall} \cdot \alpha_{wall} + \Phi_t \tag{4.30}$$

secondly there is the energy balance equation for the wall. This contains the transfer from the indoor air to the wall and the transfer from the wall to the outdoor air. Here $C_{wall} = V_{wall} \cdot \rho_{wall} \cdot c_{p\_wall}$ is the heat capacity of the wall.

$$C_{wall} \cdot \frac{dT_{wall}}{dt} = (T_r - T_{wall}) \cdot A_{wall} \cdot \alpha_{wall} + (T_{wall} - T_{amb}) \cdot A_{wall} \cdot \alpha_{wall} \tag{4.31}$$

Including the definitions of C_r and C_{wall} into **Eq. 4.30** and **4.31** and rearranging the differential equations can be obtained.

$$\begin{aligned} C_r \frac{dT_r}{dt} &= (T_{sup} - T_r) \cdot q \cdot \rho_a \cdot c_{p\_a} + (T_{wall} - T_r) \cdot A_{wall} \cdot \alpha_{wall} + \Phi_t \\ V_r \cdot \rho_a \cdot c_{p\_a} \cdot \dot{T}_r &= (T_{sup} - T_r) \cdot q \cdot \rho_a \cdot c_{p\_a} + (T_{wall} - T_r) \cdot A_{wall} \cdot \alpha_{wall} + \Phi_t \\ \dot{T}_r &= (T_{sup} - T_r) \cdot \frac{q}{V_r} + (T_w - T_r) \cdot \frac{A_w \cdot \alpha_w}{C_r} + \frac{\Phi_t}{C_r} \end{aligned} \tag{4.32}$$

$$\begin{aligned} C_{wall} \frac{dT_{wall}}{dt} &= (T_r - T_{wall}) \cdot A_{wall} \cdot \alpha_{wall} + (T_{wall} - T_{amb}) \cdot A_{wall} \cdot \alpha_{wall} \\ V_{wall} \cdot \rho_{wall} \cdot c_{p\_w} \cdot \dot{T}_{wall} &= (T_r - T_{wall}) A_{wall} \cdot \alpha_{wall} + (T_{wall} - T_{amb}) \cdot A_{wall} \cdot \alpha_{wall} \\ \dot{T}_{wall} &= (T_r - T_{wall}) \cdot \frac{A_{wall} \cdot \alpha_{wall}}{C_{wall}} + (T_{wall} - T_{amb}) \frac{A_{wall} \cdot \alpha_{wall}}{C_{wall}} \end{aligned} \tag{4.33}$$

Considering the temperatures as states and the flow-rate of the supply air as the control input the differential equations can be put in state-space form as shown by **Eq. 4.34**

$$\begin{aligned} \begin{bmatrix} \dot{T}_r \\ \dot{T}_{wall} \end{bmatrix} &= \begin{bmatrix} -\frac{A_{wall} \cdot \alpha_{wall}}{C_r} & \frac{A_{wall} \cdot \alpha_{wall}}{C_r} \\ \frac{A_{wall} \cdot \alpha_{wall}}{C_{wall}} & \frac{A_{wall} \cdot (\alpha_{amb} - \alpha_{wall})}{C_{wall}} \end{bmatrix} \begin{bmatrix} T_r \\ T_{wall} \end{bmatrix} + \begin{bmatrix} \frac{T_{sup}}{V_r} \\ 0 \end{bmatrix} q \\ &\quad + \begin{bmatrix} -\frac{q}{V_r} \\ 0 \end{bmatrix} T_r + \begin{bmatrix} \frac{\Phi_t}{C_r} \\ -\frac{A_{wall} \cdot \alpha_{amb}}{C_{wall} \cdot T_{amb}} \end{bmatrix} \\ y = Cx &= \begin{bmatrix} 1 & 0 \end{bmatrix} \begin{bmatrix} T_r \\ T_{wall} \end{bmatrix} \end{aligned} \tag{4.34}$$

This state-space formulation deviates slightly from the standard simple formulation in that there is a non-linear term. The different terms are now defined as follows:

$$\begin{aligned} A_0 &= \begin{bmatrix} -\frac{A_{wall} \cdot \alpha_{wall}}{C_r} & \frac{A_{wall} \cdot \alpha_{wall}}{C_r} \\ \frac{A_{wall} \cdot \alpha_{wall}}{C_{wall}} & \frac{A_{wall} \cdot (\alpha_{amb} - \alpha_{wall})}{C_{wall}} \end{bmatrix}, \quad B = \begin{bmatrix} \frac{T_{sup}}{V_r} \\ 0 \end{bmatrix} \\ A_1(u) &= \begin{bmatrix} -\frac{q}{V_r} \\ 0 \end{bmatrix}, \quad C = \begin{bmatrix} 1 & 0 \end{bmatrix}, \quad w = \begin{bmatrix} \frac{\Phi_t}{C_r} \\ -\frac{A_{wall} \cdot \alpha_{amb}}{C_{wall} \cdot T_{amb}} \end{bmatrix} \end{aligned} \tag{4.35}$$

which allows the state-space form to be rewritten as follows:

$$\begin{aligned} \dot{x} &= A_0 x + Bu + A_1(u)x + w \\ y &= Cx \end{aligned} \tag{4.36}$$

As it has been stated previously, x corresponds to the state vector and u is the input vector. In this case there is also a noise/disturbance vector denoted as w.

4.4.1 Parameter estimation

Isolation and heat-loss

In order to find the heat loss of the building either an experiment has to be carried out or standard values have to be used at the risk of less accuracy. In this case it is chosen to go with the experimental approach due to the age of the building and as the managers of the building consider the insulation to be particularly bad. Therefore standard values could deviate a significant amount. The experiment that is carried out is described in detail in the appendix but it is rather simple and just makes use of temperature measurements inside and outside. Two events during the test period are used to validate the heat-loss estimation. Firstly a period where the HVAC system is turned off and secondly a period where the HVAC system is providing maximum heating to the building. Particularly the second period is interesting as it here can be seen that the HVAC system barely counteracts the heat-loss during night time (see **Fig. 4.7**). As it is known how much the heating system provides the heat-loss should be fairly close to this amount.

The overall heat transfer coefficient of a single layered wall (which the wall and roof has been simplified to in this case) and with equal area inside and outside can be estimated using **Eq. 4.37**

$$\frac{1}{U} = \frac{1}{h_{ci}} + \frac{s}{k} + \frac{1}{h_{co}} \tag{4.37}$$

Where U is the overall heat transfer coefficient, k is the thermal conductivity of the materials in the wall/roof, s is the thickness of the wall/roof and lastly h_{ci}/h_{co} is the convection heat transfer coefficient of the inside and outside of the wall/roof. In this case the wall and roof is combined into a single entity with the average properties of the two separate elements and will now be referred to simple as a wall. As the area of the roof is much greater than the area of the end wall this is taken into consideration resulting in the following parameters. The thermal conductivity of the wall is found to be $1.595[W/mK]$ using a thermal conductivity of wood at $1.5[W/mK]$ and for brick $2[W/mK]$. The thickness of the wall is determined to be roughly $0.3[m]$. The convective heat transfer coefficients Could be included in the calculation. These are found as the recommended ASHRAE equation, $h_{ci} = h_{co} = 5.7 + 3.8 \cdot v$ $[W/m^2K]$, where v is the velocity of the air. However, here it is apparent that since the convective coefficients are reciprocals then these values will become smaller as the wind speed increases and due to the constant element it will always be less than $\frac{1}{5.7} = 0.18$. Comparing this to the size of the middle term $\frac{s}{k} = \frac{0.3}{1.595} = 0.1888$ it is seen that the wind speed will have a significant effect on the overall result. The average wind speed across several months in Denmark is 4 m/s and this is used for this calculation. For the indoor air velocity a value of 0.1 m/s is used as the ventilation should be running on low or medium power most of the time and due to an assumption of lower velocities near the walls and roof.

Plugging the values into **Eq. 4.37** the overall heat transfer from the indoor air to the outdoor air is found.

$$\begin{aligned}\frac{1}{U} &= \frac{1}{5.7+3.8\cdot 0.1}+\frac{0.3}{1.595}+\frac{1}{5.7+3.8\cdot 4}=0.1644+0.1888+0.0479=0.4011\\ \rightarrow U &= \frac{1}{0.4011}=2.4931[W/m^2K]\end{aligned} \tag{4.38}$$

This heat transfer coefficient already considers the different properties of the roof and the wall and therefore the heat loss can now be found by simply multiplying the surface area of the combined roof and wall and the temperature difference.

During the test period where the heater was set at full power there was a few hours where the heat-loss was great enough to counter the heating provided. As it is known that the heater provides roughly 25.5$[kW]$ this means that the heat-loss is expected to have a similar value. At that time the indoor temperature was 17.4 degrees and the outdoor temperature was 4.2 degrees.

$$P_{hl}=2.4931\cdot 1687.3\cdot(17.4-4.2)=55527=55.5[kW] \tag{4.39}$$

This value is a factor of 2 off from the expected value which could be caused by the estimation of the wall conductivity as these values are rather uncertain as the exact level of insulation is unknown. Furthermore a second possibility is that, as is described in **Sec. 4.5**, the effects of the sun can influence the temperature and thereby effectively reduce the heat-loss at certain times.

Effects of occupants exercising

As people enter a room they will start to affect the air inside. This is both in terms of dissipated heat and evaporation from sweat and breathing. Furthermore parameters such as the CO2 content in the air is also affected, however this will not be taken into consideration in this work but could be considered a topic for further study. Furthermore due to time limitations it has not been possible to develop and implement a humidity model and this is therefore also not considered.

In order to determine the contribution of heating to the room from the people present in the building data obtained in [Alber-Wallerström and Holmér 2004] has been used. This study has measured the measured the evaporative heat transfer coefficient of the subjects and found an estimation of 99 W/m^2. The average surface area of skin on the human body is assumed to be 1.8 m^2, which leads to a heat transfer of 178 W to the environment per person. Considering a sceneario where every badminton court is used for a doubles match, that will mean 4 people per court. The building contains 6 courts resulting in 24 people exercising. Using the previously mentioned heat transfer per person the resulting heat generated by the people is 4128W. This is deemed a significant amount as the maximum capacity of the heater in the system is 25 kW.

Symbol	Value [unit]	Description
$T_{amb}(t)$	[°C]	Ambient outdoor air temperature
$T_{sup}(t)$	[°C]	Temperature of air supplied to the room
$T_r(t)$	[°C]	Temperature of the room
$T_{wall}(t)$	[°C]	Temperature of the wall/roof
$q(t)$	$[m^3/s]$	Flow rate of air supplied to the room
ρ_a	1.225 $[kg/m^3]$	Density of air
ρ_{wall}	1613.9 $[kg/m^3]$	Average density of wall and roof
c_{p_a}	1.006 $[kJ/kgK]$	Specific heat capacity of air
c_{p_wall}	38.671 $[kJ/kgK]$	Specific heat capacity of wall and roof
A_{wall}	1687.3 $[m^2]$	Surface area of wall and roof
V_r	7300 $[m^3]$	internal volume of zone 1
α_w	2.5 $[W/m^2K]$	Heat transfer coefficient
α_{amb}	2.5 $[W/m^2K]$	Heat transfer coefficient
m_a	8942.5 [kg]	Total mass of the air inside zone 1
$\Phi_{Occupants}$	178 $[W]$ (per person)	Heat dissipation per person during exercise

Table 4.4: Parameters used in the room model. Only constants are shown with values

4.5 Validation of models

In order to validate the models developed throughout this chapter, the models are implemented in a simulation and weighed against measurements done on the real system. First consider the tests performed on the real system. The temperature and relative humidity of the arena over the whole period can be seen in **Fig. A.2** where the unaltered data set is located. **Fig. 4.7** shows the same data set however in this case the start and stop times of the different tests performed have been indicated with grey vertical lines. The first period indicated in this plot is from time zero and lasted 1456 minutes or roughly 24 hours. The second period starts right after this point and lasts until 4138 minutes or roughly 44.5 hours. Due to a low amount of data loggers and sensors available at the time the data loggers in the arena and outside were then moved into the HVAC unit where a series of short tests were performed in order to obtain some information about the cross-flow recuperater. These tests lasted roughly thirty minutes and is easily recognized as the shortest period on the plot. The last period of the testing starts at 4200 minutes and continues to the end of the measurements which corresponds to roughly 49.5 hours. Tests 1, 2 and 4 were different step response experiments. In test 1 and 4 the HVAC system was completely turned off in order to see the heat loss of the arena. Test 2 was a step response where the effects of the heater on full power would be seen.

A few observations can be made already at this point. Firstly One thing that was not considered during the modelling phase was the impact of the heat added to the building based on the solar effects. Naturally as the surface area of the buildings roof is rather large this means that large amounts of energy from the sun will be absorbed into the building materials. This is further amplified by the color of the roof which is a dark green which likely does not reflect large amounts of the incoming light. On top of this the poor insulation of the building means that the extra heating obtained from the sun easily can affect the indoor temperature which like are the bumps seen all over the indoor temperature

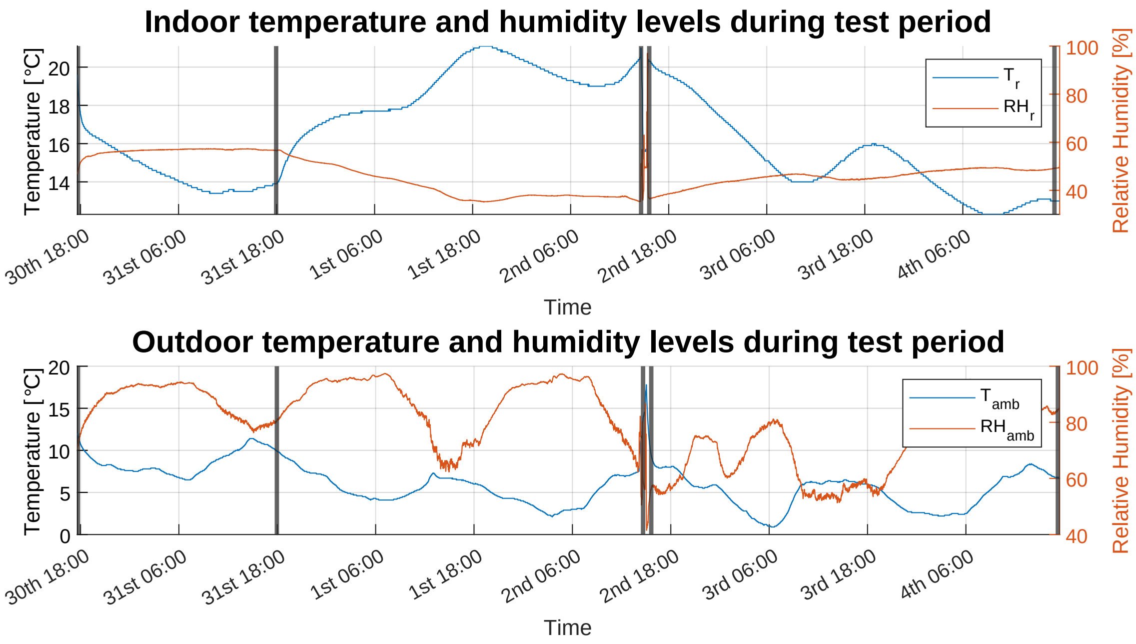

Figure 4.7: Temperature and humidity over the full test period with indicators of start and stop times. Test period is between the March 30th and April 4th.

graph in **Fig. 4.7**. This can also be seen in **Fig. A.7** where the system had been off for roughly two weeks before the start of the measurements, caused by a fault in the system. Considering the times at which the outdoor temperature rises and falls, the bumps in the indoor temperature do not fully match up. However, the building materials will work as capacitor (using an electrical analogy) in the sense that the temperature of the material will slowly increase as the sun heats it up. This heat will still be present when the sun goes down and will slowly decrease as it is slowly dissipated to the environment, both inside and outside the building. As with the capacitor analogy this effect will introduce some phase shift to the heating added by the sun and ambient temperature which will explain why the bumps in the indoor temperature appear to be offset. The effects of the sun could be considered in the model. However, in the interest of limiting model complexity further this effect is neglected for now but should be considered for further studies and work. Specially in buildings such as this one where the insulation can be poor.

Second interesting observation made from **Fig. 4.7** is that at 06:00, 1st of April, it is seen that the indoor temperature appears to level out during the period where the heater is set to provide 25kW. This is interesting as this would indicate the heat-loss being of a value close to that same amount, 25kW at this temperature difference. This is not necessarily the correct value as the the effects of the sun as described by the previous paragraph could have had some influence on the temperature leveling out. Therefore it is likely better to investigate the slope of the temperature as it is decreasing during the tests where the HVAC is off.

Last observation to make from **Fig. 4.7** is that the indoor relative humidity appears to not be influenced much by the outdoor relative humidity but simply by heating of the HVAC system. As seen on the figure, as the heater is turned on the humidity starts to drop until it reaches 40% after which the relative humidity stays rather steady. An argument could be made that a small dip in the RH can be seen at 18:00, 1st of April, which corresponds with a dip in the outdoor RH and that a small increase can be seen as the outdoor RH increases again. This same behaviour can also be observed during the last test period where the indoor RH increases over time but levels out during the day time where the outdoor RH is low. However, all of these small changes in indoor RH also correspond to the times where the bumps in temperature, from the effects of the sun, occur and therefore this is likely a better candidate for the small indoor RH variations at is already seen how much of an impact the temperature has.

For the simulations the nonlinear differential equations have been implemented and used. When the step response where the HVAC system is turned on was performed it was done with the heater giving an output of 25 kW and the ventilation was set to a value of 6 which corresponds to a flow of 0.73 m^3/s and therefore the simulations are also done under these conditions. Furthermore since the outdoor temperature and humidity was captured during this period this can also be used as inputs to the models such that similar conditions will apply.

Cross-flow recuperator

Starting off by investigating the behaviour of the cross-flow recuperater the plots of the temperatures en each of the air streams can be seen in **Fig. 4.8**, where T_{amb} is the ambient air going into the system, T_{cfs} is the heated ambient air that is sent to the main heater, T_{ret} is the warm air returning from the room and finally T_{exh} is the exhaust air after the recuperator. Here it can be seen how some of the heat is being extracted from the return air and transferred to the incoming ambient air before the return air is exhausted. Even though the indoor air temperature at the time of the test was roughly 20 degrees it is here seen that the actual measured temperature of the return air inside of the recuperator is 4-5 degrees lower. This is likely caused by some amount of heat-loss occouring when the air is going from the arena room, through the ventilation ducts and into the unit where the recuperator is found. Furthermore there is some uncertainty in terms of the accuracy of this measurement as things such as the aluminium surface on which the logger was placed could affect the measurement and furthermore the fact that a large volume of air is passing by the sensor could assist in cooling it further than the actual temperature of the air. The same uncertainties apply to the ambient temperature measurements as the outdoor temperature just before the experiment was measured to be 7.5 degrees. However as the inlet air reaches the recuperator some amount of energy has already been picked up as the temperature here is measured to be 11-12 degrees. Due to these uncertainties the actual temperature is not well known but these values obtained here are deemed to be sufficient enough to proceed. The simulation makes use of roughly the same temperatures for T_{amb} and T_{ret} as those seen in **Fig. 4.8**, the minor corrections are due to the measured temperatures not being in a complete steady state. The models used for the simulation initially assumed ideal conditions however, it has been noted that from the manufacturer of the HVAC system it is stated that the efficiency of the recuperator is roughly 70%. Therefore an additional simulation is carried out where this efficiency correction is applied to the model. The response of the model with the uncorrected efficiency can be seen in

Fig. 4.9 whereas the response of the model with the correction is seen in **Fig. 4.10**.

Temperatures	T_{amb}	T_{ret}	T_{cfs}	T_{exh}
Measured	11.5	15.75	16	14.5
Simulated ideal case	11	16	16	11
Simulated with efficiency correction	11	16	14.25	12

Table 4.5: Measured and simulated temperatures in the cross-flow recuperator

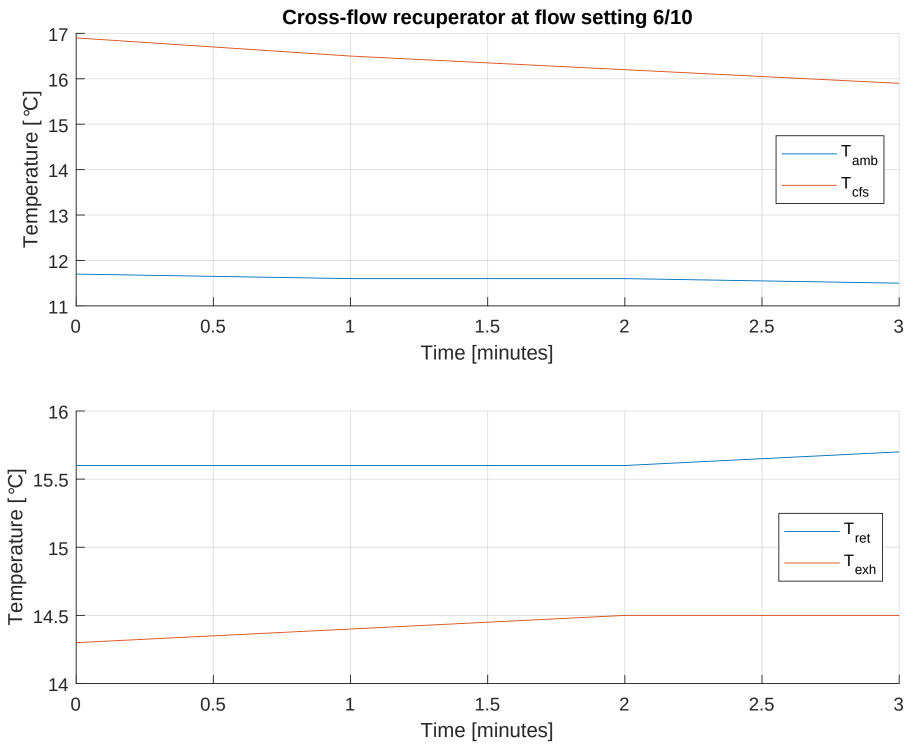

Figure 4.8: Temperatures on all sides of the cross-flow recuperator at a flow rate of 0.73 m^3/s and ambient temperatures of 7.5 degrees based on measurements shown in 4.7

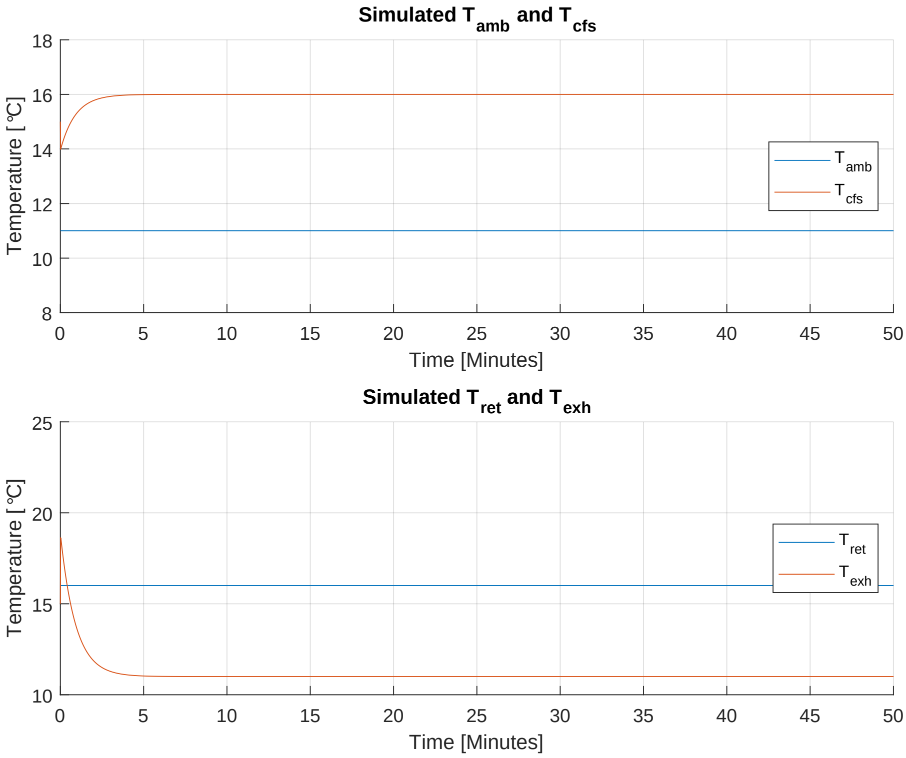

Figure 4.9: Simulated temperatures on all sides of the cross-flow recuperator under the same conditions as **Fig. 4.8**

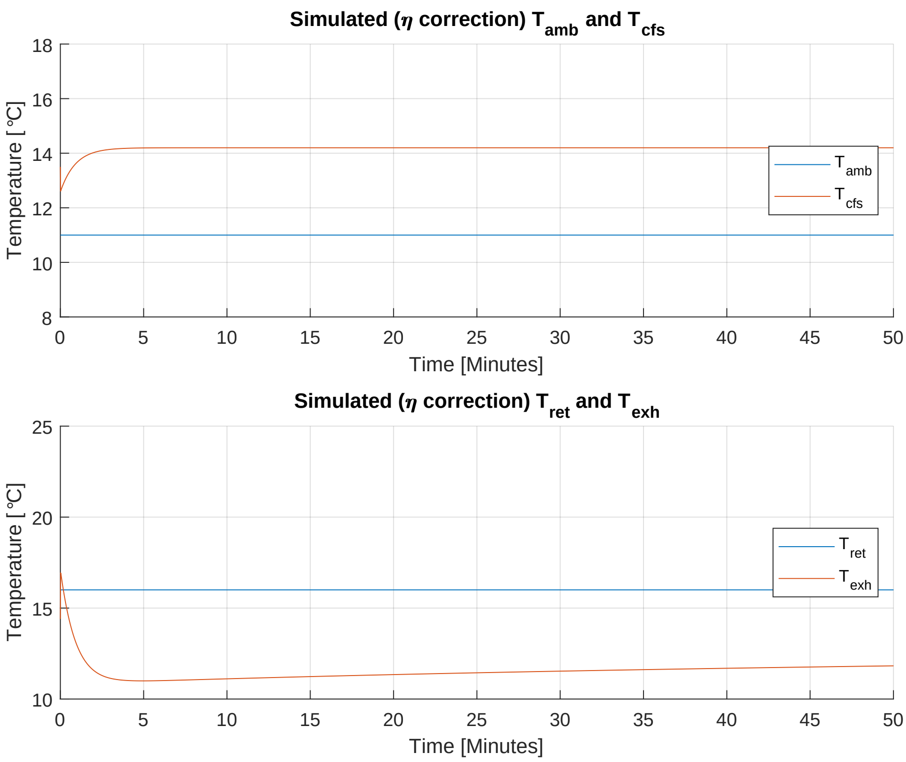

Figure 4.10: Simulated temperatures on all sides of the cross-flow recuperator under the same conditions as **Fig. 4.8** this time with an efficiency correction applied

Comparing the measurements of the temperatures in the cross-flow recuperator to the results of the simulation that consideres the efficiency of the unit, it can be seen that they do not exactly converge to the same point. However, note that T_{cfs} actually is higher than T_{ret} in the case of the measured values. As stated previously there are quite a few uncertainties to the quality of the measurements. If it is assumed that T_{ret} has a temperature closer to the measured indoor temperature just before the test, which was roughly 20 degrees, rather than the 15.75 degrees observed, the temperature of both T_{cfs} and T_{exh} will increase. As the temperature of T_{cfs} cant go above the temperature of the fluid which it is exchanging heat with T_{ret} there has to either be some external heating effect or the measured value of T_{ret} is lower than the actual value. There could be some external heat coming from the room in which the HVAC system is located however, it is deemed that this should not have a big enough effect to skew the T_{cfs} measurement this much. Instead the theory of a bad measurement of T_{ret} (caused by a collection of uncertainties as mentioned previously) is assumed to be correct such that the actual value is higher. This would cause both T_{cfs} and T_{exh} to increase in temperature and at the same time if a higher T_{ret} is applied to the simulation those values will likewise increase in the simulation. Under this assumption the model of the cross-flow recuperator can be validated.

Heater

In the case of the heater there was not enough equipment available to place a data logger and therefore the temperature of the air on the output was manually noted in intervals of one minute. Furthermore the power output of the unit was noted following a digital meter in the room with the HVAC. Lastly during the modeling of the heater a step response of the transfer function was found. Comparing these will allow for the validation of the model. Figures **Fig. 4.11a** and **Fig. 4.11b** show the manually noted temperature and power of the heater unit. By looking at the transfer function based step response of the model seen in **Fig. 4.12** it can be seen that the overall shape of the graph is the same. However there is a great difference in terms of the time constant of the two. The developed model has a very short time constant of $0.088s$ whereas it is on the scale of minutes concerning the measurements. A quick response is to be expected based on the area, materials, flow rate, heat capacity of air, etc. and the cause of the slow response of the real system is to be found in **Fig. 4.11b** where it can be seen that the effect supplied by the heater unit simply does not instantly rise to the desired amount but instead slowly increases. Considering the timescale that is to be expected when it comes to temperature changes in the arena this is not an issue however it can still be included in the simulation as a ramp applied to P_{heater}, but as this will have a quite small impact on the overall heat added to the system, the ramping is neglected.

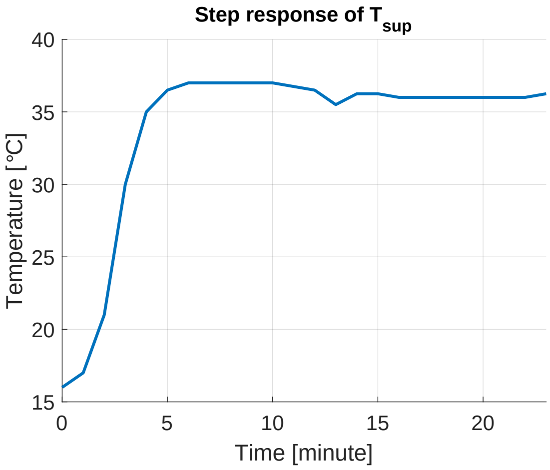

(a) Step response of measured output temperature in heater unit

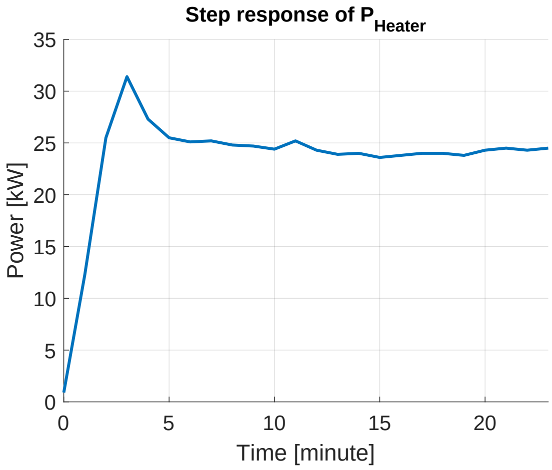

(b) Step response considering the power of the heater

Figure 4.11: Measured step responses of heater

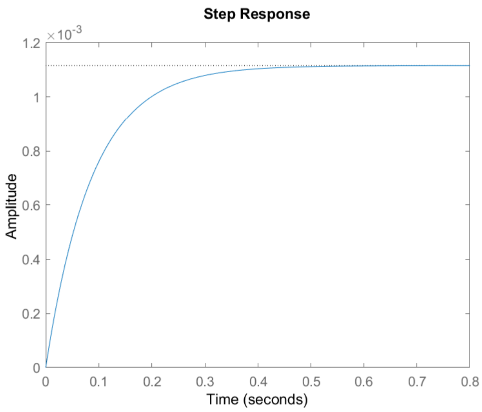

Figure 4.12: Step response based on developed heater model

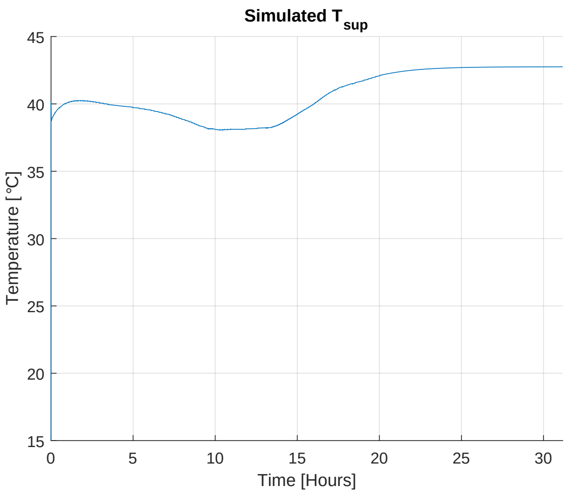

Figure 4.13: Simulated T_{sup} over a longer duration

During the experiment where the HVAC system was turned on at full power the output temperature of the heater unit was noted at various times of the day and it was noted that it stayed between 35 and 37 degrees. Looking at the simulated behaviour of the heater unit over a longer period, which can be seen in **Fig. 4.13**, it can be seen that the output temperature varies with roughly 5 degrees over a 30 hour period and in general appears to have an output that in general is about 5 degrees higher than the actual measured values. This deviation from the measured values is considered close enough to be of further use in this work without having to change elements in the model.

Arena

Finally considering the model of the main arena room. Again the bi-linear models developed in earlier sections have been used to simulate the system and are compared with the measured temperatures. **Fig. 4.14** shows the measured in- and outdoor temperatures together with the simulated indoor temperature which was based on the models and the measured outdoor temperature. Based on a quick glance the results shown on this figure are not that inspiring. However, it should be noted that the dynamics appear to be captured somewhat well when considering one effect that is not present in the model, which is the influence of the sun on the indoor temperature. As previously mentioned based on the measurements of the temperature done during the times where the HVAC system has been off, the sun appears to have a large effect on the temperature. This is likely due to the large surface area of the roof combined with the poor insulation. As an example take the first 15 hours of **Fig. 4.14**. This test was started at roughly 6 pm on a sunny day. As it has been mentioned previously the walls and roof of the building will have some capacitive effect on the temperature as the suns energy will be stored in the walls and roof as a temperature increase in the materials which then over time will be given off to the indoor and outdoor environments. This is effective visualized in this first period of the measurements where the temperature is leveling out. This could be caused by the heating unit providing just enough heat to keep the temperature leveled while the outdoor temperature is low but now consider the period between 19:00, April 1st, and 10:00, April 2nd, where it is seen that both the simulated and the measured temperatures fall. It appears that the simulated temperature drops faster than the measured, however the difference between the two is not enough to make up the same behaviour between 18:00, March 31st, and 09:00 April 1st. Other than the effects of the heating from the sun it appears that that model behaves as expected in terms of capturing the dynamics. The model is very reliable upon the ambient temperature as it can be seen that the simulated temperature follows the changes of the ambient temperature quite well, which again is due to poor insulation. With better insulation the heat transfer coefficient will be reduced whereby a smaller loss of heat will occour at the same temperature differences.

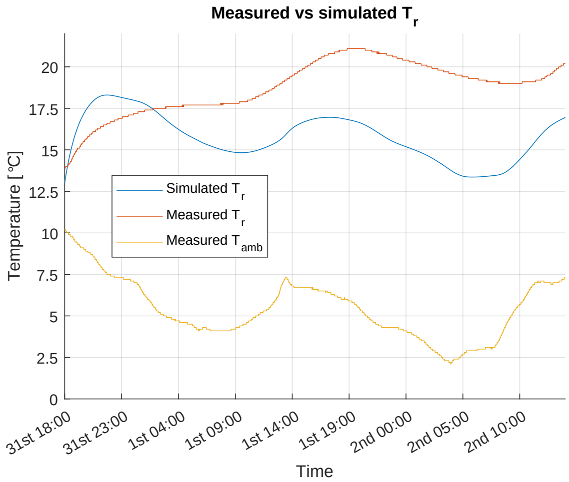

Figure 4.14: Comparison between measured and simulated room temperature together with the ambient temperature. Simulated period is between March 31st and April 2nd.

In order to improve the model the inclusion of the effects of the sun will be of great benefit. However, in the interest of avoiding too complex of a model this effect is disregarded for the moment and will be considered regarded further work and studies. Even though there is a large error of up to 5 degrees between the modelled temperature and measured temperatures this is mainly assumed to be due to the sun and therefore the current model is acceptable for further work.

5 Controller

With the system models finished a suitable controller can now be found to obtain the desired behaviour of the system that will satisfy the requirements set by the application and problem statement. This chapter will first discuss what controller that should be used and why, followed by a detailed description of how said controller works. With the theory in place the design process of the controller can begin and finally the performance of the controller when applied to the system is explored.

5.1 Choice of controller type

With the model in place the type of controller that is to be used needs to be decided. There are numerous types of controllers available and in order to choose the right type some considerations should be taken into account. First and most importantly, the controller has to be capable of providing features to solve the problem that has been outlined in the problem formulation **Sec. 2.7**. Restating the problem formulation for convenience:

How can one develop a controller that considers a multitude of factors such as activity patterns, humidity, seasonal changes etc. while keeping the same comfort levels and reducing the energy consumption, be designed and retrofitted into an aging commercial building?

From this the it is noted that the controller has to be able to account for future environmental situations that will impact the system and at the same time attempt to reach the optimal performance when it comes to the energy consumption of the system. Secondly the computational power of the platform the controller is to be implemented on has to be considered. If too much computation is required the sample rate is unable to be kept and undesireable behaviour will be seen. If there is not enough computation power available it is possible to simplify the models, however this will come at a cost of performance and can risk losing important dynamics. Lastly it has to be considered whether the controller type will work with the type of system models that have been developed. Controllers that are designed for linear systems will not work or perform very poorly on highly non-linear systems. This issue can of course be alleviated through linearization of the non-linear models however, this again comes at the cost of performance as the system deviates from the operating point. If the system is expected experience large variations in operating conditions several linearizations at different conditions can be carried out.

For this case study the models are non-linear and linearization is required. The performance of the linearized models will have to be investigated in order to ensure that they describe the system behaviour to an adequate degree. As the controller has to account for future developments in states, references and inputs, a Model Predictive Controller (MPC) is a rather obvious suggestion for a controller type. Unlike many other controller types, the MPC works through an online optimization strategy to find the best future control inputs based on current and a future predictions. The downsides of MPC is the computational power required in order to do these online predictions. As stated in the problem analysis **Ch. 2** the system would be connected to the internet such that weather data (if no outdoor sensors are present) and a schedule can be collected, or simply collected in some other way. If this is the case the unit running the control system will likely not be a dedicated MCU but a more versatile unit such as a small computer or some other embedded unit capable of these features. This together with the rapid increase of computational power in computers as well as MCU's give reason to believe that with the most significant dynamics in this system being slow, the computing capabilities will be a small, if not, non-existing issue. Due to these reasons MPC is chosen as a good candidate for a controller that can solve the goal of this work.

5.2 Model predictive control

With the choice of MPC as the controller for the system some of the theory behind the controller is to be explored before the design process can take place.

5.2.1 Theory

The main idea behind MPC is to minimize some cost function, also sometimes called an objective function. This idea is also used in controllers such as the Linear Quadratic Regulator (LQR). In the LQR, the cost function is used to determine how much effort should be put into ensuring the reference states are kept by the system while at the same time also considering the actuator effort it requires to reach this point. This is similar to the way MPC handles the cost function, however MPC also has some additional features. The first major feature MPC adds is the capability of predicting an estimate of future states as has been mentioned in previous sections. With the LQR a single optimal cost is computed and used while the MPC updates and finds the optimal value of the cost function at every iteration while at the same time also predicting an estimation of the optimal costs at future iterations, thereby allowing for the prediction of what control signal to apply in future steps to reach the target in the most optimal way in the long term. Even though several future optimal control signals can and will be calculated only the one for the next timestep is applied to the actual system and the rest is merely used in the online simulations of future behaviour of the system. This is then iterated through again when the next control signal is needed and corrections are made to the control signal that is to be applied based on the new measured states. **Fig. 5.1** can be used as a reference for the topics discussed in this section, note that this figure is simply an illustration of the behaviour and not an example of an actual controller that has been designed. As suggested by the previous paragraph there are two predictions performed by the controller.

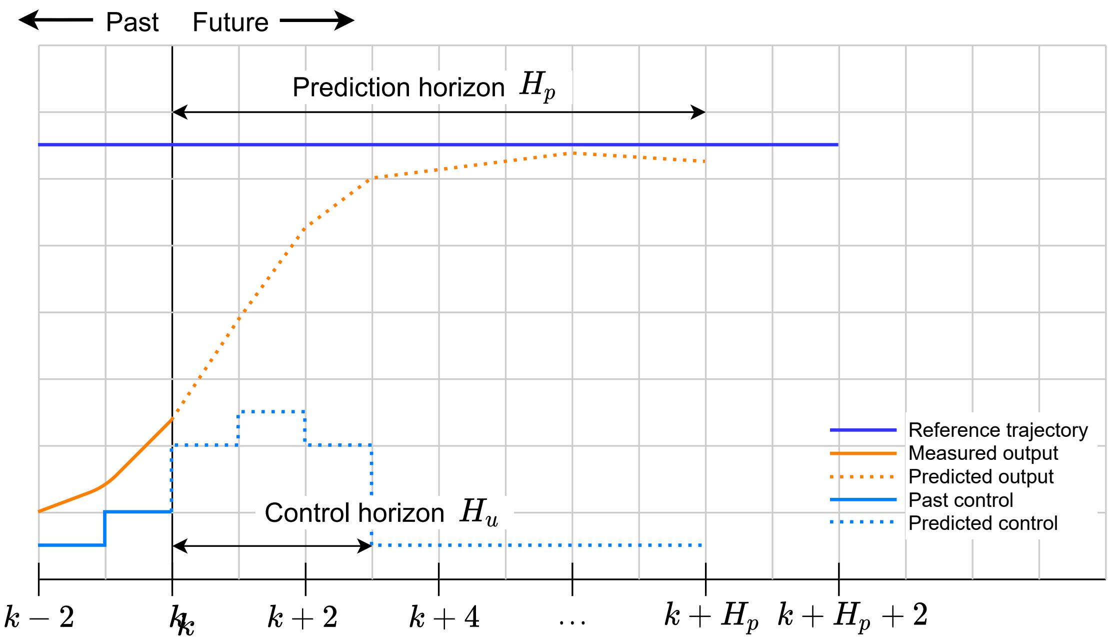

Figure 5.1

Firstly the MPC considers the current state of the system and the reference trajectory. It then tries to find an optimal solution to the control signals that will take the system closer to the reference trajectory. These control signals will be found as a sequence of inputs applied at future steps, where the sequence will have a length referred to as the control horizon H_u. These controls are applied to the linear model, resulting in an online simulation from which the state developments are found for future steps based on the optimal control sequence. The amount future time steps for which the state developments are predicted is referred to as the prediction horizon H_p. The length of H_u will always be less than or equivalent to the length of H_p. Once the prediction stage is complete the controller applies the first set of control signals in the sequence to the real system and the process repeats at the next time step. Naturally the heavy computational load of the MPC comes from finding the optimal control signals and performing online simulation. As a consequence amount of computation required can be adjusted by either increasing or lowering H_p and H_u.

Longer prediction and control horizons do not only give a negative impact on the system. With a longer horizons the online simulations performed by the controller will give further insight into the developments of the states and thereby it will be possible to obtain better predictions of the optimal control signals to apply to the system. Therefore longer extending the horizons can be beneficial if there is computational power available and increased accuracy is required. However, it has to be noted that the state predictions are dependent on the accuracy of the linearized system models. Meaning that extending the prediction horizon does not necessarily provide the system with any useful information if the models are of poor quality and in the worst case can cause predictions that can be misleading. As it is only the first control signal in the list of predicted optimal control signals that is applied to the system, bad state predictions far in the future will normally

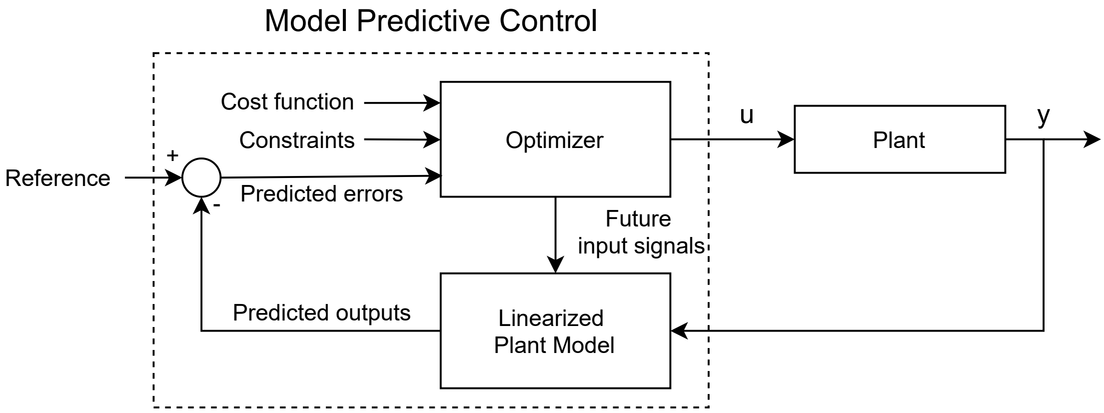

Figure 5.2: Block diagram of model predictive control

be corrected as time progresses however, it can cause worse performance of the controller if much weight is put on the bad state predictions.

Another feature of MPC is that it is possible to put limits on states and control signals which will be considered during the optimization process. There are two types of constraints available, soft constraints and hard constraints. Starting off with the hard constraints, these have to be complied with and can be used when some signal is not allowed to be exceeded in the case of a state or there is some limit to what size the control input can be. An example of a control signal that could have a hard constraint is the control signal sent to the fan motors of the system used in this case study. Here it is known that the fans can supply a maximum airflow of $1.05m^3/s$, equivalent to a value of 10 on the user input panel. This can be implemented as a hard constraint such that the MPC does not find an optimal strategy that requires an airflow of $1.2m^3/s$ for example. Similarly lower bounds can be put on the signal values. Hard constraints can also be present on the state values. For example say that the temperature in the arena is not allowed to go below 10 °C, this can be implemented as another constraint. Soft constraints are constraints that should not be exceeded, however, if it is required they can temporarily be exceeded but an extra cost will be applied. Using the same example as before with the minimum allowed temperature of the arena. Say that the indoor temperature has a hard constraint of at least 10 °C, furthermore based on the recommendations of comfortable temperature ranges shown in **Sec. 2.6**, a soft constraint can be set such that the temperature preferably would stay above 16 °C in order to reduce the risk of damage caused by moisture to the construction materials. This would be done by creating a constraint as usual but also adding and subtracting a slack variable ϵ to maximum and minimum values that represent the preferred area of operation. The slack variable then represents the size of the associated constraint violation. With the basic structure of the MPC in place the optimization algorithm is explored. the MPC algorithm takes the current states $x(k)$ as the input to the optimizer. Assuming that the prediction horizon and control horizon is of same length the algorithm can be seen as presented in **Alg. 1**. As with the LQR both the state error and actuator usage contribute to the overall cost for a given strategy. The cost of a given state error $cost_e(k+1)$ is described as the error between the states and the reference $r(k)$ normalized with some cost matrix Q. This is shown mathematically as

Algorithm 1: Model Predictive Control

initialization: x(k) = x(0);
for $k = 0 : H_p - 1$ **do**
  $x(k+1) = Ax(k) + Bu(k)$;
  $\vdots$
  $cost = cost + cost_e(k+1) + cost_u(k)$;
end

$cost_e(k+1) = ||r(k) - x(k)||^2_{Q(k)}$. A familiar structure is used for the case of the actuator usage $cost_u(k) = ||U(k)||^2_{R(k)}$ as shown in [Maciejowski 2002].

An example of the minimization problem can be shown as follows based on previous paragraphs.

$$\begin{aligned} \min_u \quad & cost \\ & \text{s.t.} \\ & \quad x(k+1) = Ax(k) + Bu(k) \\ & \quad x_{min} - \epsilon \leq x \leq x_{max} + \epsilon \\ & \quad u_{min} \leq u \leq u_{max} \\ & \quad \epsilon \geq 0 \end{aligned} \tag{5.1}$$

Where ϵ is a slack parameter which is used in conjunction with soft constraints in order to provide the extra penalty if the boundaries are exceeded. The extra penalty is defined as $cost = cost + w_\epsilon \cdot ||\epsilon||_2^2$ where w_ϵ is a constant value predetermined to tune the scale of how much extra cost is added.

The theory behind the MPC which has been mentioned in this section relies on the models used to be linear. As a result in order to use these techniques the models have to be linearized but in cases where the properties can vary a lot, a single operating point is not sufficient for good performance. Therefore other variations of the basic MPC can be used. There are the Gain Scheduled MPC and Non-linear MPC. Considering the bi-linearity of the models developed for this case study, gain scheduled MPC is a good candidate as a controller and is therefore further investigated.

Gain scheduled MPC

Gain scheduled MPC is applicable to non-linear systems through linearizing the models at a series of operating points. When in use this type of controller selects what linearized model to use based on the previous control signals that have been used. This will ensure that the model in use will correspond to conditions close to the current ones. In order for the gain scheduled MPC to perform well the bank of linearized models naturally have to be made up through operating points that cover the whole area in which the system is expected to operate. Furthermore, As there is no limit on the amount of linearized models other than the amount of memory available in the system, naturally the higher amount of linear models the better. One downside to this technique is when transitions between models happen as these often are not smooth in behaviour. One way to alleviate this issue is through bumpless transfer between the models which can be implemented through interpolation between the linearized models.

5.2.2 Implementation

Linearization and combination of system models

Before the main parts of the controller is designed the system first has to be put on a form compatible with the MPC. This means combining the subsystem models into a single complete model and furthermore linearizing the complete model.

The A and B matrices are made as a combination of the subsystem models by taking the full state and input vectors and taking the jacobian of the differential equations. As an example take entry a_{11} defined as $a_{11} = \frac{\partial \dot{T}_{exh}}{\partial T_{exh}}$.

Resulting in a state and control input vectors as seen in **Eq. 5.2**, where x_{cfh}, x_H and x_{room} are the state vectors from the cross-flow recuperator, heater and room models respectively. Furthermore small changes are made to the input vector as the ambient temperature T_{amb} and return air temperature T_{ret} are included explicitly as input parameters.

$$x = \begin{bmatrix} x_{cfh} & x_H & x_{room} \end{bmatrix}^T = \begin{bmatrix} T_{exh} & T_{div} & T_{cfs} & T_{sup} & T_r & T_{wall} \end{bmatrix}^T \tag{5.2}$$

$$u = \begin{bmatrix} q & P_{Heater} & T_{amb} & T_{ret} \end{bmatrix}^T \tag{5.3}$$

Writing out the full combined matrices results in **Eq. 5.4** where each of the entries can be seen in **Tab. 5.1**

$$\begin{aligned} A(u) &= \begin{bmatrix} a_{11} & a_{12} & 0 & 0 & 0 & 0 \\ a_{21} & 0 & a_{23} & 0 & 0 & 0 \\ 0 & a_{32} & a_{33} & 0 & 0 & 0 \\ 0 & 0 & a_{43} & a_{44} & 0 & 0 \\ 0 & 0 & 0 & a_{54} & a_{55} & a_{56} \\ 0 & 0 & 0 & 0 & a_{65} & a_{66} \end{bmatrix}, \quad B = \begin{bmatrix} b_{11} & 0 & 0 & b_{14} \\ 0 & 0 & b_{23} & b_{24} \\ b_{31} & 0 & b_{33} & 0 \\ b_{41} & b_{42} & 0 & 0 \\ b_{51} & 0 & 0 & 0 \\ 0 & 0 & b_{63} & 0 \end{bmatrix} \\ C &= \begin{bmatrix} 0 & 0 & 0 & 0 & 1 & 0 \end{bmatrix}, \quad D = 0 \end{aligned} \tag{5.4}$$

With the combined model in place the controllability and observability of the combined system is checked, as these aspects can change after the subsystems are combined. The check is done by investigating the rank of $\mathcal{C}$ and $\mathcal{O}$, where full rank means controllability and or observability. The $\mathcal{C}$ and $\mathcal{O}$ matrices are found as shown in **Eq. 5.5**. which has proven that the system is both controllable and observable.

$$\mathcal{C} = \text{rank}\left(\begin{bmatrix} B & AB & \dots & A^{n-1}B \end{bmatrix}\right) = 6 \tag{5.5}$$

$$\mathcal{O} = \text{rank}\left(\begin{bmatrix} C & CA & \dots & CA^{n-1} \end{bmatrix}^T\right) = 6 \tag{5.6}$$

a_{11}	$\frac{A_{div} \cdot \alpha_{div}}{2 \cdot V_{pHeater} \cdot c_{p\_a} \cdot \rho_a} - \frac{q}{V_{pHeater}}$	b_{11}	$-\frac{T_{exh} - T_{ret}}{V_{pHeater}}$
a_{12}	$-\frac{A_{div} \cdot \alpha_{div}}{V_{pHeater} \cdot c_{p\_a} \cdot \rho_a}$	b_{14}	$\frac{q}{V_{pHeater}} + \frac{A_{div} \cdot \alpha_{div}}{2 \cdot V_{pHeater} \cdot c_{p\_a} \cdot \rho_a}$
a_{21}	$\frac{A_{div} \cdot \alpha_{div}}{2 \cdot V_{div} \cdot c_{p\_div} \cdot \rho_{div}}$	b_{23}	$-\frac{A_{div} \cdot \alpha_{div}}{2 \cdot V_{pHeater} \cdot c_{p\_a} \cdot \rho_a}$
a_{23}	$\frac{A_{div} \cdot \alpha_{div}}{2 \cdot V_{div} \cdot c_{p\_div} \cdot \rho_{div}}$	b_{24}	$\frac{A_{div} \cdot \alpha_{div}}{2 \cdot V_{div} \dot{c}_{p\_div} \cdot \rho_{div}}$
a_{32}	$\frac{A_{div} \cdot \alpha_{div}}{V_{pHeater} \cdot c_{p\_a} \cdot \rho_a}$	b_{31}	$\frac{T_{amb} - T_{cfs}}{V_{pHeater}}$
a_{33}	$\frac{A_{div} \cdot \alpha_{div}}{2 \cdot V_{pHeater} \cdot c_{p\_a} \cdot \rho_a}$	b_{33}	$\frac{q}{V_{pHeater}} - \frac{A_{div} \cdot \alpha_{div}}{2 \cdot V_{pHeater} \cdot c_{p\_a} \cdot \rho_a}$
a_{43}	$-\frac{q}{V_{Heater}}$	b_{41}	$\frac{T_{cfs} - T_{sup}}{V_{Heater}}$
a_{44}	$\frac{q}{V_{Heater}}$	b_{42}	$\frac{1}{C_H}$
a_{54}	$\frac{q}{V_r}$	b_{51}	$\frac{T_{sup} - T_r}{V_r}$
a_{55}	$-\frac{q}{V_r} - \frac{A_{wall} \cdot \alpha_{wall}}{V_r \cdot c_{p\_a} \cdot \rho_a}$	b_{63}	$\frac{A_{wall} \cdot \alpha_{wall}}{C_w}$
a_{56}	$\frac{A_{wall} \cdot \alpha_{wall}}{V_r \cdot c_{p\_a} \cdot \rho_a}$		
a_{65}	$\frac{A_{wall} \cdot \alpha_{wall}}{V_{wall} \cdot c_{p\_w} \cdot \rho_{wall}}$		
a_{66}	$-\frac{2 \cdot A_{wall} \cdot \alpha_{wall}}{C_w}$		

Table 5.1: Combined matrix entries

Linearizing the combined model is done through inserting operating points into the obtained A and B matrices as the jacobian has already been used to find the combined matrix and therefore the two operations have been combined into one. As the controller to be designed is intended to be a gain scheduled MPC, several different linearized system models are defined. The operating points used for linearization can be seen in **Tab. 5.2**.

Linear model #	$q[m^3/s]$	T_{exh}[°C]	T_{ret}[°C]	T_{cfs}[°C]	T_{sup}[°C]	T_r[°C]	T_{amb}[°C]
1	0.45	15	18	15	35	18	10
2	0.45	15	18	15	35	18	5
3	0.45	15	18	15	35	18	0

Table 5.2: Operating points used for linearization

Discretization

Discretization of the system is done through zero-order-hold where the inputs to the system are kept constant between samples. The sample time used for the controller is 1800 s equivalent to 30 minutes. As the dynamics of this system are rather slow this is found to be sufficient. Previously it has been described how the MPC can have a heavy computational load. With a sample time of this length there is no risk of skipping samples and further small delays before a control signal is applied will have no noticable effect. If this controller is deployed on a dedicated unit it will still be important to measure the computation time to ensure that it wont cause any issues.

5.2.3 Controller tuning

With the theory and preparations done for the MPC, the next step is to tune the controller to ensure good performance. When tuning is complete the final performance of the controller is shown by applying it and the model to a months worth of temperature data.

This is described further in **Sec. 5.3**. However, in order to avoid tuning the controller to that specific sequence of temperatures a different data set is used. For convenience the outdoor temperatures measured during some of the experiments is used. The outdoor temperature is referred to as T_{amb} in the figures.

Firstly a single MPC is developed to ensure no errors in the implementation are present. Furthermore this allows for comparing the performance of a single MPC against a gain scheduled MPC.

For this work the MPC is developed using the features and functions present in the MATLAB Model Predictive Control toolbox [MATLAB 2021]. This takes care of the overall structure of the MPC such that time is not spent on that aspect, while the tuning of the controller is done by hand.

Prediction and control horizon

When it comes to the MPC parameters the first parameter to be selected is the prediction (H_p) and control (H_u) horizons. A common rule of thumb is to have a prediction horizon with a length of 20-30 steps that covers the governing dynamics of the system. In this case it has been found that a prediction horizon of 20 steps provides decent behaviour, which corresponds to simulating 10 hours ahead of the current time with a sample time of $ts = 1800s$. A second rule of thumb is to have the length of the control horizon be 20-30% of the prediction horizon. In this case $H_u = 5$ has been found to work well.

minimization problem and cost function

The cost function used for the controllers takes the form that is seen in **Eq. 5.7**. It consists of three parts, the reference tracking error, the power usage based on control signals and extra cost added by exceeding the soft constraints. First considering the control signal costs. The way these are implemented in the MATLAB MPC designer is directly through the control signals, which in this case is the flow rate and the power dissipated by the heater element. The way P_{heater} has been modelled has later been discovered to be faulty (see **Sec. 6.1** for further details) which has caused a disconnect between the heater dissipation and the flowrate of air, thereby elimination the non linearity of this part. Therefore the heater control signal can be implemented directly in this case. In the case of the fan, the power consumption is highly nonlinear as the relation between the RPM of the fan and the consumption generally can be described as a third order function. Due to the faulty modelling of the heater power it is observed that the fans are used very little by the MPC (even with usage of very small costs attached to the consumption of the fans) and furthermore the maximum amount of energy consumed by the fans is around $1500[W]$ which is significantly lower than the heater power dissipation. Due to these reasons a simple linear cost for the fan is found. Both the W_{fan} and W_{heater} is implemented by assigning a scaling parameter to the control signal that will mimic the consumption. In the case of P_{heater} a direct correlation is present, resulting in $W_{heater} = P_{heater}$ at any given sample. The consumption of the fan is scaled by a factor of 1000 which when applied to the flowrate will give a linear approximation of the power consumed. Naturally this will not be a great approximation due to the order of the relation between the RPM and power consumption but it has been found that no significant change in the behaviour of the controller is present when other costs are associated with the fans.

In terms of the reference tracking error cost J_e no scaling has been necessary in order to achieve great results. J_e is simply described as the error between the reference and the actual measurements of the corresponding state $J_e = T_{ref} - T_r$.

Furthermore weights are assigned to the costs through the Q and R matrices. In this case it has been found that using the default weights of 1 on each entry achieves adequate performance. In a scenario where the flowrate of the air is used to a greater extent to control T_r, the tuning of these weights would likely prove to have a greater significance of the final overall power consumption of the system.

The constraints applied to the problem first of all consists on the limits of the control signals defined as $u_{min} \leq u(k) \leq u_{max}$. In terms of the states and outputs, only T_r has constraints applied. First a hard constraint that makes sure the controller does not lower the temperature too much and a soft constraint that ensures T_r will stay above T_{ref} as it does not matter if the room temperature is higher than the reference, but a lower temperature should be avoided. As this is a soft constraint the slack variable is added which makes it so the temperature can go lower if necessary and the minimization will still be feasible.

$$\begin{aligned}
\min_{q,\ P_{Heater}} \quad & (||J_e||^2_{Q(k)} + ||W_{fan} + W_{Heater}||^2_{R(k)} + w_\epsilon \cdot ||\epsilon||^2_2) \\
\text{s.t.} \quad & T_{ref} \leq T_r + \epsilon \\
& T_r \geq T_{r,min} \\
& u_{min} \leq u(k) \leq u_{max} \\
& \epsilon \geq 0
\end{aligned} \tag{5.7}$$

MPC look-ahead

Initial versions of the MPC appeared to not consider future changes in reference and disturbance values. It has been found that the MATLAB MPC functions do not make use of the "look ahead" feature unless it is given sequences of future references and disturbances which had not been provided initially. This resulted in the controller effectively just working with a prediction and control horizon length of one. Naturally considering an implementation on the physical system, not all future inputs will be known before hand. The future inputs can normally be estimated to a decent degree, especially in the first few future steps. This is the principle that has been implemented in this case when possible. For example take the input that is the ambient temperature outside the building. In this case weather forecasts can be used to determine a possible sequence of future ambient temperatures. There is also the case of the return air temperatures. Here are two possibilities. First there is the possibility of simply taking hte current value and keeping it constant for future steps. This would work as a rough estimation, specially in this case where the return temperature is equivalent to the room temperature that is being controlled to be at a specific reference temperature. Another option which again can be used due to the return air being dependent on the room temperature. In this case the future states that have been found through the MPC simulating future behaviour can be pulled and used as inputs for the next samples. It has been decided to go with the approach where the MPC prediction of T_r is used as the sequence of T_{ret} for future samples. In terms of T_{amb} the input temperatures are being treated as a weather forecast. Naturally a proper weather forecast will not be as accurate and some noise could be added to the simulation input in order to accommodate this.

Reference values

The reference temperatures used for the simulations are set to 14 degrees at night $T_{r,night} = 14$ and 18 degrees during the daytime $T_{r,day} = 18$. This is at the lower end of the comfortable temperatures outlined in **Sec. 2.6**, which could cause some discomfort, however based on feedback from members of the board at HBA the reference has been lowered from the original value of 20 degrees during the day to 18 degrees, due to concerns of occupants feeling too hot while exercising. The switching between day and night references happens at specifc times of the day as it for the moment is assumed that the arena is in use every day between 08:00 in the morning and 22:00 in the evening. Therefore the reference temperature is set to 18 °C at 08:00, until 22:00 where it is switched down to 14 degrees. The reference temperatures are stored in an array and can easily be altered to fit with any known schedule and or open hours. Furthermore the reference temperature could also be altered in a specific period if there for some reason is a need for that.

Performance on data used for tuning

Running the MPC with these settings and using the ambient temperatures as described results in the behaviour seen in **Fig. 5.3**. Looking into how well the reference temperature is kept with this controller it is obvious that the reference is not kept during daytime for most of the simulation. However, by looking at the control signals during the periods where the reference is not kept, it can be seen that the heater is running at maximum capacity. Based on this the error between the reference and T_r is due to too much heat loss from the building to the environment. Furthermore when T_r reaches the reference temperature the heater power is turned down as expected. Lastly it can be seen that the heating is lowered or increased a few samples before the reference switches between day and night values. This is also expected and was the core idea of using MPC as it allows for the required temperature to be reached faster than if controllers such as PID controllers or others were to be used.

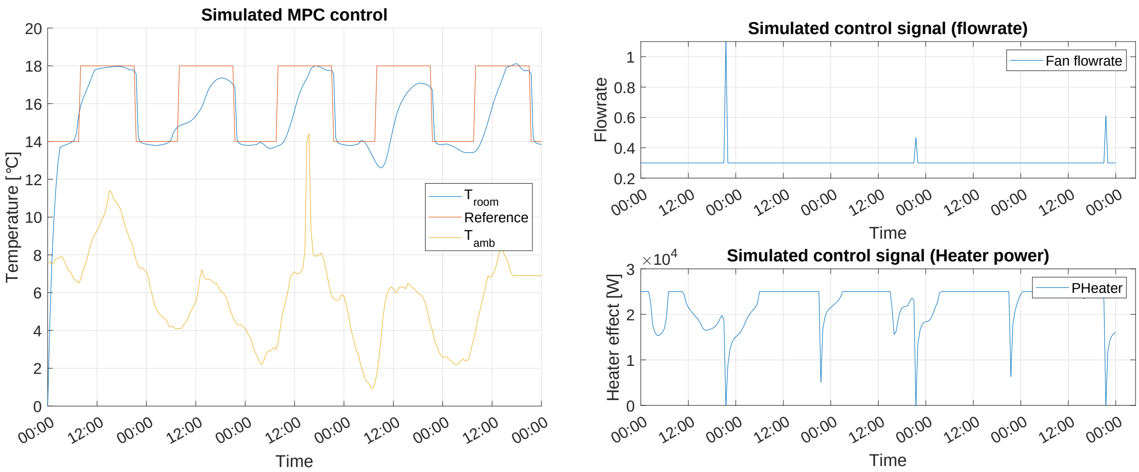

(a) T_{room} controlled through MPC (b) Applied control signals

Figure 5.3: Simulation using initial MPC design

Through this simulation the MPC is clearly functioning as expected however the scenario of T_{amb} being higher than T_r has not been tested. this scenario can be seen in **Fig. 5.4** where every sample of T_{amb} has 10 degrees added to it. With these new ambient temperatures the outdoor temperature is at times higher than the indoor temperature which means that cooling is required in the arena such that the indoor temperature does not get uncomfortable hot. In the periods where the cooling is required the flow rate is increased in the system. This makes sense as the CFR unit allows for heat transfer between the incoming air and the return air from the arena. As the outdoor air in these periods is the warmest of the two, heat will be transferred to the exhaust air, which provides a cooling effect on the supply air.

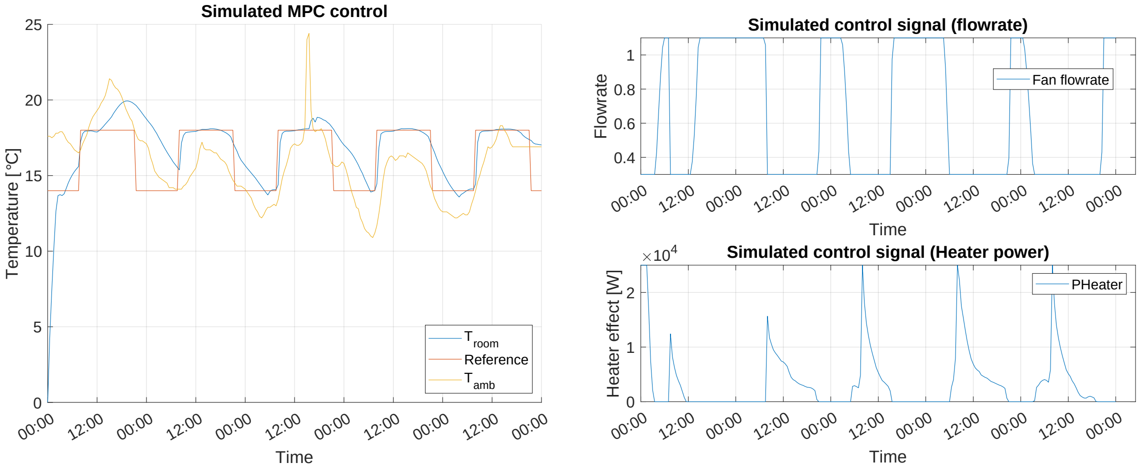

(a) T_{room} controlled through MPC (b) Applied control signals

Figure 5.4: Simulation with increased ambient temperature

MPC utilizes a linearized model to predict the future states and control inputs. The downside of this, as is the case with all linearized models, is that the linearized model degrades as the conditions move away from the operating points that were used to linearize with. For these reasons it is benefitial to use gain scheduled MPC when the controller has to cover a large operational area or if the quality of the linearized model degrades quickly. **Fig. 5.5** shows the result of a simulation where gain scheduled MPC has been used. The overall behaviour of the controller appears to not change much as gain scheduling is implemented. However, performance of the controller does improve on the days where the daytime temperatures are cooler. Such is the case on day 2 and 4 where the indoor temperature manages to reach the reference temperatures whereas this was not the case when only a single linearized model was used in **Fig. 5.3**.

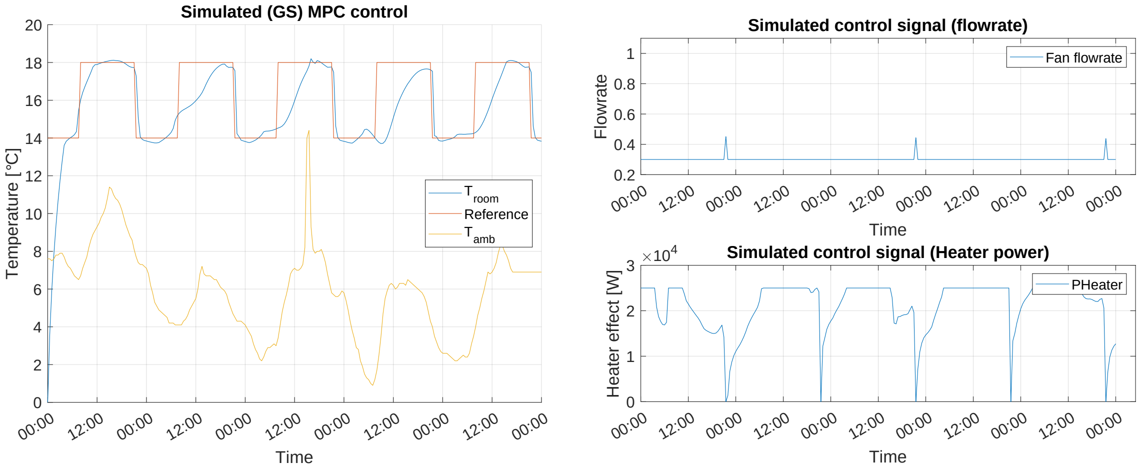

(a) T_{room} controlled through MPC (b) Applied control signals

Figure 5.5: Simulation with gain scheduled MPC and original ambient temperatures

To ensure that the MPC that is being used is actually being switched as the operating conditions change, the signal that selects what controller to use is graphed in **Fig. 5.6**. Based on these results it can be said that the gain scheduled MPC works as expected and an acceptance test can be carried out for the temperature control.

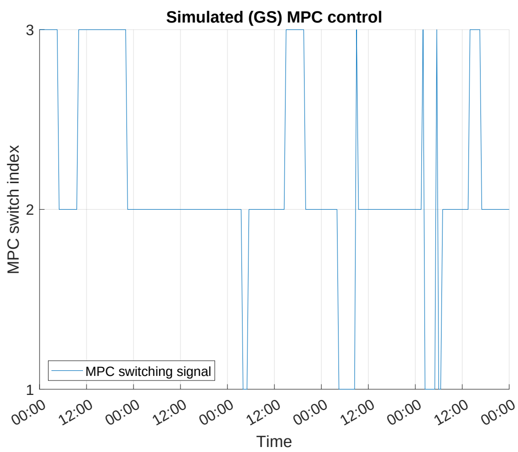

Figure 5.6: Signal showing which of the MPCs (and thereby which of the linear models) that are being used at each time step

5.3 Acceptance test and results

With the tuning of the controller complete, the acceptance test is carried out. In order to ensure an unbiased experiment the data used for the acceptance test is a set that the controller never has been applied to before. The new data set that has been used in the simulation is data from DMI's weather archive. As the arena is located in Hjørring, Denmark, the weather data for this city in particular has been retrieved.

The results of the acceptance test can in its full length be seen in **Fig. 5.7** and **Fig. 5.8**. Furthermore the first 10 days of the simulation have been isolated and is presented in **Fig. 5.9a** and **Fig. 5.9b** where the results can be seen in slightly greater detail.

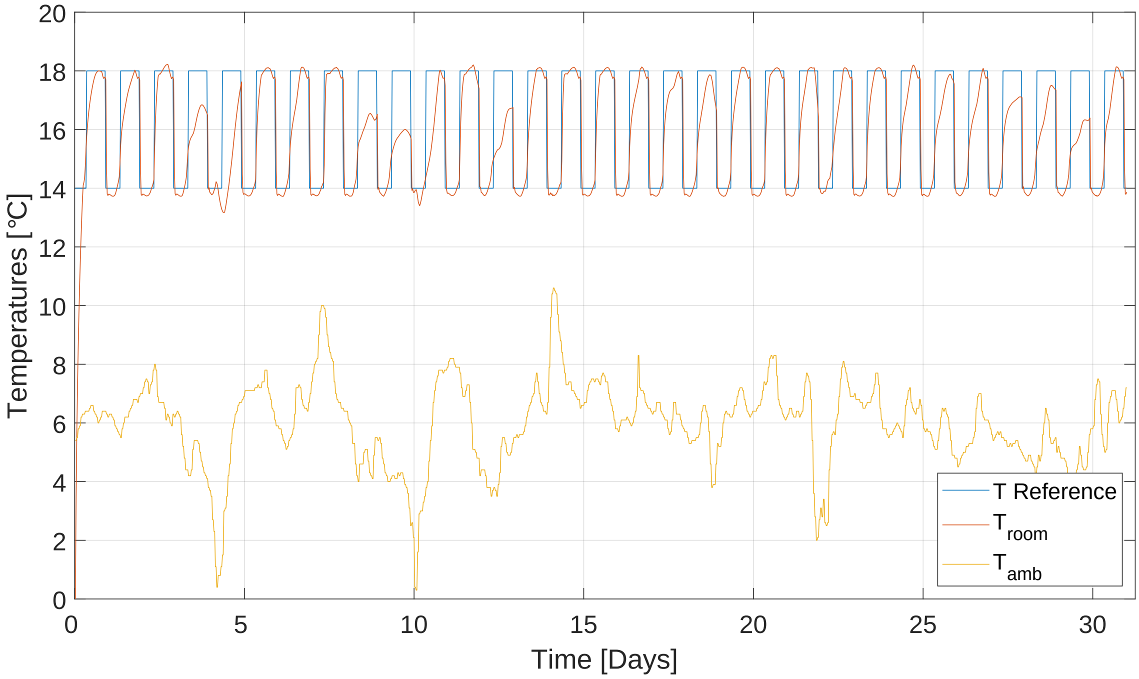

Figure 5.7: Full length acceptance test result. T_{amb} from 01-01-2020 to 31-01-2020

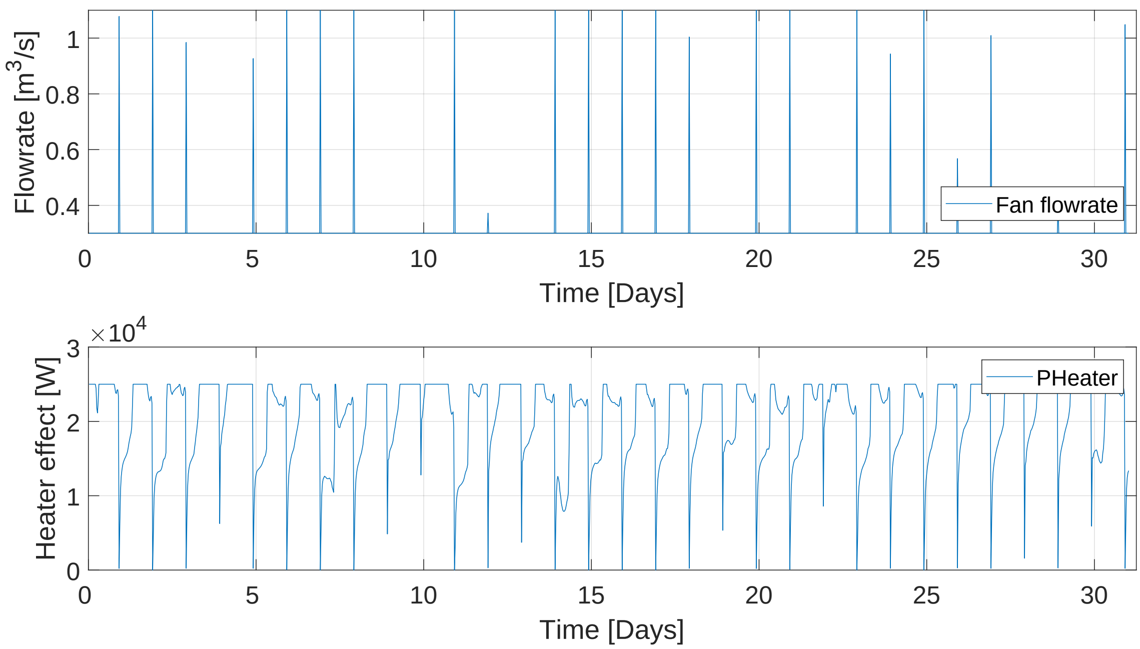

Figure 5.8: Controls applied in full length acceptance test.

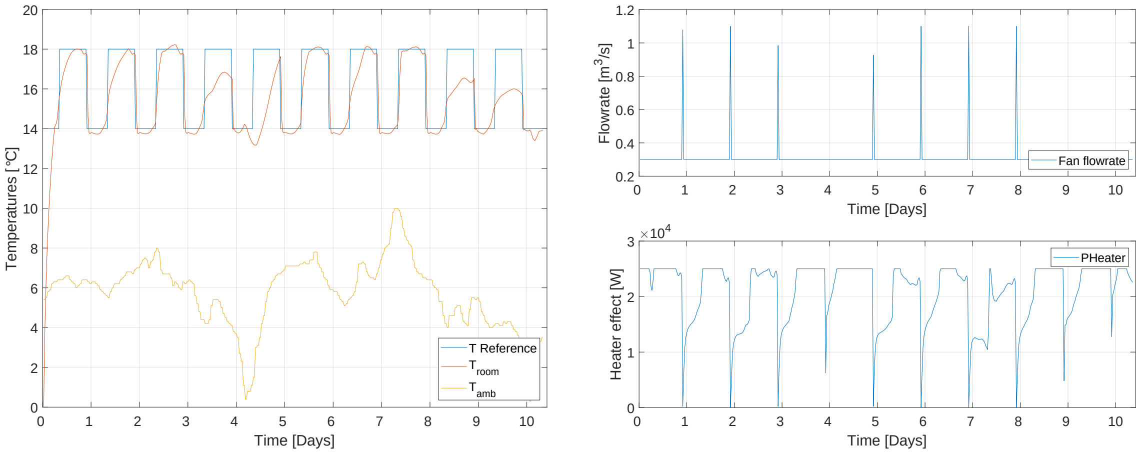

(a) First 10 days of the acceptance test.

(b) Controls applied in short acceptance test.

Figure 5.9: Simulation with gain scheduled MPC and original ambient temperatures

In general it is seen that the controller struggles to maintain the reference temperatures many of the days. This is both in terms of not meeting the required temperature at any point during some days and some other days will only reach the required temperature half or less of the day. However, looking at the control signals it is seen that for most of most of the simulation the heater is providing the maximum amount of power. Therefore the system can definitely be said to actively try to correct the error, but the heat loss in the building is too large.

The main goal of this project was to create a controller that could reduce the energy usage of the building and therefore energy consumption data has been obtained for the same period that is being simulated here. the energy consumption of the real system in this period can be seen in **Fig. 5.10**. Looking at the consumption for january 2020,

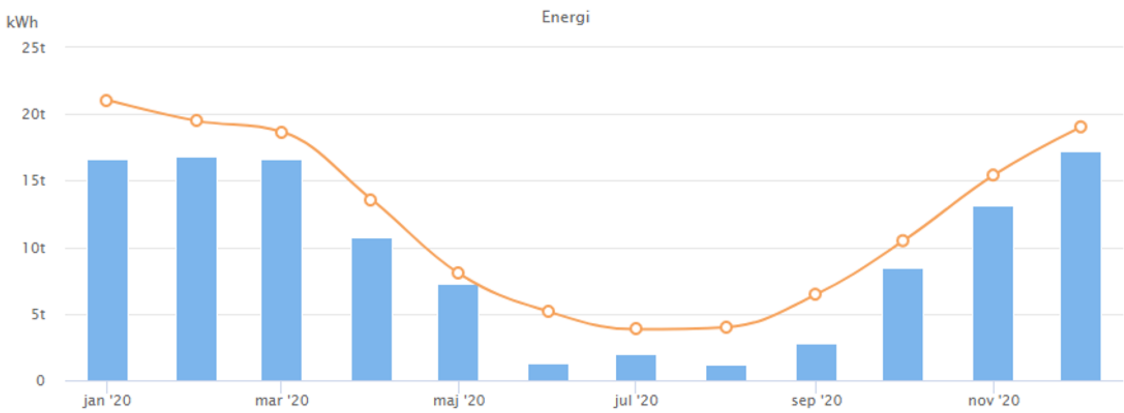

Figure 5.10: Monthly heater element energy consumption in 2020, Blue columns represent actual usage and orange graph shows expected usage.

the usage is around 16000 kWh. This data is only accounting for the consumption of the heater element and no data is available for the fan motors. In order to find the energy consumption of the simulated system the control signals have been converted into a corresponding power consumption. In the simulated period the MPC controller causes a usage of 765 kWh by both the fans combined and the heater element accounts for 15416 kWh. This results in a energy consumption decrease of $\approx 3.75\%$ when only considering the heater element. Initially this will seem like a small difference when considering that the temperatures are lowered significantly at night. However it should be noted that the model that is used here has a significantly higher loss than the real system (see **sec. 4.5**. Naturally a higher loss of heat to the environment means that more heating is required to keep a certain temperature. Therefore it is expected that the energy consumption of the system with MPC control will have a significant decrease in energy consumption if the model is improved.

Looking back at the problem statement there are a few factors to consider before concluding the acceptance test. The factors the controller has to consider and control are as follows:

- Activity patterns
- Humidity
- Seasonal changes
- Comfort levels
- Energy consumption

The humidity aspect can immediately be said to not be fulfilled as it has not been possible to include this into the model due to time constraints. When it comes to considering activity patterns and seasonal changes, these factors are deemed to be included into the design of the controller in such a way that they are fulfilled. The reference trajectory can easily be modified and updated as time progresses to take care of any special requirements and due to the implemented gain scheduled MPC new linearized models can be made and included such that the controller also handles ambient temperatures above 15 degrees well. The comfort level factor is somewhat fulfilled as the reference temperature is kept when the control signals are not saturated. However one can argue that humidity is a big factor in comfort levels and since it is not included in the model it cant be deemed a satisfying result. Finally in terms of energy consumption, the controller does appear to be able to lower the energy consumption however, due to inaccuracies in the model that is used to simulate the system the amount of energy being used is deceptively high.

Assessment 6

In this chapter the results from the different chapters throughout the report are looked further into and concluded upon.

6.1 Discussion

This section aims to discuss the decisions taken throughout the report. It also gives inspiration for what can be changed to improve the performance of the system.

6.1.1 Simulation and real environment

The work presented in this report has all been carried out through simulation and only a few measurements have been gathered from the real system. Therefore this work can at best be considered a proof of concept. This goal is considered to be accomplished as it is shown that MPC can be used to maintain adequate temperatures in a large building while at the same time lowering the energy consumption. Further developments will have to be carried out in order more accurately tell how efficient this approach is to the classic approach.

6.1.2 Improvements of room model

The main issue that removes the possibility much about the controllers potential performance on the real system is the quality of the model describing temperature changes in the main room of the badminton arena. For convenience the plot of the temperature developments when the model and real building are subjected to the same inputs can be seen in **Fig. 6.1**. From this figure it is easy to see how far the model deviates from the measurements, specially during the first night. As seen from the figure the measured temperature rises more slowly compared to the simulated temperature during the first 5 hours, which could indicate that part of the thermal mass included in the model is smaller than in the real system. This likely is due errors in the estimation of the wall parameters. Furthermore this would also somewhat explain the behaviour seen during the first night where the measured room temperature stays around 17.5 degrees. If more thermal mass is added to the model, the heat present in the building will provide a increased capacitive effect and reduce amount of heat lost over night. Furthermore as relatively large amounts of sunlight were experienced during this period it is suspected that the energy added to the system through this, has caused the walls and roof to heat up even more, which again will increase the capacitive effect and slow down the heat loss. Which in turn has allowed the heating system to maintain a constant temperature overnight. With some changes to

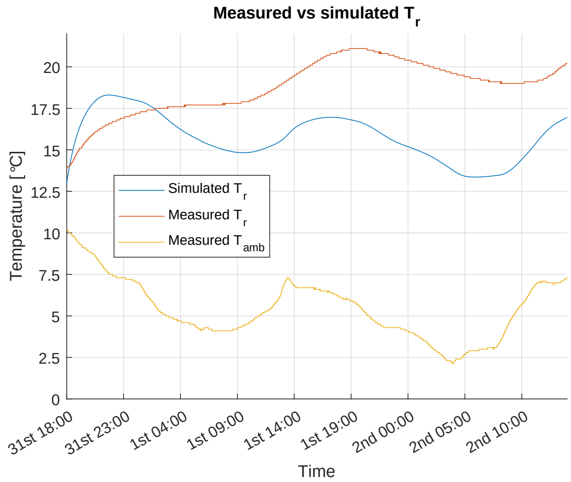

Figure 6.1: Comparison between measured and simulated room temperature together with the ambient temperature measured between March 31st and April 2nd.

the wall parameters and an added effect of energy from the sunlight it is expected that the model will have a much more similar performance to the real system. However it was not possible to implement and verify this in the project period.

6.1.3 Heater model

During the modelling of the heater element it was found that no direct control of the flow of water in the heater was possible. Therefore it is stated that a theoretical controller is implemented that provides some method of adjusting the power dissipation by manipulating the flow of water through the on/off valve. This approach resulted in **Eq. 6.1** where P_{heater} obtains a controllable value between 0 and 25000, corresponding to the power dissipation.

$$C_H \frac{dT_{sup}}{dt} = (T_{cfs} - T_{sup}) \cdot q \cdot \rho_a \cdot c_{p\_a} + P_{heater} \tag{6.1}$$

Unfortunately this approach removed a key aspect of the heater which had been overlooked until a late stage in project. Taking a step back and again considering how the heater element works, it is rather obvious that the heat dissipated by the heater will be a function of the incoming air temperature, the temperature of the metal fins in the heater and amount of air flowing through the heater. With the approach that has been used throughout this project the assumption is that the water flow that determines how much energy is being put into the metal fins of the heater can be controlled, and that this is directly correlated to the energy dissipated by the heater. However, naturally the heat dissipation will be determined by the temperature difference between the metal and the incoming air, along with how much air is passing by the metal. As the airflow increases a larger mass of air will pass by the fins and a lower temperature will be reached and more energy is pulled out of the fins. Likewise if the airflow is decreased the temperature of the air on the output will increase as the mass of the air passing by the fins is lower. the effects the air flow imposes on the heater element have been completely removed by the model that is used in this case. This has consequences which easily can be seen in the plots of the MPC control signals. Here the fans are barely ever used as the model tells the controller that the air flow has no impact on how much heat is added to the system, merely the value set by P_{heater} and the incoming air temperature. Causing the fans to only be used when cooling of the building is required (due to effects of the recuperator). In an attempt to alleviate this issue a new model that will represent the heat dissipation of the heater is created. This model utilizes forced convection to find the amount of energy that is pulled out of the metal fins and thereby transferred to the air that is being forced past the fins. The differential equation will consist of the same parameters shown in **Eq. 6.1** however P_{heater} is changed such that is described by **Eq. 6.2**. Here c_1 and c_2 are constants that vary based on the layout of the fins and the heater overall and are therefore tuned until a similar response to the one seen on the real system is obtained. T_{fins} is described as the amount of energy that is delivered by the district heating water, flow rate of the water and air and lastly by the amount of energy being pulled out from the fins and into the outgoing air.

$$\frac{dP_{heater}}{dt} = c_1 \cdot (q \cdot \rho_a)^{c_2} \cdot (T_{fins} - T_{cfs}) - P_{heater} \tag{6.2}$$

By setting $c_1 = 400$ and $c_2 = 0.65$ and assuming that some theoretical controller that handles the water flow in the heater can maintain a temperature drop from 70 degrees on the water inlet to 35 degrees on the outlet and an air flow rate $q = 0.7272$ it is found that T_{sup} obtains a response that appears similar to the one found in the step response test of the real heater, although T_{sup} is still 5-10 °C higher at a power dissipation of $25[kW]$. T_{sup} can be seen at various air flows and heater fin temperatures, with an incoming air temperature of $T_{cfs} = 15$ in **Fig. 6.2**. With these results it is assumed that implementation

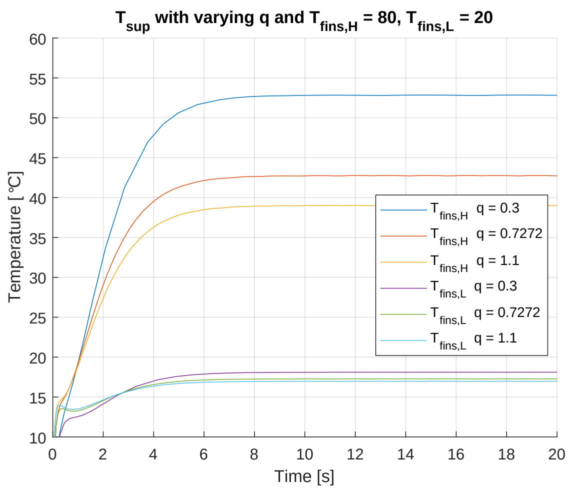

Figure 6.2: Changes in T_{sup} with new model of P_{heater}

this description of P_{heater} into the system model, the MPC will be able to utilize the fan motors more to get the desired temperatures in the building. However, it is not been possible to implement a similar model like this during the project period, due to time restrictions.

6.2 Conclusion

This section evaluates the entirety project. Firstly recall the initial problem statement.

How can one develop a controller that considers a multitude of factors such as activity patterns, humidity, seasonal changes etc. while keeping the same comfort levels and reducing the energy consumption, be designed and retrofitted into an aging commercial building?

In this work a model that describes three different system parts has been developed. The first submodel describes the behaviour of a cross-flow recuperator that is used in the system in order to pre-heat the fresh air and reduce the amount of wasted energy that is being exhausted from the system. Furthermore this unit also contains fans that determine the flow rate of air throughout the whole system. Secondly water-air heat exchanger models provides information about the transfer of energy from district heating water to the air being supplied to the building. This model has proven to be flawed and a new model has been attempted but was not possible to complete in the project period. Lastly a model has been created that describes the temperature changes in the main room of the arena. Overall the model has proven to be too aggressive in terms of loss of heat to the environment and several suggestions as to what is causing this has been found. With a complete model it has been possible to create a model predictive controller that can manage the temperatures in the building to a sufficient degree during the winter months. The goal of the controller is to reduce the operating costs through optimization of the heating in the building. As MPC estimates future developments it can account for future changes in reference values and disturbances which has allowed for the indoor temperature to be lowered when the building is unoccupied. To see the energy savings this controller creates, ambient temperature data from January 2020 has been collected and a simulation has been carried out. Furthermore actual heating usage from the real system has been obtained for the same period and it can be compared to the usage from the simulation. The MPC controller manages to reduce the energy usage by close to 600 kWh, which correlates to $\approx 3.75\%$. A better result was to be expected however, as the energy consumption is found through simulation and the model that has been developed is more aggressive in terms of heat loss, the heating needed in the simulated system to keep the same temperatures is increased. Therefore it is expected that a significant decrease in energy consumption will be seen with a more accurate model. To summarize, MPC can indeed be used to decrease energy consumption in large buildings that are not always occupied and with further developments this method of control for HVAC units in commercial buildings will likely result in large energy savings.

6.2.1 Future work

As stated in the discussion section **Sec. 6.1**, the solution developed in this work has a host of improvements that can be done. Due to this work revolving around simulations the first interesting future development would be to attempt to implement it on the real system. As the MPC in this case utilizes a model that has a higher loss of heat will likely cause excessive heating in the real system, however as the MPC not solely relies on the model but also current measurements the effects of this is expected to be manageable. Furthermore as the current model relies on being able to control the power dissipation of the heater element directly, some changes will have to be made to the control signals in the MPC and model in a similar fashion to what has been mentioned in **Sec. 6.1**. This together with an exchange of the pump in the heater element, to a pump that can be controlled through an external signal would allow for great control of the power dissipation.

Additional parameters can also be added to the model in order to improve the accuracy. It is expected that providing the MPC with information about the expected amount of sunlight together with an addition of the disturbance caused by the sunlight will allow for further energy savings if the sunlight turns out to have a significant effect. This effect still has to be proven and if it indeed turns out to be significant a model that describes the disturbance has to be developed.

During the summer periods it has been noted, based on information given by the users of the arena, that the temperatures can get very high. This is seen as a natural consequence of poor insulation and the fact that the installed system has no way of cooling down the air going into the arena other than a high air flow. Therefore inclusion of a chilling unit could be added to both the model and the real system. This would also allow for the MPC controller to more readily applicable to more HVAC systems with similar layouts.

Bibliography

Alber-Wallerström, B. and I. Holmér (2004). "Efficiency of sweat evaporation in unacclimatized man working in a hot humid environment". In: *European Journal of Applied Physiology and Occupational Physiology* 54. Accessed March 23, 2021, pp. 480–487.

American Society for Refrigeration and Air-conditioning Engineers (2001). *Ventilation for Acceptable Indoor Air Quality.* Accessed February 10, 2021. URL: `http://www.ies.al/wp-content/uploads/ASHRAE_Standard62-01_04_.pdf`.

— (2010). *Thermal Environmental Conditions for Human Occupancy.* Accessed February 12, 2021. URL: `http://arco-hvac.ir/wp-content/uploads/2015/11/ASHRAE-55-2010.pdf`.

Berardi, Umberto (2017). "A cross-country comparison of the building energy consumption and their trends". In: *Resources, Conservation and Recycling* 123 (2017), p. 230–241.

Brath, Per (1999). *Towards Autonomous Control of HVAC Systems.* Accessed March 10, 2021. URL: `https://vbn.aau.dk/ws/portalfiles/portal/316396107/fulltext`.

DMI (2021). *Danish weather archive.* Accessed February 4, 2021. URL: `https://www.dmi.dk/vejrarkiv/`.

EIA, U.S. (2020). *International Energy Outlook 2020.* Accessed February 4, 2021. URL: `https://www.eia.gov/outlooks/ieo/`.

UN-Habitat (2008). *State of the World's Cities 2010 / 2011.* ISBN: 9781849711753. Earthscan.

Intergovernmental Panel on Climate Change (2014). *Climate Change 2014: Mitigation of Climate Change.* Accessed February 9, 2021. URL: `https://www.ipcc.ch/site/assets/uploads/2018/02/ipcc_wg3_ar5_chapter9.pdf`.

Maciejowski, J.M. (2002). *Predictive Control with Constraints.* England.: Prentice Hall.

MATLAB (2021). *Model Predictive Control Toolbox.* URL: `https://se.mathworks.com/products/model-predictive-control.html`.

Orosa, Jose (Aug. 2010). "A Review of General and Local Thermal Comfort Models for Controlling Indoor Ambiences". In: ISBN: 978-953-307-131-2. DOI: `10.5772/9763`.

Petrolium, British (2010). *Statistical Review of World Energy.* Accessed February 8, 2021. URL: `http://www.dartmouth.edu/~cushman/courses/engs41/BP-StatisticalReview-2010.pdf`.

Ritchie, Hannah and Max Roser (2017). "CO2 and Greenhouse Gas Emissions". In: *Our World in Data.* https://ourworldindata.org/co2-and-other-greenhouse-gas-emissions , Accessed February 8, 2021.

Standard, Dansk (n.d.). *Norm for specifikation af termisk indeklima. DS 474.*

Appendix A

A.1 HVAC system

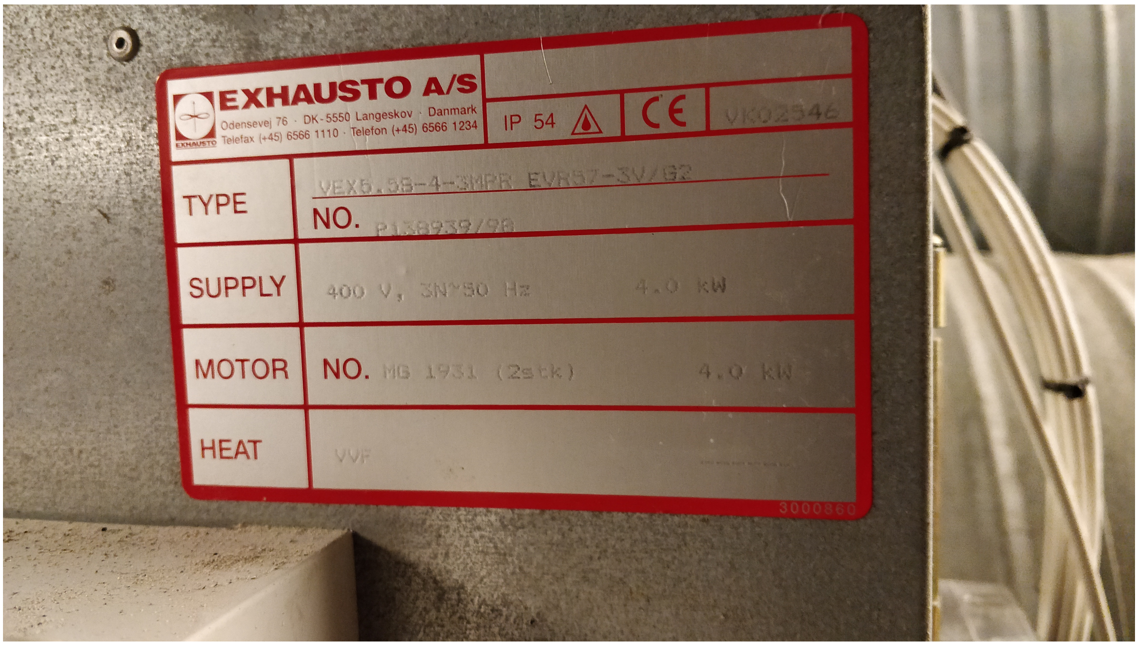

Figure A.1: Plate containing model designations and some specifications

Datasheet (only available in danish)

VEX5.5 - Luftbehandlingsaggregat

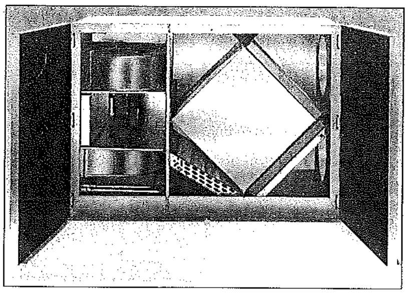

EXHAUSTO luftbehandlingsaggregat med varmegenvinding VEX5.5 har indbygget 2 ventilatorer med hver sin motor.

Motorerne er trinløst regulerbare via EVR automatik. VEX-aggregatet er lyd- og kondensisoleret på alle sider.

VEX5.5 har 2 sidehængte servicelåger, som lukkes med det medfølgende låseværktøj.

Standardfilter er F5, og som tilbehør kan der leveres F7 filter for både udsugning og indblæsning.

Aggregatet har indbygget by-pass samt filtervagt.

Kapacitetsdiagram

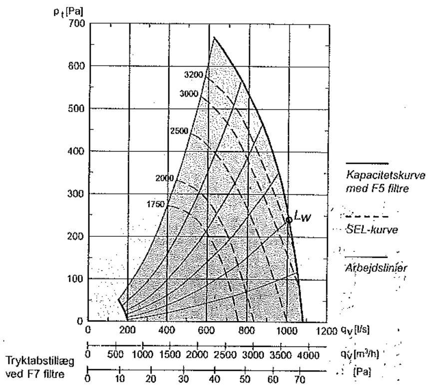

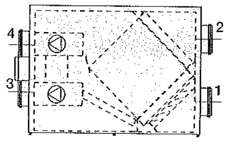

VEX5.5 standard:

VEX5.5 er standardudgave med ventilator-sektionen i venstre side.

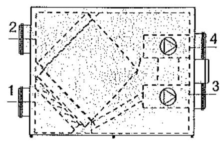

VEX5.5S spejlvendt:

VEX5.5S er spejlvendt udgave med ventilator-sektionen i højre side.

EXHAUSTO luftbehandlingsaggregater er målt med 1 m lige kanal på alle 4 tilslutningsstudse.

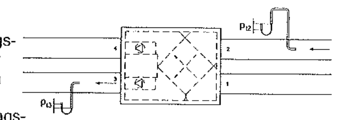

Kan denne minimumsafstand ikke opretholdes ved installationen, vil der optræde systemtryktab, hvilket der skal tages hensyn til ved projekteringen.

Størrelsen af dette systemtryktab kan beregnes ud fra faglitteraturen.

p_t er det disponible totale tryk, der er til rådighed på både udsugnings- og indblæsningssiden.

Alle interne tryktab i krydsvarmeveksler, eftervarmeflade og rene filtre (F5) er fratrukket.

De angivne arbejdslinier viser ventilatorens karakteristik ved nedregulering.

De angivne SEL-kurver viser det specifikke elforbrug i J/m³ luft, altså aggregatets totale elforbrug for begge ventilatorer incl. alle interne tryktab.

p_t = total tryk

$p_t = p_{t3} - p_{t2}$

Temperatur = 20°C

Densitet = 1,2 kg/m³

SEL = Specifikt elforbrug (J/m³)

q_V = Volumenstrøm (l/s)

P_1 = optaget effekt (W)

$P_1 = \text{SEL} \times q_V \times 10^{-3}$

$P_1 = \frac{\text{SEL (J/m}^3) \times q_V \text{ (l/s)}}{1000}$

Lyddata

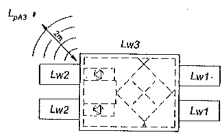

Forudsætninger for lyddata

L_{W1}: Lydeffektniveau til kanal. Sugestuds udsugning/udeluft. Målt ifølge ISO 5136.

L_{W2}: Lydeffektniveau til kanal. Trykstuds indblæsning/afkast. Målt ifølge ISO 5136.

L_{W3}: Lydeffektniveau til omgivelser. Målt ifølge ISO 3744.

L_W: Lydeffektniveau dB. Reference: 1pW. Lydniveauet er angivet ved det markerede punkt L_W (se kapacitetsdiagram).

L_p: Lydtrykniveau i 2 meters afstand fra VEX med isolerede kanaler.

Tolerance: +/-3 dB.

	L_W (dB)							L_W	L_p
Målepkt.	125	250	500	1000	2000	4000	8000	dB(A)	dB(A)
L_{W1}	80	71	64	63	57	50	44	69	
L_{W2}	88	85	83	80	75	72	65	85	
L_{W3}	78	67	60	58	52	48	38	66	52

EXHAUSTO

4.1.14

VEX5.5 - Tekniske data

Aggregatudførelse

Type	Udførelse
VEX5.5-4-3	Standard
VEX5.5S-4-3	Spejlvendt
VEX5.5-4-3FRK	Standard med frekvensomformer
VEX5.5S-4-3FRK	Spejlvendt med frekvensomformer
Udendørs montage:	VEX5.5 kan leveres i specialudgave for udendørs montage

Motordata

	Med EVR-Automatik	Uden Automatik
Udførelse:	2 motorer	2 motorer
Regulering:	Trinløst regulerbar via indbygget frekvensomformer (FRK)	ingen
Spænding:	3 x 230V fra FRK	3 x 400V
Strøm:	6,4A	5,2A
Effekt:	1,5 kW	2,2 kW
Max. omdr./min.:	1420	1420
Kapslingsklasse:	IP54	IP54
Isoleringsklasse:	F (155°C)	F (155°C)
Motorbeskyttelse:	Indbygget i FRK	Motorværn (ej EXHAUSTO leverance)

Aggregatdata

	Vandvarmeflade	Elvarmeflade 12,0	Elvarmeflade 18,0
El-forsyning	3 x 400V	3 x 400V	3 x 400V
Optaget effekt m/EVR-automatik	3,5kW	16,6kW	23,2kW
Max. fasestrøm m/EVR-automatik	14,5A*	33,5A	43,0A
Optaget effekt u/EVR-automatik	5,4kW	18,5kW	25,1kW
Max. fasestrøm u/EVR-automatik	10,4A	29,4A	38,9A

Isolering Pladekvalitet	Alle sider: 50 mm mineraluld Varmgalvaniseret Z275, Miljøklasse M2
Hovedmål (C x A x B) højde x længde x dybde	1125 x 1575 x 835 mm (excl. studse, svingningsdæmpere og automatik)
Varmeoverførselsareal Kanaltilslutning (nippelmål) Servicelåge Kondensafløb	42 m² Ø 400 mm 2 stk., sidehængte Udv./indv. = ø15/13 mm
Filter (udeluft/udsugning) Mål, L x B x D	F5 / EU5: 4,2 m² F7 / EU7: 7,0 m² (tilbehør) 592 x 592 x 48 mm
Svingningsdæmpere Bypass (indbygget) Filtervagt Vægt	8 stk. Ø 30 x 20 mm shore 50 24V motor, modulerende 2 stk. indbygget 330 kg

* *BEMÆRK: Dimensionering af nulleder.*
Den optagne strøm i de to frekvensomformere er ikke sinusformet. Nullederen skal dimensioneres så den kan klare en belastning, som er 19A.

Temperaturvirkningsgrad

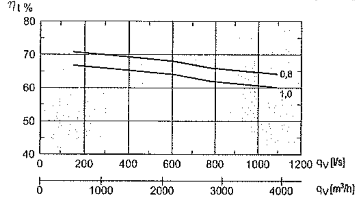

$\eta_t = \frac{t_3 - t_2}{t_1 - t_2}$ = Temperaturvirkningsgrad

t_2 = Temperatur på udeluft (friskluft)

t_3 = Temperatur på indblæsningsluft

t_1 = Temperatur på udsugningsluft

Udsugningsluft = 25°C

Udeluft (friskluft) = 5°C

Temperaturvirkningsgraden for VEX-aggregatet er vist ved forskellige volumenstrømsforhold beregnet som:

$\frac{\text{Indblæsning}}{\text{Udsugning}}$ = 0,8 og 1,0

Temperaturvirkningsgraden er anført ved tør varmegenvinding og forøges ved kondensation.

Tilbehør

Elvarmeflade ELVF **12,0** **18,0**	13,1 kW, 2 trin, modulerende 19,7 kW, 3 trin, modulerende
Vandvarmeflade VVF ved t_{ude} = -20°C, 100% varmegenvinding, luftmængde = 750 l/s og volumenstrømsforhold = 1,0	14,7kW giver en indblæsningstemperatur på 20°C ved t_F / t_R = 60/40°C
Fleksible forbindelser	4 stk. FLF 400

Styringsmuligheder

	Komplet Automatik
Type	EVR57-3
VEX5.5-4-3	
VEX5.5-4-3FRK	X

4.1.15

A.2 Temperature and humidity measurements of system

A.2.1 Test purpose

The purpose of this test is gather data such that some amount of system identification and validation data can be obtained. As the model concerns the temperature changes in different parts of the system most of these have been measured. Furthermore by measuring indoor and outdoor humidity this data can also be used together with the humidity model.

A.2.2 Measurement theory

By measuring the actual response of the system to different inputs and situations the performance of the model can be compared to the real system response. Three seperate tests are carried out, First the HVAC is turned off, providing some insight into how the temperature develops with no heating which can be used to tell how much heat is lost to the environment. Next experiment involves turning the HVAC system back on, which will show the dynamics with the heating on and give insight into things such as the rise time of the room temperature etc. For the third experiment the temperatures at the input and output vents of the recuperator is measured as this will provide some data to validate the model against.

A.2.3 Test setup

In order to do the test the following equipment is needed:

- Two or more dataloggers that can measure humidity and temperature, in this case a device called "EL-GFX-2" has been used
- Data extraction software which is available at the datalogger manufacturers website

For the experiments where the HVAC system is turned on and off the dataloggers are placed as follows. One of the loggers have to be placed outside in a shaded area such that direct sunlight does not influence the measurents. The other datalogger is placed inside the room where the data has to be measured and is preferentially placed in a location close to the center of the room to best capture the average temperatures and humidity levels. For the third experiment regarding the recuperator the experiment has to be performed multiple times with the loggers in different positions unless at least 4 loggers are available. As the recuperator has two input ducts and two output ducts a logger is placed in all of these such that the temperature can be measured at each point.

With the loggers in their positions the logging is enabled.

A.2.4 Test method

HVAC off

With the loggers placed in their respective positions the HVAC system is turned off for a set amount of hours. Preferably 24 hours or more to ensure a proper response can be captured. In this case the experiment has been carried out twice, the first time for a duration of 24 hours and the second time the duration was 49.6 hours.

HVAC on

With the loggers placed the HVAC system is turned on at a set reference temperature and airflow rate. Here the HVAC reference temperature is set to 30 degrees to ensure that the heater element is run at maximum capacity at all times and no control is used by the existing system. Furthermore the airflow rate reference is set to a value of 6 on the control panel which corresponds to $\approx 0.72m^3/s$. With these settings the temperature and humidity levels are monitored over the course of preferably more than 24 hours as with the HVAC off test. In this particular case the experiment had a duration of 44.6 hours.

recuperator

For the recuperator experiment the loggers are placed as previously stated and the HVAC system is turned on. The recuperator is a passive element that exchanges heat between two airflows and therefore the element that is varied in the test is the airflow. For this experiment the airflow was set to a setting of 2 ($\approx 0.4m^3/s$), 6 ($\approx 0.72m^3/s$) and 10 ($\approx 1.05m^3/s$), where 10 is the highest possible setting on the control panel. At each setting the data is measured over the course of a few minutes in order to allow the temperature to stabilize on each side of the unit.

A.2.5 Test results

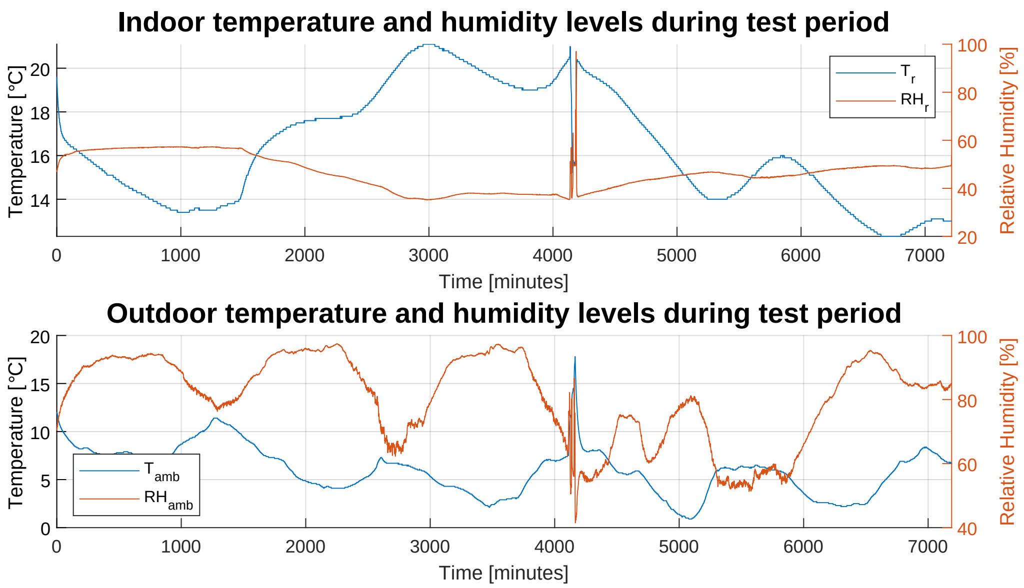

Figure A.2: Data points over the whole test period

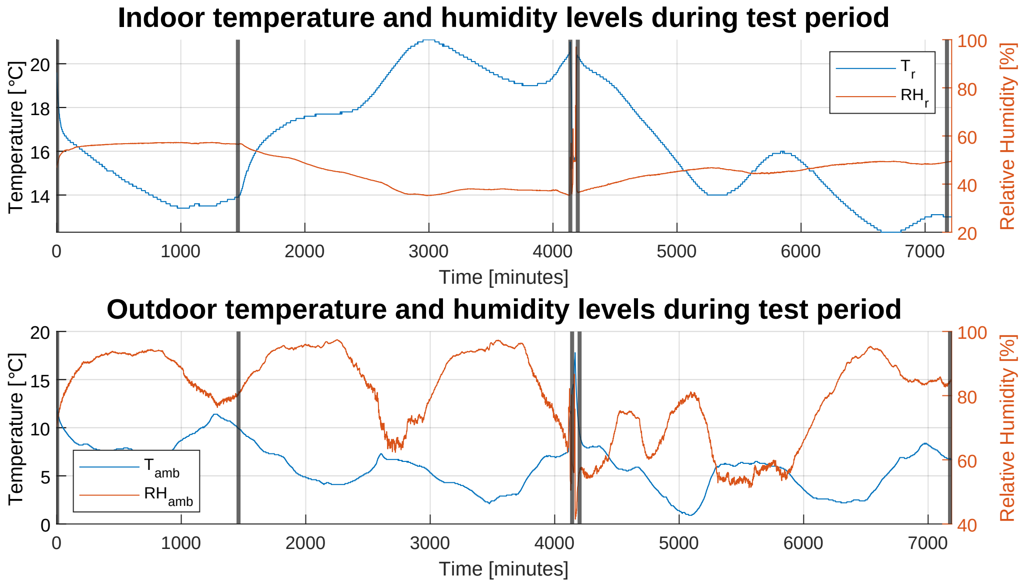

Figure A.3: **Fig A.2** where the start and stop times of experiments have been marked

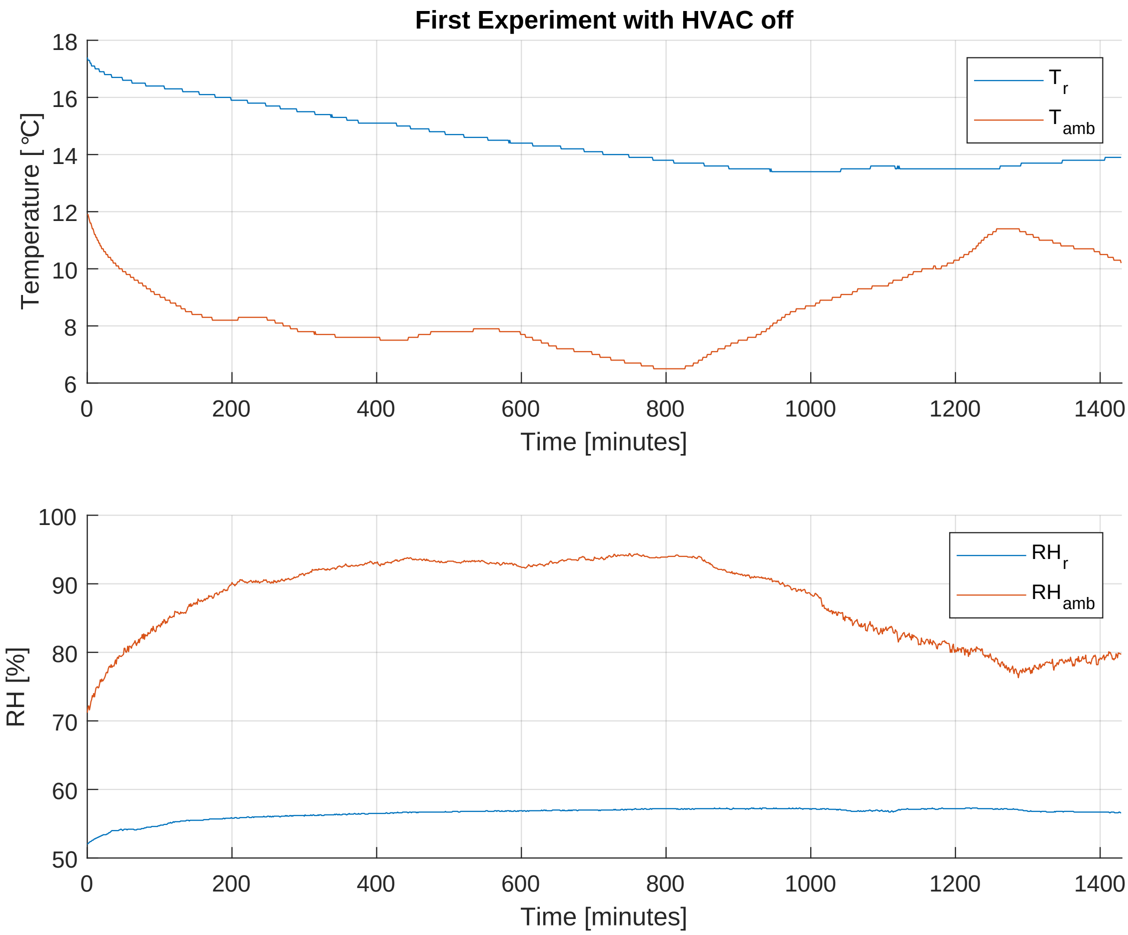

Figure A.4: Test period 1, HVAC is turned off and the temperature and RH developments are seen as the arena cools down

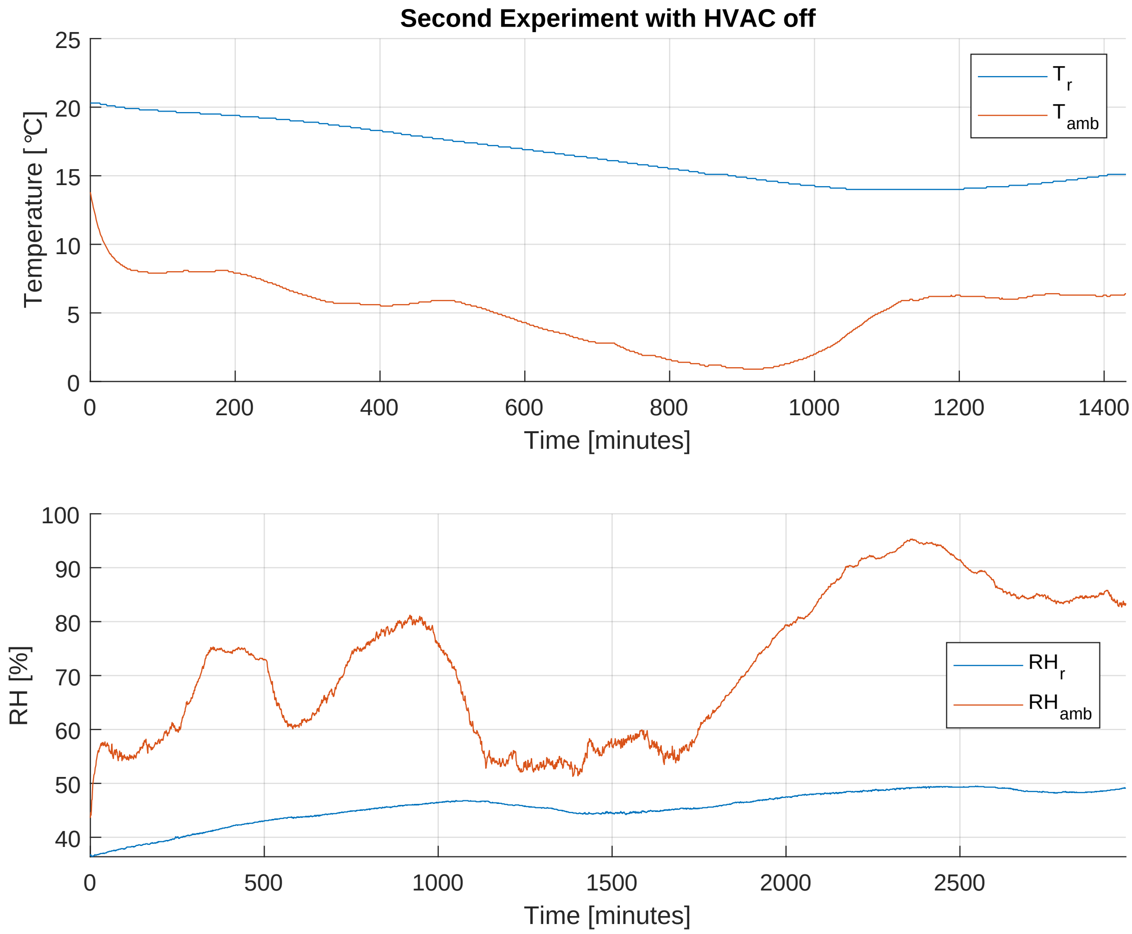

Figure A.5: Test period 4 where the HVAC system once again is turned off, however this time over a longer period

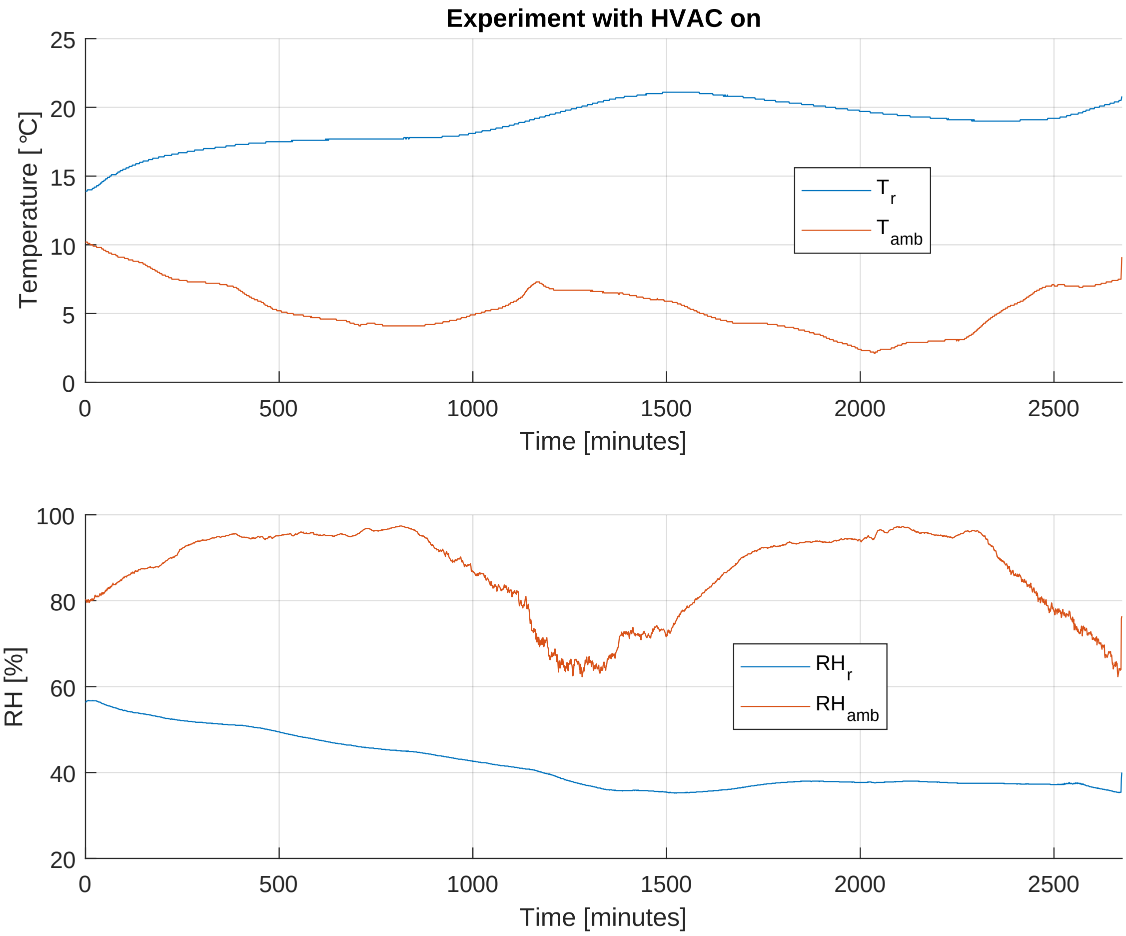

Figure A.6: Test period 2, HVAC is turned on with the heater on full power and the temperature and RH response is seen

A.2.6 Uncertainties of measurements

The main uncertainties for these experiments are present in the outdoor measurements and in the recuperator measurements. For the outdoor measurements come from the fact that the datalogger was placed inside of a black plastic box (with openings for the air to enter and not tightly sealed at the bottom) in order to protect it from direct rainfall. The placement of the box should ensure that the sun does not impact the measurements that much however, it is possible that the the measurements are a bit scewed due to the sensor being inside the box. For the recuperator measurements there are several sources of uncertainties as there is a possibility for the temperature of the surrounding aluminium to impact the temperature of the measurements as the logger had to be placed directly on it. furthermore it is unknown whether the direction of the dataloggers sensor had a large impact on the measurements when considering the large airflow surrounding the device. These uncertainties are discussed in greater detail in **Sec. 4.5**

A.2.7 Conclusion

Overall the data that has been collected through this experiment show the behaviour that was to be expected. With the data it is now possible to weigh it against the models in order to see whether they are good enough or there are some missing dynamics that have to be handled. The main difference between the measurements and the expected appearance of the data is that there is some external component that influences the indoor temperature greatly. This component is likely the sun which obviously will heat up the roof of the building and that heat will then impact the indoor air. This element was not considered before the experiment however, the data has shown that it is an important element to consider if higher accuracy of the model is wanted.

A.3 Second test period

During this period it turned out that a malfunction had caused the system to shut down a week earlier. Therefore the response seen here is the behaviour of the system when it has been fully off for at least a week.

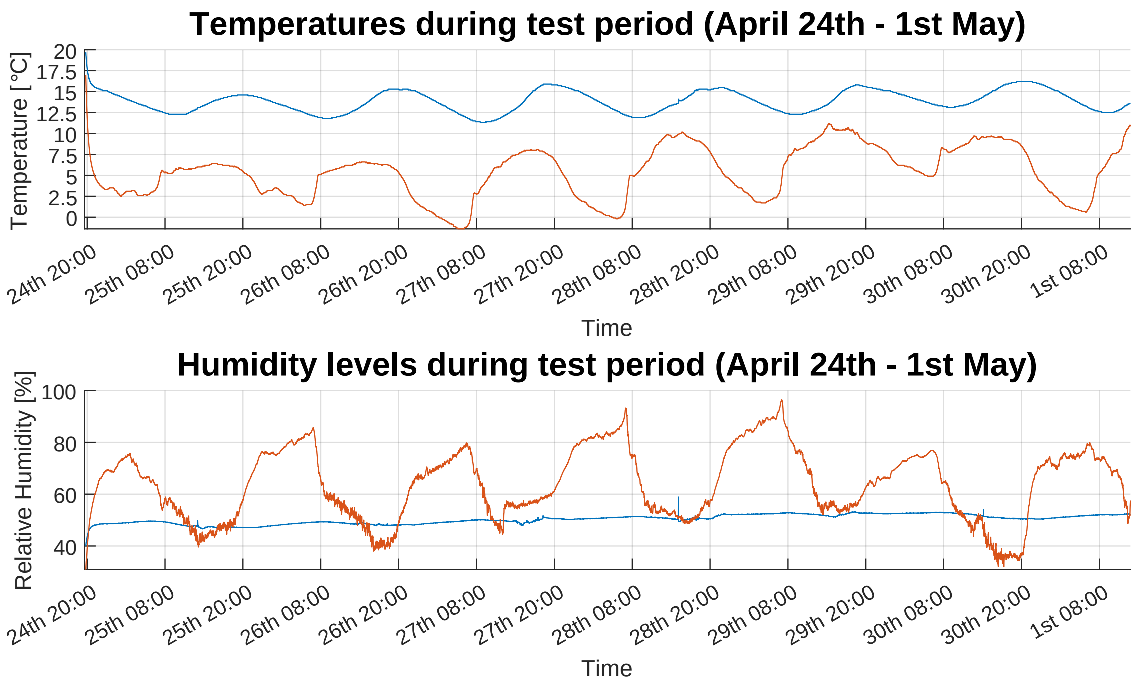

Figure A.7: Measurements of temperature and humidity levels under constant HVAC settings. Blue and orange graphs are indoor and outdoor measurements respectively